Title
The Role of DGAT1 in Triglyceride Uptake, Synthesis and Storage

Author
Haas, Joel

Publication Date
2013

Peer reviewed|Thesis/dissertation

The Role of DGAT1 in Triglyceride Uptake, Synthesis and Storage

by

Joel Theodore Haas

DISSERTATION

Submitted in partial satisfaction of the requirements for the degree of

DOCTOR OF PHILOSOPHY

in

Biochemistry and Molecular Biology

in the

GRADUATE DIVISION

of the

UNIVERSITY OF CALIFORNIA, SAN FRANCISCO

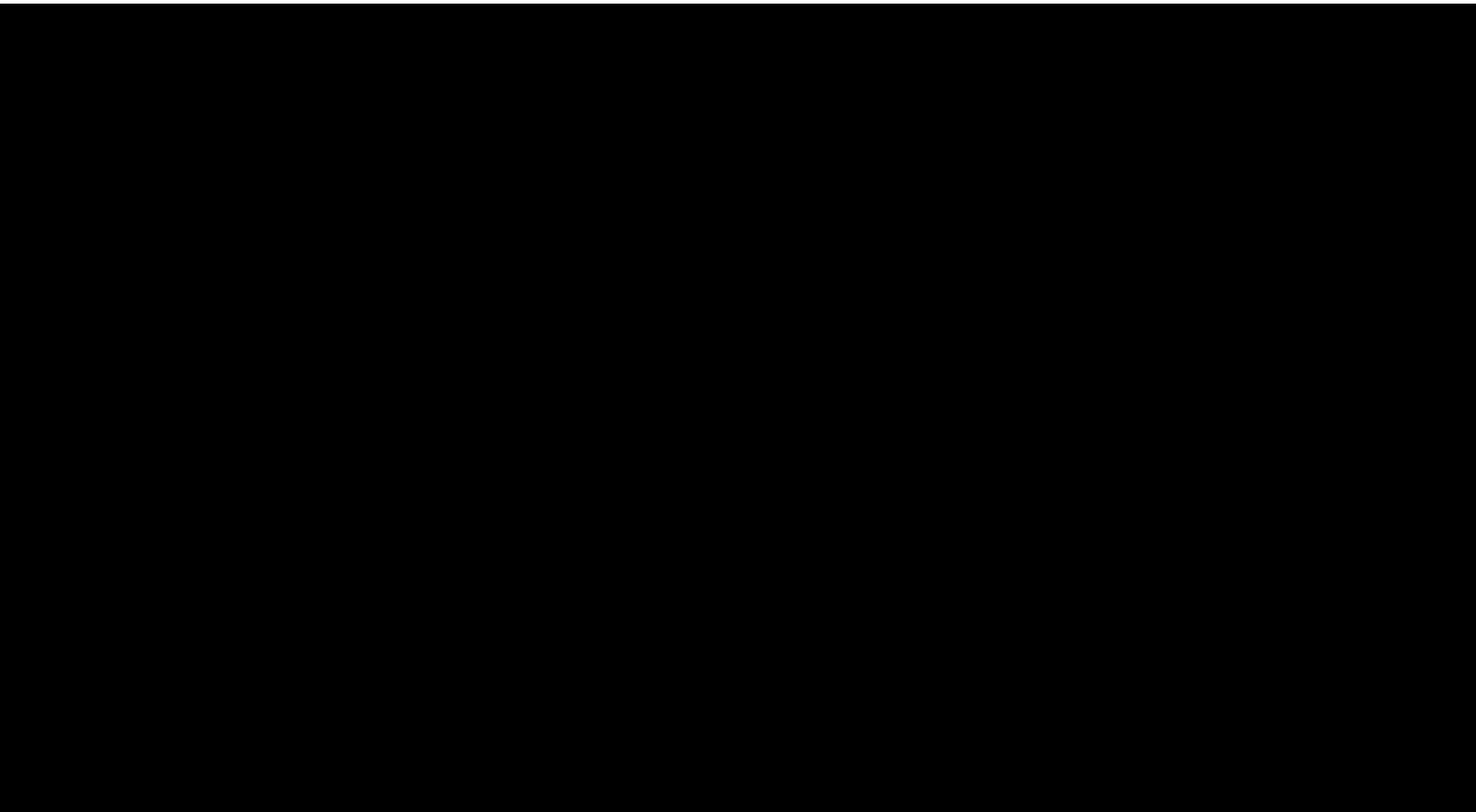

Acknowledgements

Publications and Contributions

The work in chapter 2 does not yet fit the framework of a publication. The authors of this study include Joel T. Haas, Kenneth D. Harrison, Jillian Varonin and Robert V. Farese, Jr. The experiments presented here are complementary to and build upon work not presented, performed by Scot Stone and Ping Zhou who were extremely helpful in sharing expertise and reagents. JTH and KDH designed and performed experiments, collected and analyzed data and summarized results. JV performed experiments and collected data. JTH and RVF wrote the text as it appears here. JTH was supported by a Graduate Research Fellowship from the National Science Foundation, KDH received support from the A.P. Giannini Foundation. RVF received grant support from the NIH (2R56DK56084) and The J. David Gladstone Institutes.

Work in Chapter 3 is published as a Brief Report in *The Journal of Clinical Investigation*, 2012 Dec 3, Vol. 122, No.12, pp. 4680-4 entitled "DGAT1 mutations in a family with a congenital diarrhea disorder" by Joel T. Haas*, Harland S. Winter*, Elaine Lim, Andrew Kirby, Brendan Blumenstiel, Matthew DeFelice, Stacey Gabriel, David Branski, Chaim Jalas, Carrie A. Grueter, Mauro S. Toporovski, Tobias C. Walther, Mark J. Daly**, Robert V. Farese, Jr**. *, **-authors contributed equally. The authors wish to acknowledge Sekar Kathiresan for advice, Daryl Jones for manuscript preparation, Delphine Eberlé for helpful comments, Gary Howard and Anna Lisa Lucido for editorial assistance.

This work was supported by NIH grant 2R56DK56084 (RVF), animal facilities grant NIH/NCRR CO6 RR018928, the Gladstone Institutes, the National Science Foundation (JTH), the Pediatric IBD Foundation (HSW), and funding from Martin Schlaff (HSW).

The work in chapter 4 does not yet fit the framework of a publication. Contributing authors include Joel T. Haas, Florian Wilfling, A. Rachid Thiam, Delphine C. Eberlé, Manuele Piccolis, Caroline Mrejen, Charles A. Harris, Tobias C. Walther and Robert V. Farese Jr. JTH and CAH developed the DGAT2-KO adipocyte model and performed experiments related to it. JTH performed experiments using the permeabilized cells and COS7 model. FW, ART, DCE, CM and MP planned and performed experiments. FW, ART and TCW provided invaluable discussion and guidance for the studies. JTH and RVF wrote the text as it appears here.

I addition to those listed above, I would also like to thank all of my colleagues for the opportunity to participate in collaborative studies. These positive interactions offered me valuable experience and the chance to learn and explore outside my projects in the Farese Lab. Those that have resulted in published manuscripts are listed below:

A collaboration with Dr. Charles A. Harris entitled “DGAT enzymes are required for triacylglycerol synthesis and lipid droplets in adipocytes.” by Charles A Harris, Joel T Haas, Ryan S Streeper, Scot J Stone, Manju Kumari, Kui Yang, Xianlin Han, Nicholas Brownell, Richard W. Gross, Rudolf Zechner, and Robert V. Farese Jr. published in *The Journal of Lipid Research* 2011 April;52(4):657-67.

A collaboration with Dr. Sudha Biddinger at Childrens’ Hospital of Boston entitled “Hepatic insulin signaling is required for obesity-dependent expression of SREBP-1c but not

for feeding-dependent expression." by Joel T Haas, Ji Miao, Dipanjan Chanda, Yanning Wang, Enpeng Zhao, Mary E. Haas, Matthew D. Hirschey, B. Vaitheesvaran, Robert V. Farese, Jr., Irwin J. Kurland, Mark Graham, Rosanne Cooke, Fabienne Foufelle, and Sudha B. Biddinger published in *Cell Metabolism*, 2012 June 6; 15(6):873-884.

A collaboration with Dr. Ho Yi Mak at Stowers Institute for Biomedical Research entitled "The FATP1-DGAT2 complex facilitates lipid droplet expansion at the ER-Lipid droplet interface." by Ningyi Xu, Shaobing O. Zhang, Ronald A. Cole, Sean A. McKinney, Fengli Guo, Joel T. Haas, Sudheer Bobba, Robert V. Farese, Jr., and Ho Yi Mak published in *the Journal of Cell Biology*, 2012 September 3; 198(5): 895-911.

A collaboration with Dr. Tobias Walther at Yale University entitled "Triacylglycerol synthesis enzymes mediate lipid droplet growth by relocalizing from the ER to lipid droplets." by Florian Wilfling, Huajin Wang, Joel T. Haas, Natalie Krahmer, Travis J. Gould, Aki Uchida, Ji-Xin Cheng, Morven Graham, Romain Christiano, Florian Fröhlich, Xinran Liu, Kimberly K. Buhman, Rosalind A. Coleman, Joerg Bewersdorf, Robert V. Farese, Jr., and Tobias C. Walther, published in *Developmental Cell*, 2013 February 25; 24(4): 384-399.

A collaboration with Dr. Melanie Ott at The Gladstone Institutes/University of California-San Francisco entitled "Diacylglycerol acyltransferase-1 localizes hepatitis C virus NS5A protein to lipid droplets and enhances NS5A interaction with the viral capsid core." by Gregory Camus, Eva Herker, Ankit A. Modi, Joel T. Haas, Holly R. Ramage, Robert V. Farese Jr., and Melanie Ott, published in *the Journal of Biological Chemistry*, 2013 April 5; 288: 9915-9923.

Personal Acknowledgements

There is a long list of individuals to whom I am indebted for advice, reagents, support, mentorship and friendship. They helped to make the last five years enjoyable and fulfilling and generally made all of the suffering worth it.

None of the work presented here would have been possible without, my mentor Bob Farese. I owe Bob my eternal gratitude for providing a great environment and good people with whom to share the bench. From taking me out for bike rides to sharing insights about balancing family and a career in science, he offered a truly holistic mentoring experience. He was incredibly supportive through the ups and downs of research science and gave me the freedom to explore and experiment. It has been an incredibly valuable experience.

I would also like to thank Tobias Walther who provided critical of cell biology experience and a lot of frank advice. He was a constant observer of the elephant in the room and really helped me to focus on things that matter. Despite the fact that he was either halfway across the world or all the way across the country, he was indispensible to the success of the studies presented here.

The other members of my committee, Drs. Peter Walter and Keith Yamamoto, were extremely supportive and pushed me to try different things, get outside my comfort zone and really make the most of the outstanding environment at UCSF. Peter was a great advocate who helped me think differently about problems and strongly reinforced the importance of good presentations. Keith was a consistently positive but critical voice on my committee who really helped me frame my research in a broader context. I am also grateful for their support in helping to establish meaningful financial assistance for graduate student parents. I really aspire to be as thoughtful, critical and thorough as my four scientific advisors.

All the members of the Farese and Walther Labs have helped me along the way. During my rotation, Dr. Charlie Harris, took me under his wing and, like every trainee, had me do all the quantitative PCR that he did not want to do. He was a great friend and a valued colleague who had incredible insight into metabolic interrogation and was a great sounding board for crazy ideas (with many of his own). Thanks to Lauren Herl Martens and Erin Currie, the other graduate students, who could always take time to commiserate about a bad experiment, a great breakthrough, or a long weekend. Drs. Yi Guo and Kenneth Harrison, who were good friends and collaborators for all things DGAT and lipid droplets. On the Walther lab side, I am grateful to have met Natalie Krahmer, Florian Wilfling, Rachid Thiam, Nora Kory, Huajin Wang, Yuan Xue and Romain Christiano. Flo and Rachid were always great for scientific discussion, were extremely helpful collaborators and great friends. Thanks to Nora, Huajin, Flo and Romain for their hospitality when I visited Yale and introducing me to wings at the Archie Moore's.

I owe a debt of gratitude to my classmates, who are an outstanding and talented group of people who happen to be scientists. I was extremely apprehensive about leaving the network I had established in Boston, but they made the transition across the US a really enjoyable experience. It is such an honor to be included among them.

I want to thank my parents, Ted and Dianne Haas, for their steadfast support and eagerness to visit and take care of Louise. Thanks to my sisters, Heather McClellan and Rachel Lohman and their spouses for reminding me that there are important things outside of science and for all the gifts and smiles shared with Louise. It is an incredible asset to have such an encouraging family.

Last, but not least, I would like to thank my wife Delphine Eberlé and our daughter Louise. There have been exciting and great times and there have been depressing and difficult times the last five years. Through it all, it has been an immense comfort to have your emotional support, and your expert scientific opinion to beat me over the head when I was being foolish. I look forward to it for years to come.

Abstract

Every living organism is must balance constant energy requirements against variable nutrient availability. One mechanism that has evolved to serve this purpose is the storage of energy as triglycerides (TGs). However, the nature of these molecules poses a problem; how can cells store an extremely hydrophobic molecule, shielding it from the hydrophilic cell environment, while maintaining easy access to the energy substrate? The answer is the lipid droplet (LD), a unique and ubiquitous organelle consisting of a phospholipid monolayer that shields a neutral lipid core, composed mostly of TGs and sterol esters (SE) in variable ratios. LDs also have a dynamic protein coat that varies among cell types and among LDs in the same cell. In the work presented here, we focus on the enzymes that synthesize TG, the diacylglycerol acyltransferase (DGAT) enzymes. We previously showed that cells lacking DGAT1 and DGAT2 are unable to synthesize TG and also lack LDs.

In chapter 2, we attempted to elucidate the cellular signals that drive TG synthesis and found that there is significant regulation of DGAT activity during the transition between fasting and feeding. Interestingly, DGAT1 and DGAT2 appear to play opposite roles in this regulation; DGAT1 is more active in fasting than during refeeding, while DGAT2 is more active during refeeding. We also observed significant decreases in activity with phosphatase treatment and identified several phosphorylation sites on both human and murine DGAT1. We were unable to determine whether the phosphorylation was linked to the change in activity observed *in vivo.*

In chapter 3, we identified and characterized family with a novel mutation in the DGAT1 gene. We determined that the mutation induced incorrect splicing of the DGAT1 mRNA and led to the omission of exon 8 from the full length mRNA. Removing exon 8 excises 75 base pairs from the mRNA, leading to an in-frame deletion of 25 amino acids. This protein product was not detectable when expressed as cDNA and was insufficient to rescue TG synthesis in mouse embryonic fibroblasts lacking DGAT1 and DGAT2. These results indicate the mutated gene gives rise to an unstable protein that is likely misfolded and rapidly degraded.

Finally, in chapter 4, we sought to develop model systems in which LD formation could be rapidly induced from a null background. We used adipocytes lacking DGAT2 combined with chemical inhibition of DGAT1 to block LD formation throughout the differentiation process. We found LD formation was not affected by nocodazole, brefeldinA or cycloheximide treatment. Inhibitors of fatty acid synthesis were also insufficient to block LD formation. However, 2-bromopalmitate did block LD formation. In permeabilized cells, we found that short chain diacylglycerols induced a dramatic change in the size of LDs as compared to the usual 1,2-dioleoylglycerol. We believe this is due to the surface active properties of the diacylglycerols. Finally, we found that treating cells with Bodipy-C12, a fluorescent fatty acid analog induced spots that appeared to be nascent LDs. However, these spots were not blocked in cells lacking both DGATs, nor were the spots coated by the LD-specific proteins perilipin 2 or perilipin 3. When assessing the biochemical nature of these spots by TLC, we found they were incorporated into in glycerolipids, but we were unable to identify the lipid species present. Still, we can conclude that with endogenous lipid substrates TG synthesis and LD formation were always absolutely correlated. Of all the tested

conditions, we were only able to alter LD formation by addition of short-chain diacylglycerols. Thus, we believe LD formation is likely a biophysical process that may be modified by protein action, but is primarily driven by the physical properties of TG accumulation in the membrane bilayer.

These three chapters highlight the importance and complexity of TG synthesis at the cellular and organismal level. Here we have defined a framework for investigating the signals that control TG synthesis in vivo, a physiological context for when TG synthesis is important, and three cellular systems for understanding how triglycerides are packaged into lipid droplets.

Table of Contents

List of Tables

List of Figures

An Introduction to Neutral Lipid Synthesis and Lipid Droplet Formation

Lipid droplet formation and energy homeostasis

Every living organism requires constantly requires energy to survive. For most living things, sources of energy are not constantly available. These two facts require that organisms develop the ability to store energy to sustain it through periods with no available nutrient sources. In eukaryotes, cells do this by storing energy as highly reduced long chain fatty acids, which are then esterified to a glycerol backbone forming a triglyceride molecule. These triglycerides are then subsequently packaged into a unique organelle called the lipid droplet.

Lipid droplets (LDs) are unique because they are composed of a hydrophobic core surrounded by a phospholipid monolayer, rather than a membrane bilayer. The core is composed of a mixture of primarily triglycerides (TG) and sterol esters that varies in composition depending on the cell type. These cytosolic fat globules were originally thought to be an inert storage depot with no function in the cell. However, many recent studies have shown the dynamic nature of LDs with respect to their size and protein coat. Thus, we are beginning to understand the important role of LDs in cellular physiology.

Despite these advances, there are many questions related to the basic biology of LDs that remain unsolved. These include: How and where do LDs form? How do proteins target their surface? Do all LDs in the same cell have the same function? For my thesis, I chose to focus on the question of LD formation. In particular, I wanted to look at the processes that govern TG LD formation because of the relationship to energy balance and metabolic diseases.

In addition to the relevance to metabolic disease, LD formation presents an interesting biophysical problem for the cell. The enzymes that synthesize the neutral lipid core of LDs localize to the endoplasmic reticulum (ER). However, a "mature" LD exists in the cytosol and is delineated by a phospholipid monolayer (Tauchi-Sato et al., 2002). It remains unclear how a membrane bilayer gives rise to a monolayer, while still maintaining the integrity of the donor bilayer. Additionally, it is unknown what determines the localization of an LD formation site. The ubiquity of LDs across cell types and species suggests there may be a conserved mechanism that controls their formation.

A number of groups have taken a genetic approach to try to identify genes involved in LD homeostasis. Using yeast as a model organism (Fei et al., 2008; Szymanski et al., 2007), two groups screened the deletion collection and found ~ 100 genes that modify LD morphology, though only 3 hits overlap between the two studies. In higher organisms, there is much more diversity in the morphology of LDs than in yeast. Two such screens have been published using *Drosophila* cells (Beller et al., 2008; Guo et al., 2008). Guo, et al. identified 5 classes of LD phenotypes related to their size, number and clustering. Both studies found that the COP-I complex regulates lipid droplet size. Finally, Ashrafi, et al. identified ~300 genes in *Caenorhabditis elegans* that modify LD content and morphology as assessed by Nile red staining (Ashrafi et al., 2003). Among all these screens, no single hit genetic manipulation has been sufficient to completely block LD formation.

However, there are two known genetic mutants that completely lack lipid droplets. In yeast, a strain was engineered to lack the two TG synthesizing enzymes (Dga1p and Lro1p) as well as the two sterol ester synthesizing enzymes (Are1p and Are2p). This compound mutant, called the Δ4, lacks lipid droplets by virtue of its lack of neutral lipid synthesis

enzymes (Sandager et al., 2002). The mammalian corollary was generated by making the compound mutant of the two TG synthesizing enzymes (DGAT1 and DGAT2) in adipocytes (Harris et al., 2011). Thus, the only way currently known to completely abolish LD formation is by inactivating the enzymes that fill the core.

To establish a framework to interrogate LD formation, we decided to focus on the enzymes that synthesize TG in mammalian cells. Our work presented here addresses first the activation of TG synthesis in chapter 2, a physiological context for when TG synthesis is necessary in chapter 3 and the process of packaging TG into LDs in chapter 4.

Triglyceride Synthesis and Uptake

The first step of LD formation requires the synthesis and accumulation of TG in a membrane bilayer. The diacylglycerol:acyl-coA acyltransferase (DGAT) reaction is the final and only committed step of TG synthesis as the products of every preceding reaction can be shunted into other pathways, such as phospholipid synthesis. Indeed, we were the first group to show that knocking out the DGAT enzymes in mammalian cells completely ablates the cells' ability to form LDs (Harris et al., 2011).

In mammals there are two DGAT enzymes, DGAT1 and DGAT2, which together account for more than 95% of the TG synthesis capacity (Harris et al., 2011). These enzymes are structurally different, are from different protein families, and have different physiological function as indicated by their knockout phenotypes (**Figure 1.1A-C**). DGAT2-KO mice are not viable, dying within hours after birth due to a skin barrier defect (Stone et al., 2004). They are severely runted and have nearly 90% reduced total carcass TG content compared to wildtype (WT) littermates. Conversely, DGAT1-KO mice are viable and have many favorable metabolic characteristics, such as resistance to diet-inducted obesity (Smith et al., 2000), increased longevity (Streeper et al., 2012), and increased energy expenditure (Streeper et al., 2006). These findings catalyzed the development of chemical inhibitors of DGAT1, several of which are currently in clinical trials (Birch et al., 2010; Cao et al., 2012; Devita and Pinto, 2013; Yin et al., 2012).

One active area of research of the DGAT enzymes is understanding the contribution of each isoenzyme to net TG synthesis capacity of the cell and under which conditions one can substitute for the other. For example, it has been proposed that hepatic DGAT1, and not DGAT2, may orient TG toward the ER lumen, facilitating ApoB lipidation and VLDL

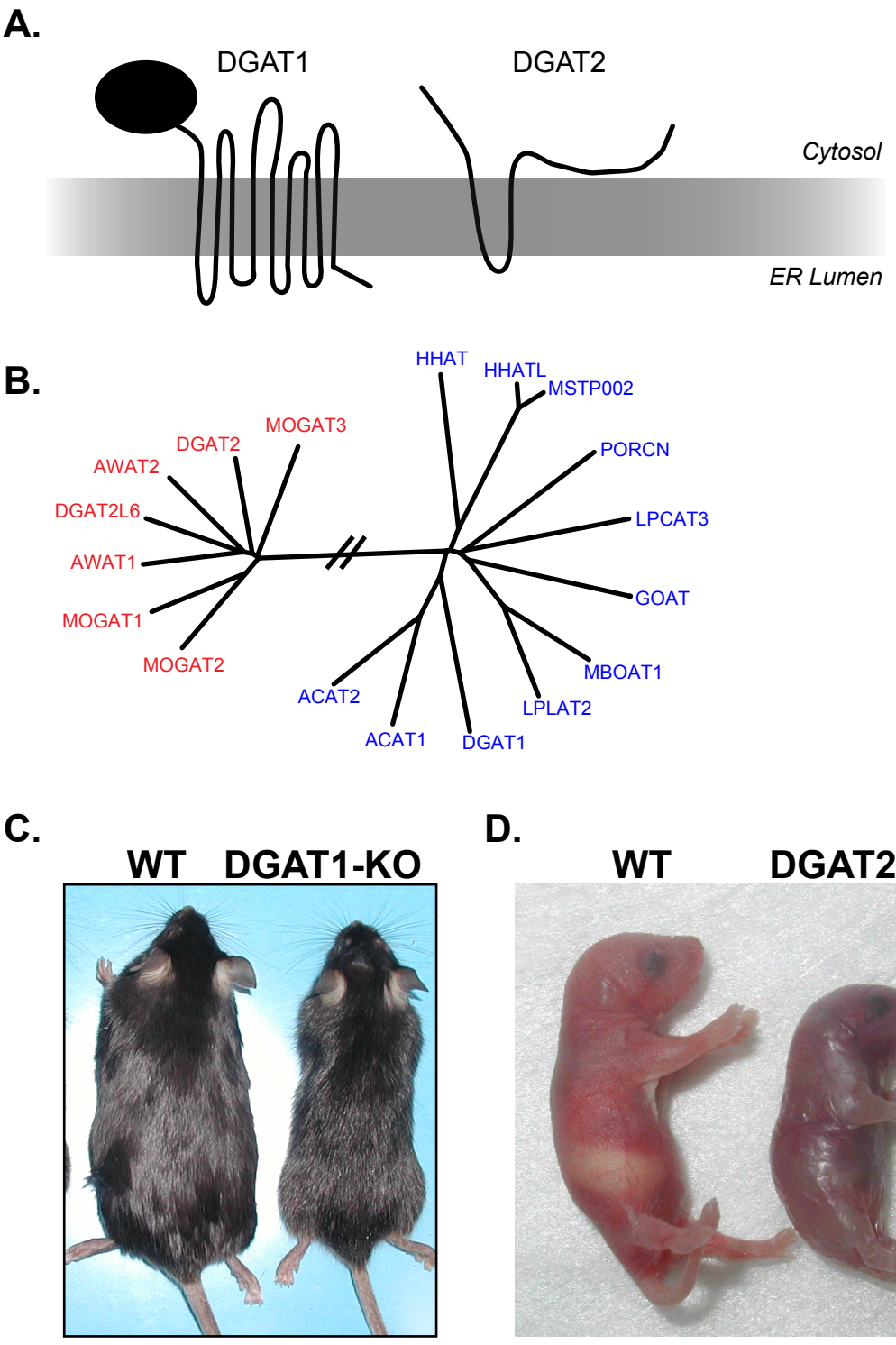

Figure 1.1: The Two DGAT enzymes are from different gene families and have different physiological functions. A. The predicted transmembrane topology of DGAT1 and DGAT2. **B.** A phylogenetic tree of DGAT1 (MBOAT) and DGAT2 (DAGAT) families from humans. **C.** Wildtype and DGAT1-KO mice fed a high fat diet. **D.** Wildtype and DGAT2-KO pups.

secretion (Owen and Zammit, 1997; Waterman et al., 2002). However, studies using antisense oligonucleotides against DGAT2 show a significant decrease in VLDL secretion relative to controls, indicating DGAT2 may play a more important role (Liu et al., 2008).

Studies on the role of DGATs during lipolysis have been similarly conflicting. In vitro lipolysis studies from our lab (C. Harris, unpublished observations) and others (Wurie et al., 2012) found increased free fatty acid (FFA) and glycerol release when blocking DGAT1. We thus suspected DGAT1 may be important for attenuating the rate of lipolysis to conserve FFA. However, recent work has uncovered that DGAT2 and other upstream enzymes are localized to the lipid droplet surface (Kuerschner et al., 2008; Stone et al., 2009; Wilfling et al., 2013; Xu et al., 2012). Further, the major triglyceride lipase (ATGL) apparently generates 1,3-diacylglycerols, a preferred substrate for DGAT2, whereas DGAT1 prefers 1,2-diacylglycerols. These results suggest that DGAT2 is in the right location and uses the correct substrate to be the major lipolysis re-esterification enzyme. Thus, it remains unclear which enzyme dominates during lipolysis or whether one enzyme can compensate for the other.

In chapter 2, we established a fasting and feeding paradigm to investigate the activity of the different DGAT enzymes in conditions favoring lipolysis or de novo TG synthesis. We seek to determine the relative activity of DGAT1 and DGAT2 in the white adipose tissue under these nutritional states and determine how the activity is controlled. We and others have proposed DGAT1 may be regulated by phosphorylation (Haagsman et al., 1981; Lau and Rodriguez, 1996). Together with the coordinate, phosphorylation-dependent control of the lipases through PKA, it seems plausible that DGAT1 or DGAT2 could be regulated by phosphorylation during lipolysis.

The phenotype of the DGAT1-KO mouse (Chen et al., 2002; Smith et al., 2000; Streeper et al., 2012) generated interest into whether DGAT1 inhibitors could be used to treat obesity and associated diseases. Inhibitor studies using rodent subjects generally reproduce the knockout phenotype (Birch et al., 2009; Cao et al., 2011), however their efficacy in humans and other higher mammals is completely untested. Among the strongest findings in the DGAT1-KO mouse are the elevated levels of GLP-1 and PYY (Lin et al., 2013; Okawa et al., 2009), gut peptide hormones that enhance glucose-stimulated insulin secretion and suppress appetite, respectively. Interestingly, over-expression of DGAT1 specifically in the small intestine of the DGAT1-KO mouse was recently shown to reverse many effects of the global knockout (Lee et al., 2010), suggesting an important role for DGAT1 in normal function of the intestine.

In chapter 3, we characterized a new mutation in *DGAT1* in a human cohort. Based on available information, we hypothesized it should be a loss of function mutation. These studies are particularly relevant due to the interest in DGAT1 inhibition as a therapy for obesity and associated cardiovascular diseases.

Formation of a Triglyceride Lipid Droplet

Two key questions surrounding LD formation are: what defines an LD formation site, and what determines the size of nascent LDs. To define a formation site, we must first consider the nature of the molecules involved and possibilities that could give rise to the cytosolic LD delineated by a monolayer. We feel there are essentially two possibilities; (1) as TG accumulates in the membrane bilayer, it can freely diffuse until the local concentration increases and drives the spontaneous formation of an LD, and (2) TG and other neutral lipids are sequestered by a protein or complex that facilitates LD formation in a specialized subdomain.

Current literature overwhelmingly favors the second possibility and several candidates have emerged. For example, PLIN3 has been shown to bind phospholipids directly (Bulankina et al., 2009) and forms punctate structures in adipocytes within minutes of fatty acid loading (Wolins et al., 2005). Several groups have found that knockdown of PLIN3 reduces, but does not completely abolish, LDs (Bulankina et al., 2009; Nose et al., 2013). Still, yeast and many lower eukaryotes do not have identifiable homologs to PAT proteins, yet still have lipid droplets. Thus, it is unlikely that PLIN3 and PLIN4 are absolutely required for LD formation.

Fat storage-inducing transmembrane protein 2 (FIT2) is another appealing candidate that is an evolutionarily conserved protein that is widely expressed in mammalian cell types. Altering expression levels of FIT2 dramatically affects the quantity of LDs in a cell without altering TG synthesis and only moderately raising overall TG levels. Thus, FIT2 appears to affect TG partitioning between the ER and LDs (Kadereit et al., 2008). Interestingly, FIT2 binds TG specifically and the relative ability of mutants to bind TG is positively correlated

with LD size(Gross et al., 2011). While these studies are relatively recent, FIT2 may likely affect LD formation directly, though this has not yet been addressed experimentally.

Lastly, seipin (BSCL2) and lipin1 (LPIN1) have been implicated as mediators of LD formation. Interestingly, loss of function mutations of these proteins in mammals give rise to congenital lipodystrophy, with malformed adipose tissue and severe hepatic steatosis (Cui et al., 2011; Magre et al., 2001; Reue et al., 2000). The yeast homolog of seipin (Fld1p) was found in two independent yeast screens to give a fewer LD phenotype (Fei et al., 2008; Szymanski et al., 2007). Similarly, deletion of the yeast homolog of lipin (Pah1p) gives rise to fewer lipid droplets with a similar amount of total neutral lipids, though TG is significantly reduced (Adeyo et al., 2011). This is likely due to lipin's function as a phosphatidic acid (PA) phosphatase, converting PA to DAG (Han et al., 2006). Conversely, the precise molecular function of seipin remains unknown, though it may regulate the surface composition LDs giving rise to conditions favoring LD fusion (Fei et al., 2011). From these data, seipin and lipin have a clear role in maintaining a normal LD morphology in yeast and have important functions in the adipose tissue of higher organisms. More focused studies are needed to address whether these effects are related to LD formation specifically or other aspects of LD biology.

There is essentially no experimental literature addressing TG LD formation from a biophysical perspective. However, there are some interesting theoretical papers (Khandelia et al., 2010; Ohsaki et al., 2009) as well as abundant research on the properties of water in oil in water (W/O/W) emulsions (Hayward et al., 2006; Teixeira et al., 2000) that the properties of the membranes and lipids themselves may play a previously underappreciated role in LD

formation. Aside from the membrane lipids, it is also important to consider where the TG itself is synthesized.

We are just beginning to understand the differences in subcellular localization between DGAT1 and DGAT2. The first evidence of differing ER domains comes from plants, where over-expression of DGAT1 and DGAT2 revealed that the two enzymes localize to ER subdomains that exclude each other (Shockey et al., 2006). This appears to hold true in mammals as well. DGAT2 localizes to the endoplasmic reticulum and lipid droplets (Stone et al., 2009) (**Figure 1.2A**). Interestingly, LD targeting is greatly enhanced upon fatty acid loading (Kuerschner et al., 2008; Stone et al., 2009). Sequence analysis of DGAT2 shows a weak mitochondrial targeting sequence that is sufficient to target a fluorescent protein to mitochondria (Stone et al., 2009).

Conversely, DGAT1 appears to be confined to the ER and no similar LD-targeting has been observed (Stone et al., 2009). When co-expressed with the pan-ER marker KDEL, DGAT1 overlaps nearly perfectly (**Figure 1.2B**). It can be excluded from certain ER subdomains, as coexpression with a marker for ER-exit sites yields distinct localization (**Figure 1.2C**). Based on localization, we expect DGAT1-derived LD formation to occur at the ER, while DGAT2-derived LD formation could occur at either ER or mitochondrial membranes.

The major impediment to a clearer understanding is a clear definition of what LD formation means and the paucity of model systems which allow us to study it directly. In chapter 4, we confine LD formation to the first minutes after TG synthesis begins and saturates the membrane with TG. We will focus on constructing a mammalian model system

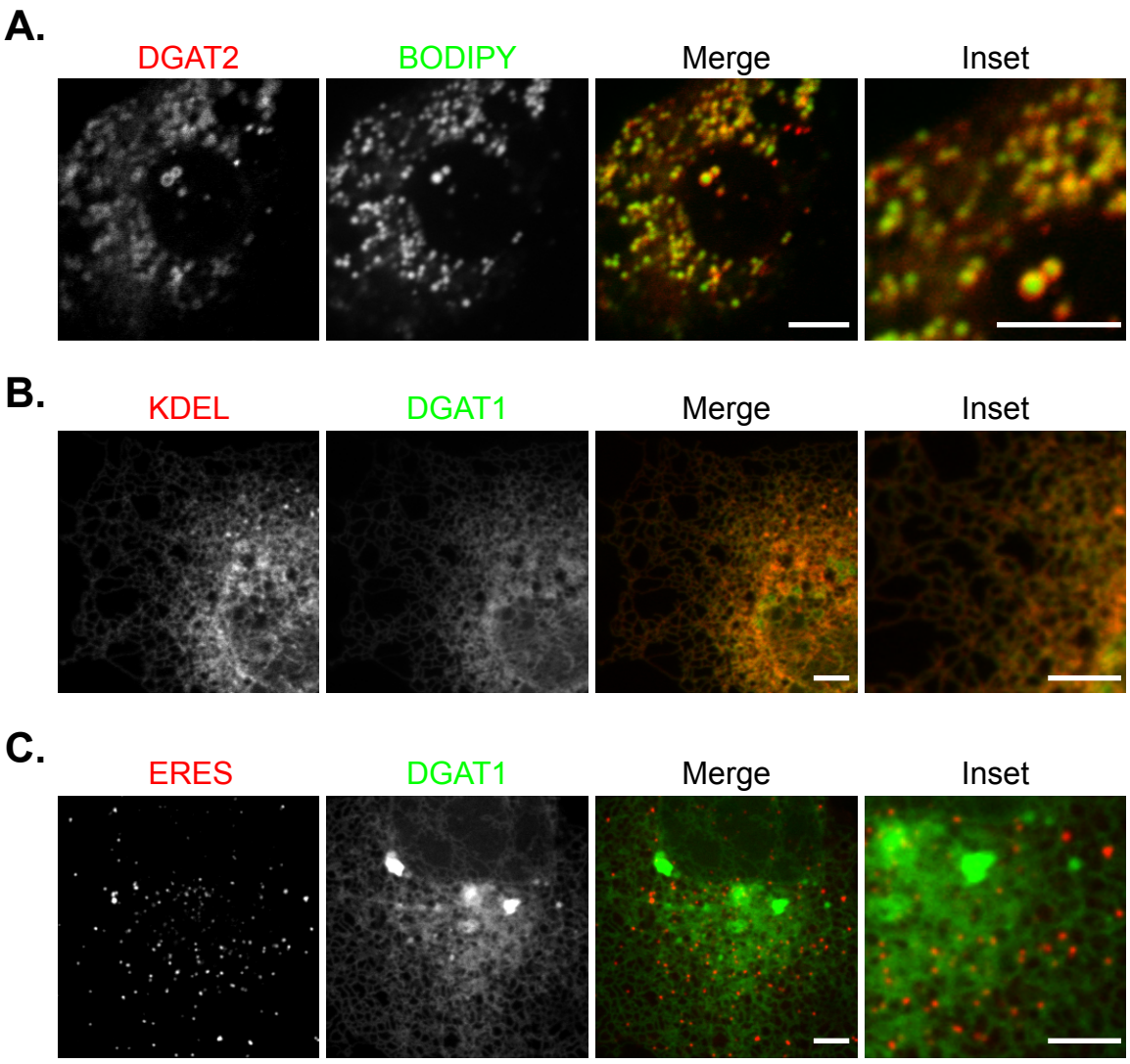

Figure 1.2: DGAT2 and DGAT1 localize to different subcellular domains. A. DGAT2 localizes to lipid droplets and endoplasmic reticulum. **B.** Overexpressed DGAT1 in COS7 cells colocalizes with a KDEL marker. **C.** DGAT1 is excluded from ER exit sites marked by Sec16B. Scale = 5 μm

in which LDs can be formed de novo, in the absence of existing droplets. We will explore whether various cellular pathways that have been implicated in LD formation (including PAT proteins (Wolins et al., 2005; Wolins et al., 2003), the secretory pathway (Soni et al., 2009) and lipodystrophy genes (Adeyo et al., 2011; Fei et al., 2008; Szymanski et al., 2007)) truly affect LD formation directly or exert influence on the steady-state balance between TG synthesis and breakdown.

Lipid droplets are important organelles that are central to lipid metabolism. Recent work has uncovered important processes that govern LD morphology, including local TG synthesis, availability of PC, and LD fusion proteins. Still, the components that govern LD formation remain unknown. Current work in the field is focused on finding the markers of LD formation sites and assessing the role of various LD associated proteins. We believe the next big advances in the field will come from a more focused approach on the biophysical behavior of the lipids making up LDs themselves.

References

Adeyo, O., Horn, P.J., Lee, S., Binns, D.D., Chandrahas, A., Chapman, K.D., and Goodman, J.M. (2011). The yeast lipin orthologue Pah1p is important for biogenesis of lipid droplets. J Cell Biol 192, 1043-1055.

Ashrafi, K., Chang, F.Y., Watts, J.L., Fraser, A.G., Kamath, R.S., Ahringer, J., and Ruvkun, G. (2003). Genome-wide RNAi analysis of Caenorhabditis elegans fat regulatory genes. Nature 421, 268-272.

Beller, M., Sztalryd, C., Southall, N., Bell, M., Jackle, H., Auld, D.S., and Oliver, B. (2008). COPI complex is a regulator of lipid homeostasis. PLoS Biol 6, e292.

Birch, A.M., Birtles, S., Buckett, L.K., Kemmitt, P.D., Smith, G.J., Smith, T.J., Turnbull, A.V., and Wang, S.J. (2009). Discovery of a potent, selective, and orally efficacious pyrimidinooxazinyl bicyclooctaneacetic acid diacylglycerol acyltransferase-1 inhibitor. J Med Chem 52, 1558-1568.

Birch, A.M., Buckett, L.K., and Turnbull, A.V. (2010). DGAT1 inhibitors as anti-obesity and anti-diabetic agents. Curr Opin Drug Discov Devel 13, 489-496.

Bulankina, A.V., Deggerich, A., Wenzel, D., Mutenda, K., Wittmann, J.G., Rudolph, M.G., Burger, K.N., and Honing, S. (2009). TIP47 functions in the biogenesis of lipid droplets. J Cell Biol 185, 641-655.

Cao, G., Konrad, R.J., Li, S.D., and Hammond, C. (2012). Glycerolipid acyltransferases in triglyceride metabolism and energy homeostasis-potential as drug targets. Endocr Metab Immune Disord Drug Targets 12, 197-206.

Cao, J., Zhou, Y., Peng, H., Huang, X., Stahler, S., Suri, V., Qadri, A., Gareski, T., Jones, J., Hahm, S., Perreault, M., McKew, J., Shi, M., Xu, X., Tobin, J.F., and Gimeno, R.E. (2011). Targeting Acyl-CoA:diacylglycerol acyltransferase 1 (DGAT1) with small molecule inhibitors for the treatment of metabolic diseases. J Biol Chem 286, 41838-41851.

Chen, H.C., Smith, S.J., Ladha, Z., Jensen, D.R., Ferreira, L.D., Pulawa, L.K., McGuire, J.G., Pitas, R.E., Eckel, R.H., and Farese, R.V., Jr. (2002). Increased insulin and leptin sensitivity in mice lacking acyl CoA:diacylglycerol acyltransferase 1. J Clin Invest 109, 1049-1055.

Cui, X., Wang, Y., Tang, Y., Liu, Y., Zhao, L., Deng, J., Xu, G., Peng, X., Ju, S., Liu, G., and Yang, H. (2011). Seipin ablation in mice results in severe generalized lipodystrophy. Hum Mol Genet 20, 3022-3030.

Devita, R.J., and Pinto, S. (2013). Current Status of the Research and Development of Diacylglycerol O-acyltransferase 1 (DGAT1) Inhibitors. J Med Chem.

Fei, W., Shui, G., Gaeta, B., Du, X., Kuerschner, L., Li, P., Brown, A.J., Wenk, M.R., Parton, R.G., and Yang, H. (2008). Fld1p, a functional homologue of human seipin, regulates the size of lipid droplets in yeast. J Cell Biol 180, 473-482.

Fei, W., Shui, G., Zhang, Y., Krahmer, N., Ferguson, C., Kapterian, T.S., Lin, R.C., Dawes, I.W., Brown, A.J., Li, P., Huang, X., Parton, R.G., Wenk, M.R., Walther, T.C., and Yang, H. (2011). A role for phosphatidic acid in the formation of "supersized" lipid droplets. PLoS Genet 7, e1002201.

Gross, D.A., Zhan, C., and Silver, D.L. (2011). Direct binding of triglyceride to fat storage-inducing transmembrane proteins 1 and 2 is important for lipid droplet formation. Proc Natl Acad Sci U S A 108, 19581-19586.

Guo, Y., Walther, T.C., Rao, M., Stuurman, N., Goshima, G., Terayama, K., Wong, J.S., Vale, R.D., Walter, P., and Farese, R.V. (2008). Functional genomic screen reveals genes involved in lipid-droplet formation and utilization. Nature 453, 657-661.

Haagsman, H.P., de Haas, C.G., Geelen, M.J., and van Golde, L.M. (1981). Regulation of triacylglycerol synthesis in the liver: a decrease in diacylglycerol acyltransferase activity after treatment of isolated rat hepatocytes with glucagon. Biochim Biophys Acta 664, 74-81.

Han, G.S., Wu, W.I., and Carman, G.M. (2006). The Saccharomyces cerevisiae Lipin homolog is a Mg2+-dependent phosphatidate phosphatase enzyme. J Biol Chem 281, 9210-9218.

Harris, C.A., Haas, J.T., Streeper, R.S., Stone, S.J., Kumari, M., Yang, K., Han, X., Brownell, N., Gross, R.W., Zechner, R., and Farese, R.V., Jr. (2011). DGAT enzymes are required for triacylglycerol synthesis and lipid droplets in adipocytes. J Lipid Res 52, 657-667.

Hayward, R.C., Utada, A.S., Dan, N., and Weitz, D.A. (2006). Dewetting instability during the formation of polymersomes from block-copolymer-stabilized double emulsions. Langmuir 22, 4457-4461.

Kadereit, B., Kumar, P., Wang, W.J., Miranda, D., Snapp, E.L., Severina, N., Torregroza, I., Evans, T., and Silver, D.L. (2008). Evolutionarily conserved gene family important for fat storage. Proc Natl Acad Sci U S A 105, 94-99.

Khandelia, H., Duelund, L., Pakkanen, K.I., and Ipsen, J.H. (2010). Triglyceride blisters in lipid bilayers: implications for lipid droplet biogenesis and the mobile lipid signal in cancer cell membranes. PLoS One 5, e12811.

Kuerschner, L., Moessinger, C., and Thiele, C. (2008). Imaging of lipid biosynthesis: how a neutral lipid enters lipid droplets. Traffic 9, 338-352.

Lau, T.E., and Rodriguez, M.A. (1996). A protein tyrosine kinase associated with the ATP-dependent inactivation of adipose diacylglycerol acyltransferase. Lipids 31, 277-283.

Lee, B., Fast, A.M., Zhu, J., Cheng, J.X., and Buhman, K.K. (2010). Intestine-specific expression of acyl CoA:diacylglycerol acyltransferase 1 reverses resistance to diet-induced hepatic steatosis and obesity in Dgat1-/- mice. J Lipid Res 51, 1770-1780.

Lin, H.V., Chen, D., Shen, Z., Zhu, L., Ouyang, X., Vongs, A., Kan, Y., Levorse, J.M., Kowalik, E.J., Jr., Szeto, D.M., Yao, X., Xiao, J., Chen, S., Liu, J., Garcia-Calvo, M., Shin, M.K., and Pinto, S. (2013). Diacylglycerol acyltransferase-1 (DGAT1) inhibition perturbs postprandial gut hormone release. PLoS One 8, e54480.

Liu, Y., Millar, J.S., Cromley, D.A., Graham, M., Crooke, R., Billheimer, J.T., and Rader, D.J. (2008). Knockdown of acyl-CoA:diacylglycerol acyltransferase 2 with antisense oligonucleotide reduces VLDL TG and ApoB secretion in mice. Biochim Biophys Acta 1781, 97-104.

Magre, J., Delepine, M., Khallouf, E., Gedde-Dahl, T., Jr., Van Maldergem, L., Sobel, E., Papp, J., Meier, M., Megarbane, A., Bachy, A., Verloes, A., d'Abronzo, F.H., Seemanova, E., Assan, R., Baudic, N., Bourut, C., Czernichow, P., Huet, F., Grigorescu, F., de Kerdanet, M., Lacombe, D., Labrune, P., Lanza, M., Loret, H., Matsuda, F., Navarro, J., Nivelon-Chevalier, A., Polak, M., Robert, J.J., Tric, P., Tubiana-Rufi, N., Vigouroux, C., Weissenbach, J., Savasta, S., Maassen, J.A., Trygstad, O., Bogalho, P., Freitas, P., Medina, J.L., Bonnicci, F., Joffe, B.I., Loyson, G., Panz, V.R., Raal, F.J., O'Rahilly, S., Stephenson, T., Kahn, C.R., Lathrop, M., and Capeau, J. (2001). Identification of the gene altered in Berardinelli-Seip congenital lipodystrophy on chromosome 11q13. Nat Genet 28, 365-370.

Nose, F., Yamaguchi, T., Kato, R., Aiuchi, T., Obama, T., Hara, S., Yamamoto, M., and Itabe, H. (2013). Crucial Role of Perilipin-3 (TIP47) in Formation of Lipid Droplets and PGE2 Production in HL-60-Derived Neutrophils. PLoS One 8, e71542.

Ohsaki, Y., Cheng, J., Suzuki, M., Shinohara, Y., Fujita, A., and Fujimoto, T. (2009). Biogenesis of cytoplasmic lipid droplets: from the lipid ester globule in the membrane to the visible structure. Biochim Biophys Acta 1791, 399-407.

Okawa, M., Fujii, K., Ohbuchi, K., Okumoto, M., Aragane, K., Sato, H., Tamai, Y., Seo, T., Itoh, Y., and Yoshimoto, R. (2009). Role of MGAT2 and DGAT1 in the release of gut peptides after triglyceride ingestion. Biochem Biophys Res Commun 390, 377-381.

Owen, M., and Zammit, V.A. (1997). Evidence for overt and latent forms of DGAT in rat liver microsomes. Implications for the pathways of triacylglycerol incorporation into VLDL. Biochem Soc Trans 25, 21S.

Reue, K., Xu, P., Wang, X.P., and Slavin, B.G. (2000). Adipose tissue deficiency, glucose intolerance, and increased atherosclerosis result from mutation in the mouse fatty liver dystrophy (fld) gene. J Lipid Res 41, 1067-1076.

Sandager, L., Gustavsson, M.H., Stahl, U., Dahlqvist, A., Wiberg, E., Banas, A., Lenman, M., Ronne, H., and Stymne, S. (2002). Storage lipid synthesis is non-essential in yeast. J Biol Chem 277, 6478-6482.

Shockey, J.M., Gidda, S.K., Chapital, D.C., Kuan, J.C., Dhanoa, P.K., Bland, J.M., Rothstein, S.J., Mullen, R.T., and Dyer, J.M. (2006). Tung tree DGAT1 and DGAT2 have nonredundant functions in triacylglycerol biosynthesis and are localized to different subdomains of the endoplasmic reticulum. Plant Cell 18, 2294-2313.

Smith, S.J., Cases, S., Jensen, D.R., Chen, H.C., Sande, E., Tow, B., Sanan, D.A., Raber, J., Eckel, R.H., and Farese, R.V., Jr. (2000). Obesity resistance and multiple mechanisms of triglyceride synthesis in mice lacking Dgat. Nat Genet 25, 87-90.

Soni, K.G., Mardones, G.A., Sougrat, R., Smirnova, E., Jackson, C.L., and Bonifacino, J.S. (2009). Coatomer-dependent protein delivery to lipid droplets. J Cell Sci 122, 1834-1841.

Stone, S.J., Levin, M.C., Zhou, P., Han, J., Walther, T.C., and Farese, R.V., Jr. (2009). The endoplasmic reticulum enzyme DGAT2 is found in mitochondria-associated membranes and has a mitochondrial targeting signal that promotes its association with mitochondria. J Biol Chem 284, 5352-5361.

Stone, S.J., Myers, H.M., Watkins, S.M., Brown, B.E., Feingold, K.R., Elias, P.M., and Farese, R.V., Jr. (2004). Lipopenia and skin barrier abnormalities in DGAT2-deficient mice. J Biol Chem 279, 11767-11776.

Streeper, R.S., Grueter, C.A., Salomonis, N., Cases, S., Levin, M.C., Koliwad, S.K., Zhou, P., Hirschey, M.D., Verdin, E., and Farese, R.V., Jr. (2012). Deficiency of the lipid synthesis enzyme, DGAT1, extends longevity in mice. Aging (Albany NY) 4, 13-27.

Streeper, R.S., Koliwad, S.K., Villanueva, C.J., and Farese, R.V., Jr. (2006). Effects of DGAT1 deficiency on energy and glucose metabolism are independent of adiponectin. Am J Physiol Endocrinol Metab 291, E388-394.

Szymanski, K.M., Binns, D., Bartz, R., Grishin, N.V., Li, W.P., Agarwal, A.K., Garg, A., Anderson, R.G., and Goodman, J.M. (2007). The lipodystrophy protein seipin is found at endoplasmic reticulum lipid droplet junctions and is important for droplet morphology. Proc Natl Acad Sci U S A 104, 20890-20895.

Tauchi-Sato, K., Ozeki, S., Houjou, T., Taguchi, R., and Fujimoto, T. (2002). The surface of lipid droplets is a phospholipid monolayer with a unique Fatty Acid composition. J Biol Chem 277, 44507-44512.

Teixeira, H., Dubernet, C., Rosilio, V., Benita, S., Lepault, J., Erk, I., and Couvreur, P. (2000). New bicompartmental structures are observed when stearylamine is mixed with triglyceride emulsions. Pharm Res 17, 1329-1332.

Waterman, I.J., Price, N.T., and Zammit, V.A. (2002). Distinct ontogenic patterns of overt and latent DGAT activities of rat liver microsomes. J Lipid Res 43, 1555-1562.

Wilfling, F., Wang, H., Haas, J.T., Krahmer, N., Gould, T.J., Uchida, A., Cheng, J.X., Graham, M., Christiano, R., Frohlich, F., Liu, X., Buhman, K.K., Coleman, R.A., Bewersdorf, J., Farese, R.V., Jr., and Walther, T.C. (2013). Triacylglycerol synthesis enzymes mediate lipid droplet growth by relocalizing from the ER to lipid droplets. Dev Cell 24, 384-399.

Wolins, N.E., Quaynor, B.K., Skinner, J.R., Schoenfish, M.J., Tzekov, A., and Bickel, P.E. (2005). S3-12, Adipophilin, and TIP47 package lipid in adipocytes. J Biol Chem 280, 19146-19155.

Wolins, N.E., Skinner, J.R., Schoenfish, M.J., Tzekov, A., Bensch, K.G., and Bickel, P.E. (2003). Adipocyte protein S3-12 coats nascent lipid droplets. J Biol Chem 278, 37713-37721.

Wurie, H.R., Buckett, L., and Zammit, V.A. (2012). Diacylglycerol acyltransferase 2 acts upstream of diacylglycerol acyltransferase 1 and utilizes nascent diglycerides and de novo synthesized fatty acids in HepG2 cells. FEBS J 279, 3033-3047.

Xu, N., Zhang, S.O., Cole, R.A., McKinney, S.A., Guo, F., Haas, J.T., Bobba, S., Farese, R.V., Jr., and Mak, H.Y. (2012). The FATP1-DGAT2 complex facilitates lipid droplet expansion at the ER-lipid droplet interface. J Cell Biol 198, 895-911.

Yin, W., Carballo-Jane, E., McLaren, D.G., Mendoza, V.H., Gagen, K., Geoghagen, N.S., McNamara, L.A., Gorski, J.N., Eiermann, G.J., Petrov, A., Wolff, M., Tong, X., Wilsie, L.C., Akiyama, T.E., Chen, J., Thankappan, A., Xue, J., Ping, X., Andrews, G., Wickham, L.A., Gai, C.L., Trinh, T., Kulick, A.A., Donnelly, M.J., Voronin, G.O., Rosa, R., Cumiskey, A.M., Bekkari, K., Mitnaul, L.J., Puig, O., Chen, F., Raubertas, R., Wong, P.H., Hansen, B.C., Koblan, K.S., Roddy, T.P., Hubbard, B.K., and Strack, A.M. (2012). Plasma lipid profiling across species for the identification of optimal animal models of human dyslipidemia. J Lipid Res 53, 51-65.

Post-translational regulation of DGAT1 activity in mammals

Abstract

Triacylglycerols (TG) are a critical cellular energy source whose synthesis is regulated at several levels. The enzymes that synthesize TGs, the diacylglycerol acyltransferases (DGATs) catalyze the final and only committed step of TG synthesis. Despite many recent advances into understanding the molecular functions of the two DGATs (DGAT1 and DGAT2), little is known about what regulates their activity. We first measured the activity of DGAT1 and DGAT2 under fasted and fed conditions in the white (WAT) and brown (BAT) adipose tissue. In WAT, DGAT1 activity during fasting was increased 2-fold over the refed state, while DGAT2 was more active in the refed state. In BAT, DGAT1 activity was not different between the two nutritional states, while DGAT2 followed the same pattern as in WAT. Through ^{32}P incorporation and mass spectrometry, we found that both human and murine DGAT1 are multiply phosphorylated. We subsequently mutated these phosphorylation sites and found no effect on DGAT1 activity. However, phosphatase treatment of microsomes dramatically reduced DGAT1 activity in our experiments. Taken together, these findings indicate DGAT1 is regulated in a tissue and nutrient state specific manner and suggest a phosphorylation-dependent mechanism may be responsible. However, the identity of the phosphorylation site and the precise stimulus remains unknown.

Introduction

Precise control of triglyceride synthesis is critical for cells to maximize the storage of available nutrients. The substrates for TG synthesis, diacylglycerols and fatty acyl-coAs, can be alternatively used for TG or phospholipid (PL) synthesis. These metabolic fates are controlled in a nutritional-state dependent way, i.e. lipogenic vs. lipolytic states. Another layer of complexity arises from the needs of different tissues under these different nutritional states. Thus, there exists a need for rapid, careful control of the TG synthesis and storage.

In the context of animal physiology, known lipid metabolic processes (e.g. lipolysis) are under hormonal control and mediated by phosphorylation-dependent events. Indeed, there is considerable evidence that DGAT1 may be regulated post-transcriptionally, likely by direct phosphorylation. Several studies lead by Haagsman indicate microsomal DGAT activity from hepatocytes treated with glucagon (Haagsman et al., 1981) or fatty acids (Haagsman and Van Golde, 1981) is decreased or increased, respectively. This group further determined that a cytosolic factor can inactivate DGAT activity under conditions favoring phosphorylation, and that the inactivation is reversible. Interestingly, re-activation can be blocked by addition of the serine-threonine phosphatase inhibitor NaF, boiling the cytosolic fraction or trypsin digestion of the cytosol. Another study led by Lau found similar results using microsomes purified from rat epididymal fat pads (Lau and Rodriguez, 1996). However, these results suggested tyrosine phosphorylation was the major regulator of activity. Taken together, these early studies provide strong evidence for the phosphoregulation of in vitro DGAT activity.

Subsequent to cloning, several lines of evidence suggest that DGAT1, and not DGAT2, is subject to post-transcriptional regulation. First, in vitro activity is overwhelmingly biased for DGAT1 (Cases et al., 2001) indicating that previous in vitro work likely reflects DGAT1 activity (Haagsman et al., 1981; Haagsman and Van Golde, 1981; Lau and Rodriguez, 1996). Studies in 3T3L1 adipocytes demonstrated that over-expression of human DGAT1 raised mRNA levels more than 20-fold, while protein levels only increased roughly 4-fold (Yu et al., 2002). This group also measured the protein half-life of DGAT1 and found it to be roughly 18 hrs. This likely excludes the possibility of protein turnover as a major regulator of microsomal DGAT activity. Interestingly, when a putative tyrosine phosphorylation Y316 site was mutated to alanine, no difference in DGAT activity or TG synthesis in cells was measured.

To attempt to reconcile these findings in light of our current knowledge of the DGAT enzymes, we sought to identify the physiological contexts in which phosphorylation could be important for regulating DGAT1 activity. We concurrently mapped more than 6 phosphorylation sites in both the mouse and human proteins through over-expression studies and demonstrated a decrease in ^{32}P-orthophosphate incorporation in alanine mutants of these phosphorylation sites. Unfortunately, we found no differences in *in vitro* activity of the various phospho-mutants of DGAT1.

Materials and Methods

Animal Studies

Dgat1-KO and wildtype (WT) littermate controls were housed in a 12hr/12hr light/dark cycle and given *ad libitum* access to standard chow diet and water. For fasting and refeeding studies, 4-5 month old WT and Dgat1-KO mice were fasted for 24 hrs (*fasted*) or fasted for 24 hr and refed 4 hrs (*refed*). Mice were sacrificed by cervical dislocation, and epididymal (WAT) and intra-scapular (BAT) fat pads were removed and immediately frozen. All animal procedures were carried out under an approved protocol reviewed by the UCSF Institutional Animal Care and Use Committee.

In vitro DGAT assay

In vitro DGAT activity assays were performed as described previously (Cases et al., 1998). For WAT and BAT assays, 5-10 μg and 50 μg of microsomal protein was used, respectively. For assays on cell extracts, up to 50 μg of microsomal protein or up to 100 μg of total cellular protein was used.

^{32}P Phosphate incorporation

HEK293T cells were transfected with FLAG-mDGAT1 using Lipofectamine 2000 (Invitrogen, Carlsbad, CA) according to manufacturer's instructions. Twenty four hours post-transfection, cells were switched to phosphate-free medium and labeled with 250 μCi of ^{32}P orthophosphate for 4 hours.

FLAG-DGAT1 immunoprecipitation

Cells were immediately lysed in RIPA buffer containing 20 mM orthovanadate, 1 mM NaF, 1 mM β-glycerophosphate and 1 μM okadaic acid. FLAG IP was performed using magnetic FLAG (M2, Sigma Aldrich, St. Louis, MO.) beads and protein was eluted using FLAG peptide.

Site Directed Mutagenesis

Site directed mutagenesis of FLAG-DGAT1 constructs was performed using the Lightning Site-Directed Mutagenesis Kit (Stratagene) according to manufacturer's instructions. Primers were designed using publicly available software at https://www.genomics.agilent.com/

Phosphorylation site mapping

FLAG-DGAT1 constructs were transfected into HEK293T cells or McArdle RH7777 cells in 10 cm dishes. Cells were lysed and FLAG-DGAT1 was immunoprecipitated and separated by SDS-PAGE. Bands corresponding to FLAG-DGAT1 were excised and subjected to in-gel digestion by trypsin. Alternatively, IP eluate was digested in solution with trypsin, GluN or LysC.

Bioinformatics

Protein sequences of DGAT1 for 39 higher eukaryotes were retrieved by querying the UniProt(2013) database. We selected sequences representing the full length protein for each species available. These sequences were subsequently aligned using Clustal Omega (Goujon et al., 2010). The human DGAT1 protein sequence (O75907) was processed using TMHMM (Goujon et al., 2010; Krogh et al., 2001) and NetPhos 2.0 (Blom et al., 1999).

Phosphatase Treatment

For phosphatase treatment, whole cell lysates or microsomal protein was incubated with either buffer or buffer containing 1 U calf intestinal phosphatase (CIP, New England Biolabs, Ipswich, MA) per μg protein. Samples were incubated at 37 °C for 30 mins and immediately used for DGAT activity assays.

Results

DGAT1 activity is regulated under fasted and refed conditions

Lipolysis is a critical metabolic process mediated by stimulation of the beta-adrenergic receptors and subsequent intracellular accumulation of cAMP. This triggers a well studied phosphorylation cascade mediated by cyclic AMP dependent kinase, Protein Kinase A (PKA). It has been proposed that DGAT activity may also be regulated in this state to attenuate the generation of free fatty acids during lipolysis and act as a conservation mechanism for TG. We thus sought to determine the adipose DGAT activity under fasted and refed conditions and the relative contributions of DGAT1 and DGAT2 to this total activity. In vitro activity assays were performed on microsomal protein from WAT and BAT of fasted or refed mice as described in the methods. By measuring WT samples under conditions specific for DGAT1 and measuring total DGAT activity in *Dgat1*-KO samples, we were able to dissect the contribution of each enzyme and compare their relative activity in the different metabolic states.

In WAT, we found that DGAT1 was active during fasting and activity reduced roughly 50% in the refed state. DGAT2 showed the opposite and was more active in the refed state. (**Figure 2.1A**) Interestingly, the BAT showed that DGAT1 was more active in the refed state and reduced during fasting, while DGAT2 showed no difference between refed or fasted state. (**Figure 2.1B**) These data indicate that DGAT1 activity is regulated in conjunction with physiological state and in a tissue dependent manner.

DGAT1 activity is decreased by dephosphorylation

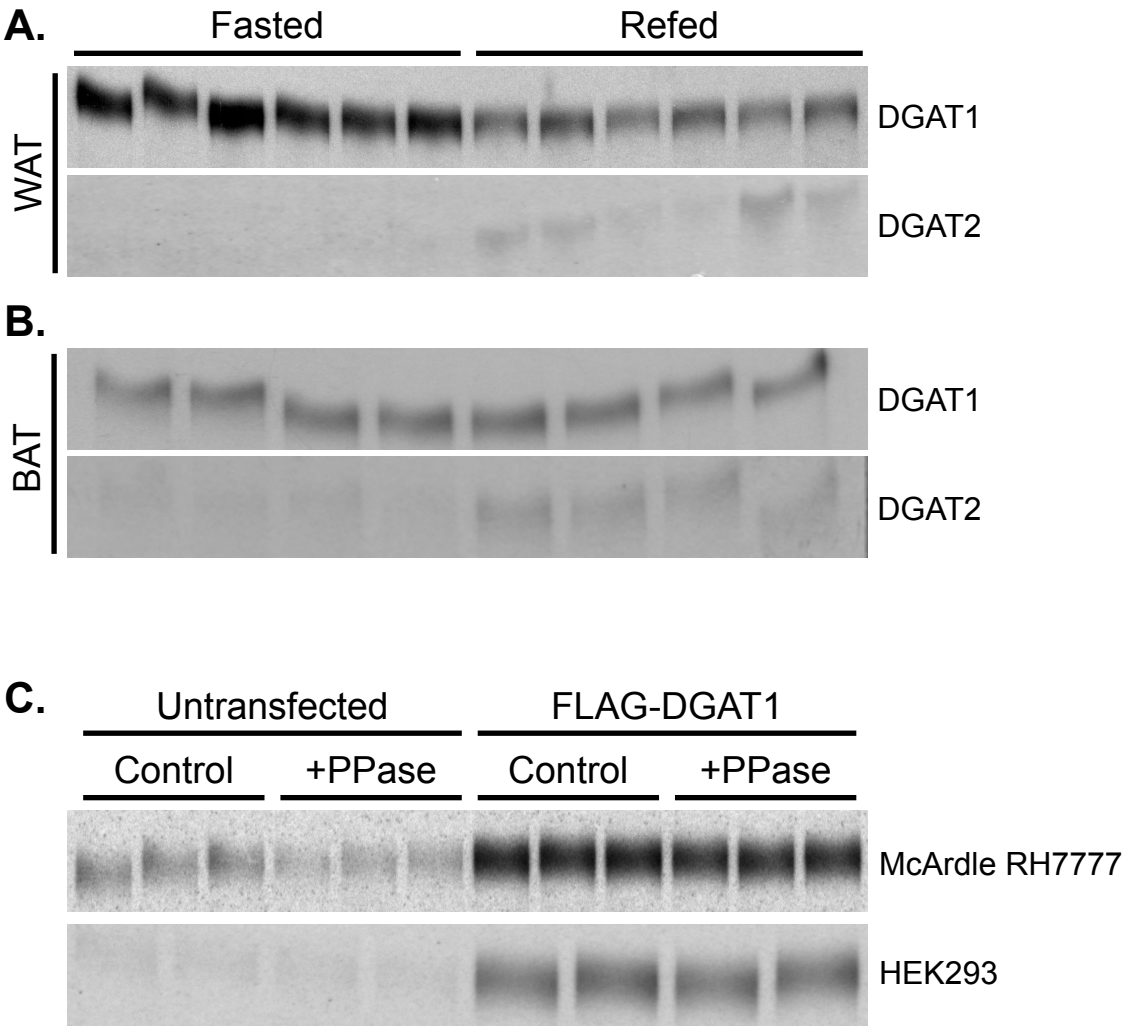

Figure 2.1. DGAT Activity is regulated by nutritional status and may reflect phospho-regulation. A. DGAT activity of microsomes isolated epididymal fat pads. **B.** DGAT activity of microsomes isolated from intra-scapular brown adipose tissue. **C.** DGAT activity of whole cell lysates from different cell types to measure the effect of phosphatase treatment.

To determine whether the changes in activity seen with nutritional status could be explained by changes in phosphorylation, we treated microsomes in vitro with phosphatase and measured the activity (**Figure 2.1C**). When using McArdle RH7777 cells were used, phosphatase treatment decreased in vitro DGAT activity roughly 50%. Transfection with FLAG-mDGAT1 blunted the effect of phosphatase treatment. Interestingly, when using HEK293 cells, there was no effect of phosphatase treatment in transfected or untransfected. This is in opposition to previously performed experiments in our lab (Ping Zhou, Scot Stone, unpublished observations) and published studies that show decreased in vitro activity in conditions favoring phosphorylation (Haagsman et al., 1982).

DGAT1 has many predicted phosphorylation sites

To begin dissecting the possible phosphorylation sites on DGAT1, we took a bioinformatic approach to map predicted sites and their relative conservation across 39 higher eukaryotes. (**Figure 2.2A**) Using the human sequence, we generated a model of the predicted topology of DGAT1. (**Figure 2.2B**) This was based on the topology of ACAT1, which shares roughly 20% sequence identity and has been carefully mapped experimentally (Guo et al., 2005), and the bioinformatic analysis performed as described in the methods.

The current working model of ACAT1 topology suggests 9 transmembrane domains, with a cytosolic N-terminus and luminal C-terminus (Guo et al., 2005). For DGAT1, experimental evidence suggests it also has this orientation, though with only 3 transmembrane domains(McFie et al., 2010). It is important to note that this differs from the bioinformatic prediction shown in Figure 2.2B. A similar discrepancy exists between studies that map ACAT1 and seems to arise from the experimental protocol, with epitope tag

A.

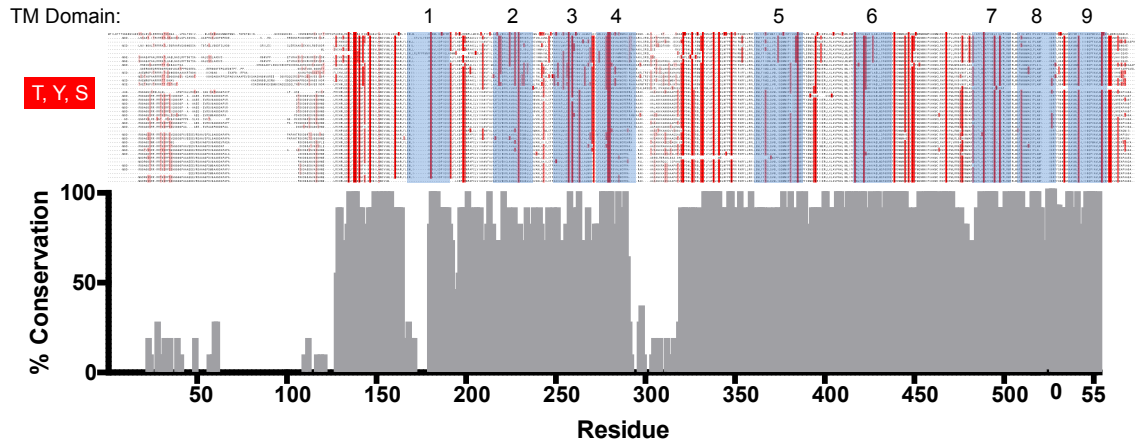

B.

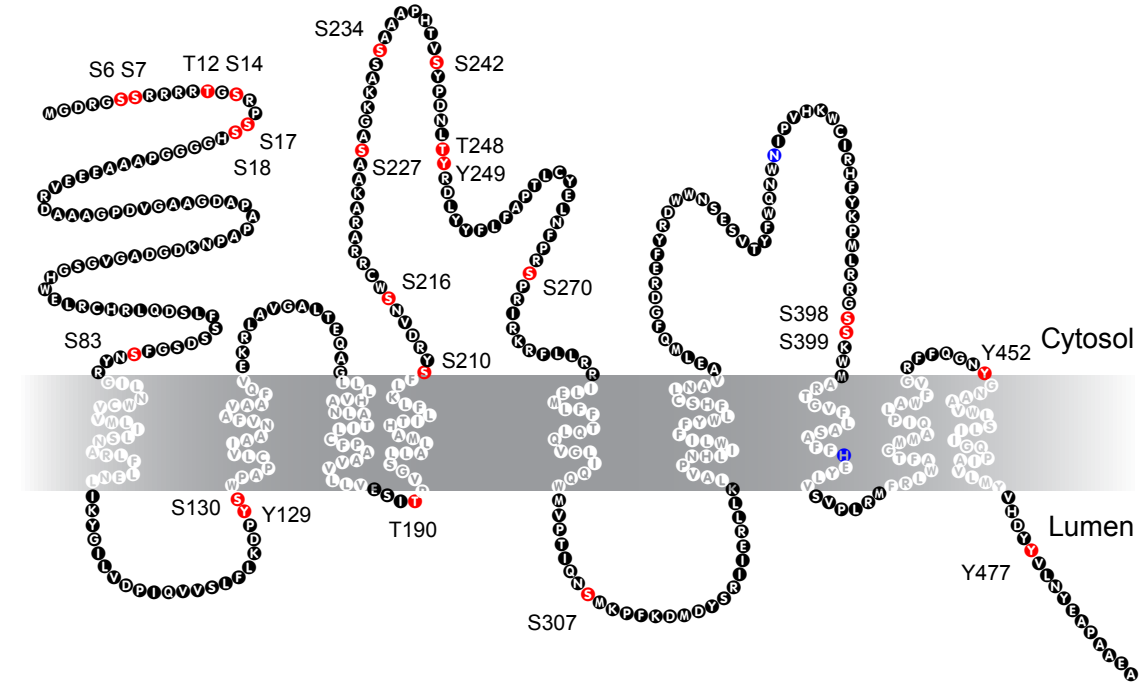

Figure 2.2 DGAT1 has many highly conserved phosphorylation sites. A. A sequence alignment of the amino acid sequence of DGAT1 across 39 species. Predicted transmembrane domains are in light blue, every T, S and Y is marked in red. The relative conservation of each amino acid is plotted immediately below. **B.** A predicted model of human DGAT1 structure based on the transmembrane predictions and experimental results mapping ACAT1. Predicted phosphorylation sites are marked in red.

insertion (Joyce et al., 2000; Lin et al., 1999) generally yielding fewer TM domains than cysteine modification (Guo et al., 2005).

Upon Inspection of the soluble domains of DGAT1, several highly conserved phosphorylatable residues are apparent. These are summarized with their associated predicted kinase in **Table 2.I**. Of note are Y361 and T160, whose homologs in *Tropaeolum majus* DGAT1 have a demonstrated affect on activity (Taylor et al., 2009). Similarly, murine sites T15, S17, S20, S25, S40, S67 and S244 have been identified in recent large-scale phosphoproteomics studies (Beltrao et al., 2012; Humphrey et al., 2013; Huttlin et al., 2010) as well as human site Y316 (Beltrao et al., 2012).

DGAT1 incorporates ^{32}P phosphate at more than 5 sites

We next wanted to verify that DGAT1 is phosphorylated and identify the sites. We performed ^{32}P orthophosphate labeling in transfected HEK293 cells and McArdle RH7777 stably expressing FLAG-mDGAT1 (**Figure 2.3A**). FLAG immunopurification (IP) and subsequent autoradiography reveals a band at the size corresponding to mDGAT1 in both cell types. This is consistent with previous experiments performed in the lab (S Stone & P Zhou, unpublished observations).

To identify residues that are phosphorylated on DGAT1 in vitro, we performed mass spectrometry (MS) on IP FLAG-mDGAT1 and FLAG-hDGAT1. The results of 3 replicate experiments for each species are summarized in **Figure 2.3B**. We obtained ~35% coverage of both mouse and human proteins, mostly in the N-terminus. In murine DGAT1, we found 6 sites: T15, S17, S20, S25, S40 and S280. From human DGAT1, we identified only 4: T12, S14, S17 and S18. We subsequently mutated the phosphorylated residues to alanines in

A.

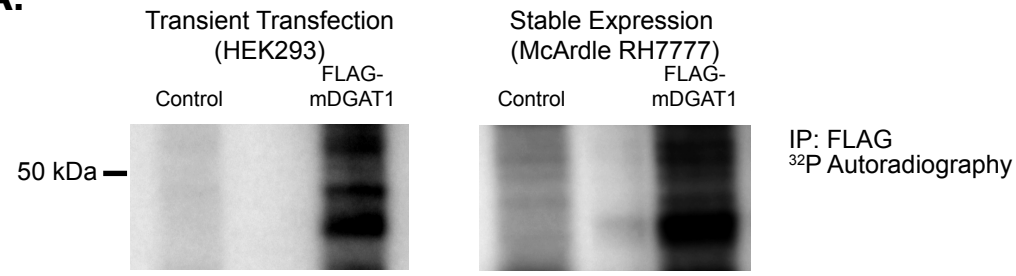

B.

mouse DGAT1

MGDRGGAGSSRRRRT*GS*RVS*VQGGS*GPKVEEDEVRDAAVS*PDLGAGGDAPAPAPAPAHTRDKDGRTSVGD
GYWDLRCHRLQDSLFSSDSGFSNYRGILNWCVVMLILSNARLFLENLIKYGILVDPIQVVSLFLKDPYSWPAP
CVIIASNIFVVAAFQIEKRLAVGALTEQMGLLLHVVNLATIICFPAAVALLVESITPVGSVFALASYSIMFLK
LYSYRDVNLWCRQRRVKAKAVSTGKKVSGAAAQQAVSYPDNLTYRDLYYFIFAPTLCYELNFPRSPRIRKRFL
LRRVLEMLFFTQLQVGLIQQWMVPTIQNSMKPFKDMDYSRIIERLLKLAVPNHLIWLIFFYWFFHSCLNAVAE
LLQFGDREFYRDWWNAESVTYFWQNWNIPVHKWCIRHFYKPMLRHGSSKWVARTGVFLTSAFFHEYLVSVPLR
MFRLWAFTAMMAQVPLAWIVGRFFQGNYGNAAVWVTLIIGQPVAVLMYVHDYYVLNYDAPVGV

human DGAT1

MGDRGSSRRRRT*GS*RPS*S*HGGGGPAAAEEEVRDAAAGPDVGAAGDAPAPAPNKDGDAGVGS*GHWELRCHR
LQDSLFSSDSGFSNYRGILNWCVVMLILSNARLFLENLIKYGILVDPIQVVSLFLKDPYSWPAPCLVIAANVF
AVAAFQVEKRLAVGALTEQAGLLLHVANLATILCFPAAVVLLVESITPVGSLLALMAHTILFLKLFSYRDVNS
WCRRARAKAASAGKKASSAAAPHTVSYPDNLTYRDLYYFLFAPTLCYELNFPRSPRIRKRFLLRRILEMLFFT
QLQVGLIQQWMVPTIQNSMKPFKDMDYSRIIERLLKLAVPNHLIWLIFFYWLFHSCLNAVAELMQFGDREFYR
DWWNSESVTYFWQNWNIPVHKWCIRHFYKPMLRRGSSKWMARTGVFLASAFFHEYLVSVPLRMFRLWAFTGMM
AQIPLAWFVGRFFQGNYGNAAVWLSLIIGQPIAVLMYVHDYYVLNYEAPAAEA

C.

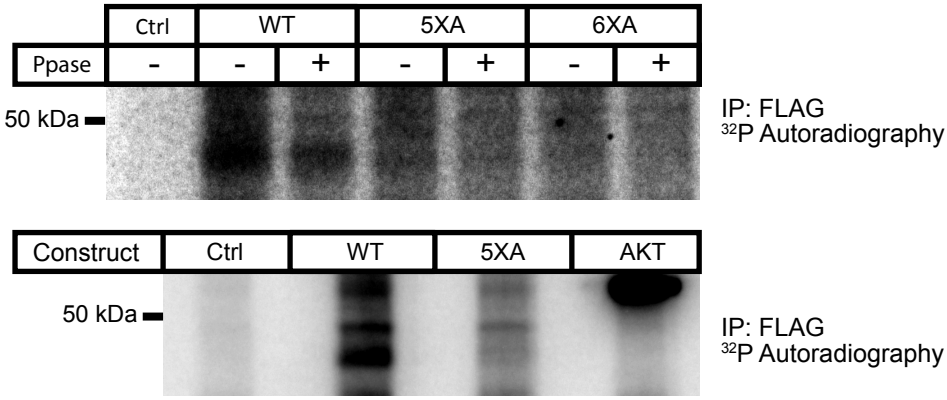

Figure 2.3: DGAT1 is phosphorylated on at least 6 sites. A. ^{32}P incorporation performed in HEK293 cells or McArdle RH7777 cells. **B.** The summary of three independent mass spectrometry runs including all identified phosphorylation sites. **C.** ^{32}P incorporation performed in transiently transfected McArdle RH7777 cells with various phosphorylation mutants of murine DGAT1.

successive versions T15A, S17A and S20A (3XA); 3XA with S25A and S40A (5XA); 5XA with S280A (6XA).

To determine the extent to which ^{32}P incorporation was reduced, we expressed 5XA and 6XA mutants in McArdle cells and performed FLAG-IP with subsequent autoradiography detection (**Figure 2.3C**). As before, the WT protein shows abundant ^{32}P signal by autoradiography. ^{32}P incorporation in the 5XA mutant is dramatically reduced, whereas the 6XA mutant is undetectable. These results indicate that transfected DGAT1 is phosphorylated on at least 6 residues in basal conditions.

Basal phosphorylation state does not affect in vitro DGAT activity

To determine whether the phosphorylation status of the identified sites affects DGAT activity, we measured in vitro activity of the phospho-null mutants. Using the mouse constructs, we measured protein levels (**Figure 2.4A**) and in vitro DGAT activity (**Figure 2.4B**) of WT, 3XA, 5XA transfected HEK293 cells. We found no differences in among the three phospho mutants with respect to protein levels or in vitro activity. We next wondered whether reducing the basal phosphorylation might uncover additional regulation through CIP treatment (**Figure 2.4C**). Thus, we measured in vitro activity of WT, 5XA and 6XA constructs that had been treated with phosphatase. We again saw no differences in *in vitro* DGAT activity among the treatments. This result differs from our earlier test of CIP treatment and likely indicates this is a cell-type specific phenomenon.

Finally, we wanted to test whether the phospho-sites identified in human DGAT1 affected in vitro activity. We generated constructs with T12, S14 (2XA) and S270A (3XA) mutants and expressed them in HEK293 cells. We observed that protein levels were similar

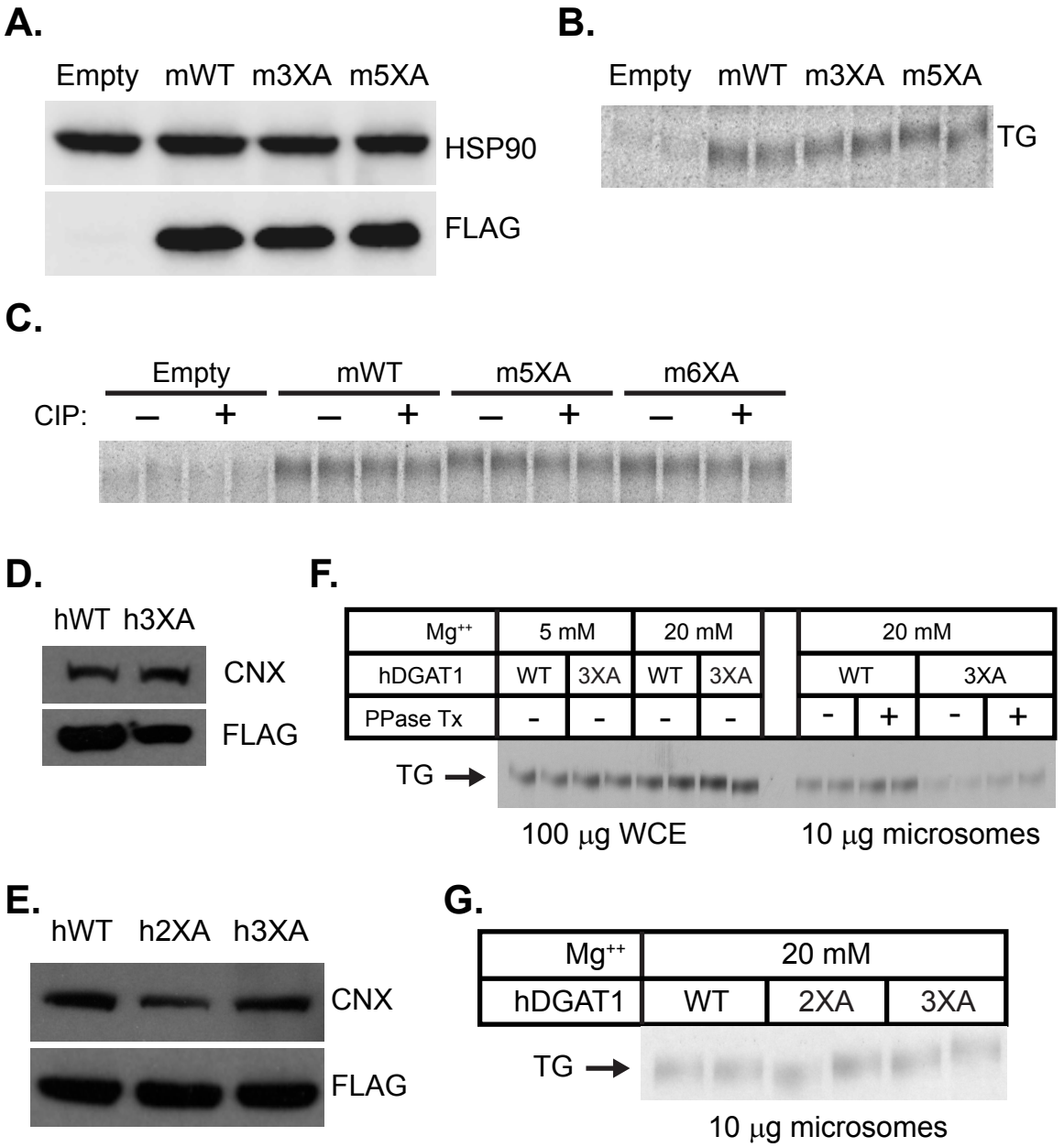

Figure 2.4: Basal phosphorylation mutants do not reproducibly affect DGAT1 activity. A. WB of WT and phospho-null mutants of murine DGAT1 confirming equal expression. **B.** A DGAT1 assay performed on cells transfected with phospho-null mutants of murine DGAT1 showing no differences between WT, 3XA and 5XA. **C.** Additional phosphatase treatment of DGAT1 phospho-null mutants does not alter activity. **D.** WB of WT and phospho-null mutants of human DGAT1 showing slightly reduced expression of 3XA mutant. **E.** DGAT1 activity testing the effect of Mg++ and phosphatase treatment on activity of WT and 3XA hDGAT1 mutants. **F.** WB of WT and phospho-null mutants of human DGAT1. **G.** DGAT1 activity assay of microsomes isolated from cells overexpressing phospho-null mutants of hDGAT1.

between WT, 2XA and 3XA (**Figures 2.4D and 2.4E**). When measured against WT alone, the 3XA mutant was roughly 50% less active in vitro (**Figure 2.4F**). However, these results were not repeated when comparing the WT, 2XA and 3XA mutants (**Figure 2.4G**). Altogether, these results strongly suggest a role for phosphorylation in regulating DGAT1 activity, though it is likely a cell-type and perhaps species specific phenomenon.

Discussion

In this study we have demonstrated that adipose DGAT1 and DGAT2 activity is regulated in a nutritional state-dependent manner. We went on to show that phosphatase treatment affects DGAT activity in vitro in a cell-type specific manner. Through mass spectrometry, we identified 6 phosphorylation sites in murine DGAT1 and 5 sites in human DGAT1 that are phosphorylated under basal conditions. These findings indicate it is possible that DGAT1 activity is regulated by phosphorylation under normal physiological conditions. However, we have been unable to identify the sites or physiological states under which the regulation occurs.

Our measurements of ^{32}P incorporation of the 6XA mutant (**Figure 2.3C**) indicate that we have identified the majority of the high-frequency phosphorylation sites by MS. However, because of the limitations of our purification and MS scheme, we cannot completely rule out the existence of addition phosphorylation sites that exist below the detection limit of the ^{32}P assay. Indeed, the results of the in vitro phosphatase treatment experiments suggest that additional sites exist and are important for the regulation of activity.

One major limitation of our current approach is that we did not attempt to mimic different physiological states through in vitro treatment. Indeed, it will be important to determine whether inducing lipolysis conditions in the cellular model affects in vitro DGAT activity in the same way as fasting conditions in the animal. Previous studies (Beynen et al., 1981; Haagsman et al., 1981, 1982; Haagsman and Van Golde, 1981, 1984) have generally relied on perfusion of animal tissue as their experimental paradigm. These types of approaches are also more likely to uncover differences that genuinely affect activity, rather than any basal phosphorylation that may be present.

Table 2.I. A Summary of predicted and identified phosphorylation sites on DGAT1

Site (Human Numbering)	Score	Predicted Kinase	Notes	Ref.
S6	0.994	PKC	NetPhos Predicted	
S7	0.995	PKC, PKA, CDC2	NetPhos Predicted	
T12	0.960	PKC, PKA	Mouse ortholog identified	17, 18
S14	0.966	RSK, PKB, PKC, PKA, GSK3	Mouse ortholog identified	17
S17	0.994	CKI	Mouse ortholog identified	18
S18	0.996	CKI	NetPhos Predicted	
S83	0.954		NetPhos Predicted	
Y129	0.903	INSR	NetPhos Predicted	
S130	0.563		NetPhos Predicted	
S188	0.006		Mouse ortholog identified	
T190	0.571	p38MAPK	NetPhos Predicted	
S210	0.949	PKC	NetPhos Predicted	
S216	0.581		NetPhos Predicted	
S227	0.771		NetPhos Predicted	
S233	0.270		Mouse ortholog identified	19
S234	0.776	PKC	NetPhos Predicted	
S242	0.939		NetPhos Predicted	
T248	0.659		NetPhos Predicted	
Y249	0.794		NetPhos Predicted	
S270	0.912	p38MAPK, GSK3, CDK5	NetPhos Predicted	
S307	0.928	PKC, PKG	NetPhos Predicted	
Y316	0.408		Identified by phosphoproteomics	18
S398	0.997	RSK, PKC, PKA, PKG	NetPhos Predicted	
S399	0.890	RSK, PKA	NetPhos Predicted	
Y452	0.750		NetPhos Predicted	
Y477	0.813		NetPhos Predicted	

References

(2013). Update on activities at the Universal Protein Resource (UniProt) in 2013. Nucleic Acids Res 41, D43-47.

Beltrao, P., Albanese, V., Kenner, L.R., Swaney, D.L., Burlingame, A., Villen, J., Lim, W.A., Fraser, J.S., Frydman, J., and Krogan, N.J. (2012). Systematic functional prioritization of protein posttranslational modifications. Cell 150, 413-425.

Beynen, A.C., Haagsman, H.P., Van Golde, L.M., and Geelen, M.J. (1981). The effects of insulin and glucagon on the release of triacylglycerols by isolated rat hepatocytes are mere reflections of the hormonal effects on the rate of triacylglycerol synthesis. Biochim Biophys Acta 665, 1-7.

Blom, N., Gammeltoft, S., and Brunak, S. (1999). Sequence and structure-based prediction of eukaryotic protein phosphorylation sites. J Mol Biol 294, 1351-1362.

Cases, S., Smith, S.J., Zheng, Y.W., Myers, H.M., Lear, S.R., Sande, E., Novak, S., Collins, C., Welch, C.B., Lusis, A.J., Erickson, S.K., and Farese, R.V., Jr. (1998). Identification of a gene encoding an acyl CoA:diacylglycerol acyltransferase, a key enzyme in triacylglycerol synthesis. Proc Natl Acad Sci U S A 95, 13018-13023.

Cases, S., Stone, S.J., Zhou, P., Yen, E., Tow, B., Lardizabal, K.D., Voelker, T., and Farese, R.V., Jr. (2001). Cloning of DGAT2, a second mammalian diacylglycerol acyltransferase, and related family members. J Biol Chem 276, 38870-38876.

Goujon, M., McWilliam, H., Li, W., Valentin, F., Squizzato, S., Paern, J., and Lopez, R. (2010). A new bioinformatics analysis tools framework at EMBL-EBI. Nucleic Acids Res 38, W695-699.

Guo, Z.Y., Lin, S., Heinen, J.A., Chang, C.C., and Chang, T.Y. (2005). The active site His-460 of human acyl-coenzyme A:cholesterol acyltransferase 1 resides in a hitherto undisclosed transmembrane domain. J Biol Chem 280, 37814-37826.

Haagsman, H.P., de Haas, C.G., Geelen, M.J., and van Golde, L.M. (1981). Regulation of triacylglycerol synthesis in the liver: a decrease in diacylglycerol acyltransferase activity after treatment of isolated rat hepatocytes with glucagon. Biochim Biophys Acta 664, 74-81.

Haagsman, H.P., de Haas, C.G., Geelen, M.J., and van Golde, L.M. (1982). Regulation of triacylglycerol synthesis in the liver. Modulation of diacylglycerol acyltransferase activity in vitro. J Biol Chem 257, 10593-10598.

Haagsman, H.P., and Van Golde, L.M. (1981). Synthesis and secretion of very low density lipoproteins by isolated rat hepatocytes in suspension: role of diacylglycerol acyltransferase. Arch Biochem Biophys 208, 395-402.

Haagsman, H.P., and van Golde, L.M. (1984). Regulation of hepatic triacylglycerol synthesis and secretion. Vet Res Commun 8, 157-171.

Humphrey, S.J., Yang, G., Yang, P., Fazakerley, D.J., Stockli, J., Yang, J.Y., and James, D.E. (2013). Dynamic adipocyte phosphoproteome reveals that Akt directly regulates mTORC2. Cell Metab 17, 1009-1020.

Huttlin, E.L., Jedrychowski, M.P., Elias, J.E., Goswami, T., Rad, R., Beausoleil, S.A., Villen, J., Haas, W., Sowa, M.E., and Gygi, S.P. (2010). A tissue-specific atlas of mouse protein phosphorylation and expression. Cell 143, 1174-1189.

Joyce, C.W., Shelness, G.S., Davis, M.A., Lee, R.G., Skinner, K., Anderson, R.A., and Rudel, L.L. (2000). ACAT1 and ACAT2 membrane topology segregates a serine residue essential for activity to opposite sides of the endoplasmic reticulum membrane. Mol Biol Cell 11, 3675-3687.

Krogh, A., Larsson, B., von Heijne, G., and Sonnhammer, E.L. (2001). Predicting transmembrane protein topology with a hidden Markov model: application to complete genomes. J Mol Biol 305, 567-580.

Lau, T.E., and Rodriguez, M.A. (1996). A protein tyrosine kinase associated with the ATP-dependent inactivation of adipose diacylglycerol acyltransferase. Lipids 31, 277-283.

Lin, S., Cheng, D., Liu, M.S., Chen, J., and Chang, T.Y. (1999). Human acyl-CoA:cholesterol acyltransferase-1 in the endoplasmic reticulum contains seven transmembrane domains. J Biol Chem 274, 23276-23285.

McFie, P.J., Stone, S.L., Banman, S.L., and Stone, S.J. (2010). Topological orientation of acyl-CoA:diacylglycerol acyltransferase-1 (DGAT1) and identification of a putative active site histidine and the role of the n terminus in dimer/tetramer formation. J Biol Chem 285, 37377-37387.

Taylor, D.C.S., Xu, J.S., Mietkiewska, E.S., and Francis, T.S. (2009). Acyl-coa-dependent diacylglycerol acyltransferas 1 (dgat1) gene from tropaeolum majus, protein encoded thereby and uses thereof. (US).

Yu, Y.H., Zhang, Y., Oelkers, P., Sturley, S.L., Rader, D.J., and Ginsberg, H.N. (2002). Posttranscriptional control of the expression and function of diacylglycerol acyltransferase-1 in mouse adipocytes. J Biol Chem 277, 50876-50884.

A DGAT1 mutation in a Family with a Congenital Diarrhea Disorder

Abstract

Congenital diarrheal disorders (CDD) are rare, heterogeneous enteropathies with early onset and often severe outcomes. Here, we report a family with two of three children affected by CDD, presenting 3 days after birth with severe intractable diarrhea. One child died from complications at age 17 months. The second child resolved most symptoms at 10–12 months of age. Exome sequencing identified homozygousity for a rare splice-site mutation in *DGAT1* in both affected children. Molecular analysis of the mutant allele revealed a total loss of function, with no detectable DGAT1 protein or activity produced. The cause of diarrhea is unknown, but likely relates to abnormal fat absorption in the intestinal mucosa. Our results identify *DGAT1* loss-of-function mutations as a rare cause of CDD and prompt concern for DGAT1 inhibition in humans, which is being assessed for treating metabolic diseases.

Introduction

Congenital diarrheal disorders (CDD) are rare and heterogeneous enteropathies, often with severe clinical manifestations (Berni Canani et al., 2010; Terrin et al., 2012). Those with ascribed etiology typically result from autosomal recessive mutations. Affected genes include those related to disaccharidase deficiency, ion or nutrient transport defects, pancreatic insufficiency, or lipid trafficking (Berni Canani et al., 2010). Some types of CDD can be treated with dietary modification, but many present challenging clinical conditions, often requiring chronic nutritional support.

Here, we identified and characterized a rare *DGAT1* mutation in a family with CDD. *DGAT1* encodes one of two acyl CoA:diacylglycerol acyltransferases (DGATs), which catalyze the final step in triglyceride (TG) synthesis (Yen et al., 2008). *DGAT1* is expressed ubiquitously, with highest expression in human intestine (Cases et al., 1998). Mice lacking DGAT1 have normal fat absorption, although absorption is delayed and more fat reaches distal intestinal regions (Buhman et al., 2002). Because of the favourable metabolic phenotype of DGAT1-knockout mice (Smith et al., 2000), DGAT1 inhibitors have been developed (Cao et al., 2011; Nakada et al., 2010; Zhao et al., 2008) and proven efficacious in animal studies (Cao et al., 2011; McLaren et al., 2011). Several are being evaluated in clinical trials (Birch et al., 2010; Cao et al., 2012; Yin et al., 2012). However, mutations in human *DGAT1* have not been reported, and information about human DGAT1 deficiency is limited.

Methods

Experimental procedures are provided in detail in Supplemental Methods.

Genetic screening and verification

Exome capture was with Agilent Whole Exome SureSelect v2 kit. Single-nucleotide-variant search parameters are described in text. For RFLP analysis, PCR products were digested with *Fnu*4-HI. Bands are 165, 32, and 3 bp (wildtype); 122, 43, 32, and 3 bp (mutant).

Molecular Characterization

Mouse embryonic fibroblasts (MEFs) were isolated and immortalized (Willnow and Herz, 1994). DGAT activity was assayed (Cases et al., 1998) with conditions specific for DGAT1 (50 mM $MgCl_2$). Total RNA was isolated with Trizol (Invitrogen) and reverse-transcribed (RT) with iScript cDNA Synthesis kit (BioRad). Antibodies were FLAG antibody M2 (Sigma, 1:2000), DGAT1 antibody NB110-41487 (1:1000, Novus), and HSP90 (1:2000, BD Biosciences). HRP secondary antibodies (1:5000, Amersham) were used with ECL (Pierce).

Statistics

The probability of Δ8 mutation causing CDD was empirically determined from the frequency of any homozygous or compound heterozygous deleterious mutations occurring in the reference exome sets ((ESP); Project, 2010).

Study Approval

Written informed consents for all adult participants and the parents of the children were obtained. The genetic study proposal was approved by the Partners Institutional Review Board.

Results and Discussion

Clinical summary

The affected family is a non-consanguineous couple of Ashkenazi Jewish descent with three children from full-term, uncomplicated pregnancies. The first boy was unaffected. The second child (Case 1), a girl, weighed 3.18 kg at birth and was fed with breast milk and cow's milk formula. Three days after birth, she developed vomiting, colicky pain, and non-bloody, watery diarrhea, 8–10 times daily. She was treated with oral rehydration solution and changed to soy-based formula, but diarrhea continued. Cultures for bacterial pathogens, rotavirus, and adenovirus were negative. She exhibited protein-losing enteropathy, with stool alpha-1 antitrypsin of 8–20 mg/g (normal <3 mg/g stool), and hypoalbuminemia. She required total parenteral nutrition and intermittent infusions of albumin. Stomach, duodenum and colon biopsies were negative for chronic granulomatous disease, autoimmune enteropathy, food protein-induced enterocolitis, microvillous inclusion disease, and tufting enteropathy (**Figure A1.1**). Neuroendocrine cells were present in intestinal biopsies. Congenital lymphangiectasia, a cause of protein-losing enteropathy, was excluded by CT scan and histology. There was evidence of dystrophic microvilli in the duodenum. Immunological tests were unremarkable except for slightly decreased IgG (275 mg/dL) with normal subclasses.

The child exhibited hyperlipidemia with fasting serum TG of 325 mg/dL at age 1 month [subsequently 81–631 mg/dL; mean of 264 mg/dL (n = 55)] (**Table 3.I**). The father had elevated fasting TG (118–481 mg/dL) and total cholesterol levels (140–260 mg/dL), with

HDL cholesterol 33–39 mg/dL. The mother also had elevated fasting TG (144–229 mg/dL) and total cholesterol levels (174–220 mg/dL), with HDL cholesterol 39–42 mg/dL.

At 14 months of age, the child was below the first percentile for weight, despite parenteral nutrition and feeding per gastrostomy tube. She had recurrent episodes of sepsis, presumably related to a venous catheter. Eventually, she tolerated tube feedings (80 kcal/kg/day) with amino acid–based formula containing maltodextrin and medium chain TGs, but did not gain weight and continued to lose protein in her stool. She died at age 17 months from complications of malnutrition and sepsis.

The third child (Case 2), a boy, weighed 3.7 kg at birth. He initially tolerated breast milk and soy formula, but developed diarrhea 3 days after birth. His stools were non-bloody, 4–6 times daily, and watery. Six days after birth, he was admitted for dehydration, metabolic acidosis, and hyponatremia. Stool cultures were negative for bacterial pathogens, rotavirus, and adenovirus. Stool sodium and potassium levels were normal. Serum IgG was normal, but fecal alpha-1 antitrypsin was increased to 4.7–7.9 mg/g. He required intravenous albumin to correct the protein-losing enteropathy. Light and electron microscopy of duodenum at age 2 months revealed findings similar to Case 1 (**Figure A1.2A and A1.2B**). With nutritional support of amino acid–based formula and parenteral nutrition, he began to gain weight, and by 10 months of age was no longer losing protein in his stool. A second duodenal biopsy, performed when his diarrhea improved (age 13 months), showed improved enterocyte morphology (**Figure A1.2C and A1.2D**) and increased eosinophils. Because of combined hyperlipidemia (elevated serum total cholesterol and TG—**Table 3.I**), he was treated with cholestyramine at age 27 months, and fasting serum lipid levels decreased. He was thriving at age 46 months on an unrestricted diet.

Mutation identification and characterization

The identical phenotype and onset in two affected siblings suggested a recessive mutation (**Figure 3.1A**). To identify candidates, exome sequencing was performed on DNA from both parents and Case 2 (Supplemental Methods). Utilizing published sequence databases ((ESP); Project, 2010), we searched for rare alleles (frequency <1%) that were predicted loss-of-function (nonsense, splice, frameshift) or were non-synonymous and predicted deleterious by PolyPhen2 (Adzhubei et al., 2010). A single candidate gene (*DGAT1*) was identified in which the child was homozygous (and both parents heterozygous) for a splice variant (chr8:145541756 A→G), in the splice donor site 3′ of exon 8, altering the invariant GT to GC. We identified three individuals in ~12,500 control exomes as carriers for this mutation and estimate probability of homozygousity of 1 in ~50–100 million births, revealing a novel and severe recessive disorder.

Using PCR and RFLP, we confirmed both affected children as homozygous carriers of the mutation. The maternal grandmother, paternal grandfather, both parents, and unaffected child were heterozygous (**Figure 3.1B**). The known founder effect of the Ashkenazi Jewish subpopulation likely explains why two unrelated families carry such a rare mutation (Slatkin, 2004).

The predicted result of the mutation is skipping of exon 8 (Krawczak et al., 2007), yielding an in-frame deletion of 75 bp (**Figure 3.1C**). Using RT-PCR with primers flanking exon 8 (**Figure 3.1D**), we confirmed cDNA products corresponding to the wildtype and exon 8–deleted (Δ8) allele in the parents and unaffected child, and only the mutant in the affected

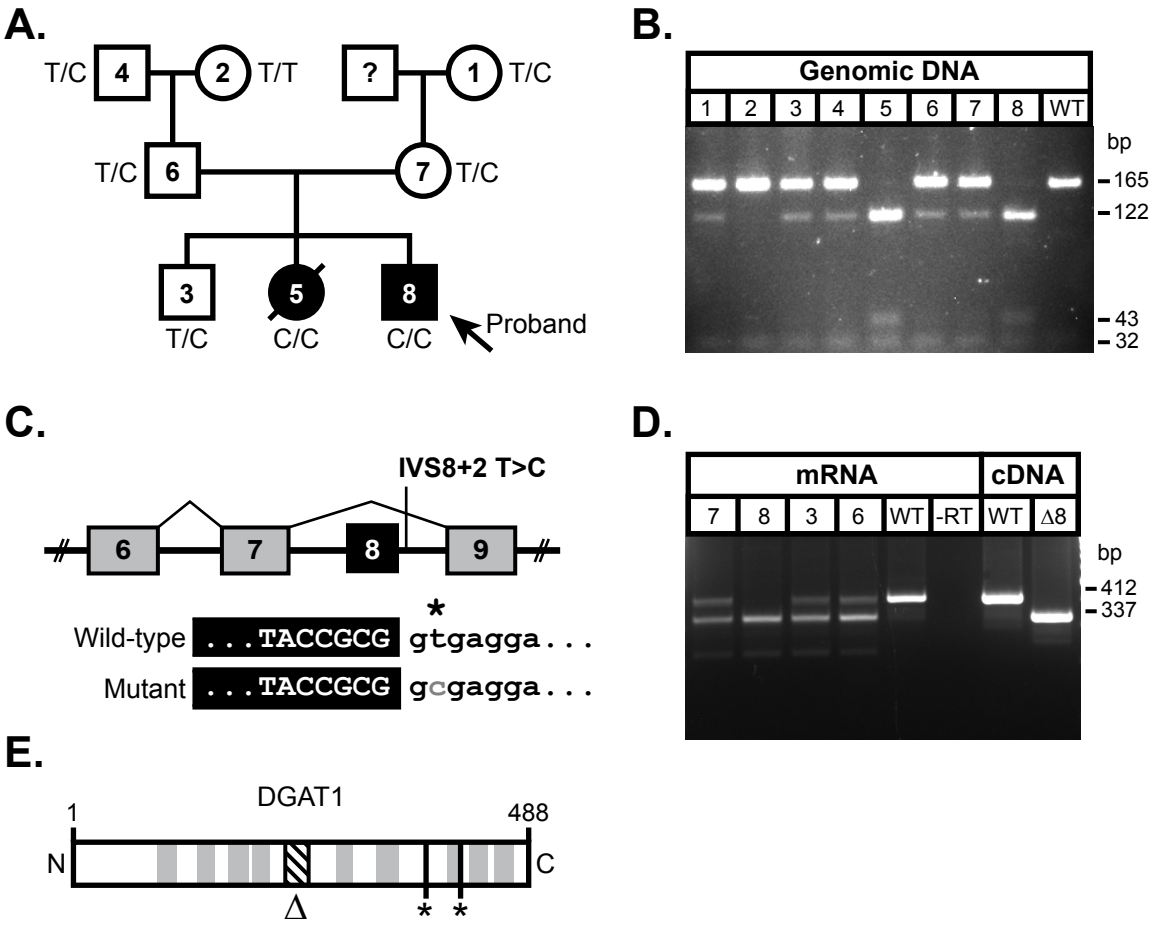

Figure 3.1. Mutation in DGAT1 segregates with congenital diarrhea and protein-losing enteropathy. A. Pedigree of affected family indicating inheritance of diarrheal phenotype and DGAT1 genotype. T, wild-type allele; C, mutant allele. **B.** RFLP assay of genomic DNA from family, demonstrating mutation inheritance. PCR product was digested with Fnu4HI to yield 165 and 32 for the reference (A), and 122, 43 and 32 bp for the mutant allele (G). **C.** Schematic of predicted splicing result for wildtype and mutant alleles. **D.** RT-PCR analysis of mRNA isolated from blood of the proband, unaffected sibling, and parents. Mutant DGAT1 allele yields exon 8–deleted (Δ8) mRNA. **E.** Diagram of DGAT1 protein including predicted transmembrane domains (grey), putative catalytic residues (*), and deleted region corresponding to exon 8 (Δ, diagonals).

child (**Figure 3.1D**). No other gene-specific products were detected. Exon 8 deletion removes 25 amino acids from the highly conserved MBOAT domain of DGAT1 but does not affect putative active site residues (Hofmann, 2000) (**Figure 3.1E)**.

To determine the mutation's effects on DGAT1 activity, we expressed full-length and □8 cDNAs (FLAG-tagged and untagged) in mouse embryonic fibroblasts (MEFs) lacking *Dgat1* (Harris et al., 2011) (DGAT1-KO). Although both mRNA species were present, neither DGAT1 protein nor in vitro DGAT1 activity was detected in cells expressing Δ8 cDNA (**Figure 3.2A**). We also expressed the constructs in MEFs lacking both DGAT1 and DGAT2 (DGAT1,2-KO) (Harris et al., 2011). DGAT1,2-KO MEFs expressing wildtype DGAT1 and incubated with [^{14}C]-oleate accumulated TGs, but cells expressing Δ8 did not (**Figure 3.2B**). These results indicate that DGAT1 protein and activity are lost with the Δ8 mutation.

To determine whether Δ8 protein is rapidly degraded, we used MG132 to inhibit proteasomal degradation and found, indeed, Δ8 protein was detected after 4 hours (**Figure 3.2C**). Nevertheless, DGAT1,2-KO cells treated with MG132 accumulated TG only when expressing wildtype *DGAT1* but not Δ8 (**Figure 3.2D**). Thus, the Δ8 allele yields an unstable protein that, even when present, is likely inactive.

Our findings show that homozygous *DGAT1* loss-of-function is associated with CDD. The reported mutation results in deletion of exon 8 and a null allele. The frequency of randomly occurring homozygous or compound heterozygous mutations in the exome database indicate it is highly likely ($p<0.01$) that the Δ8 mutation causes CDD. *DGAT1* function in the intestine and potential relevance to the phenotypes supports this conclusion.

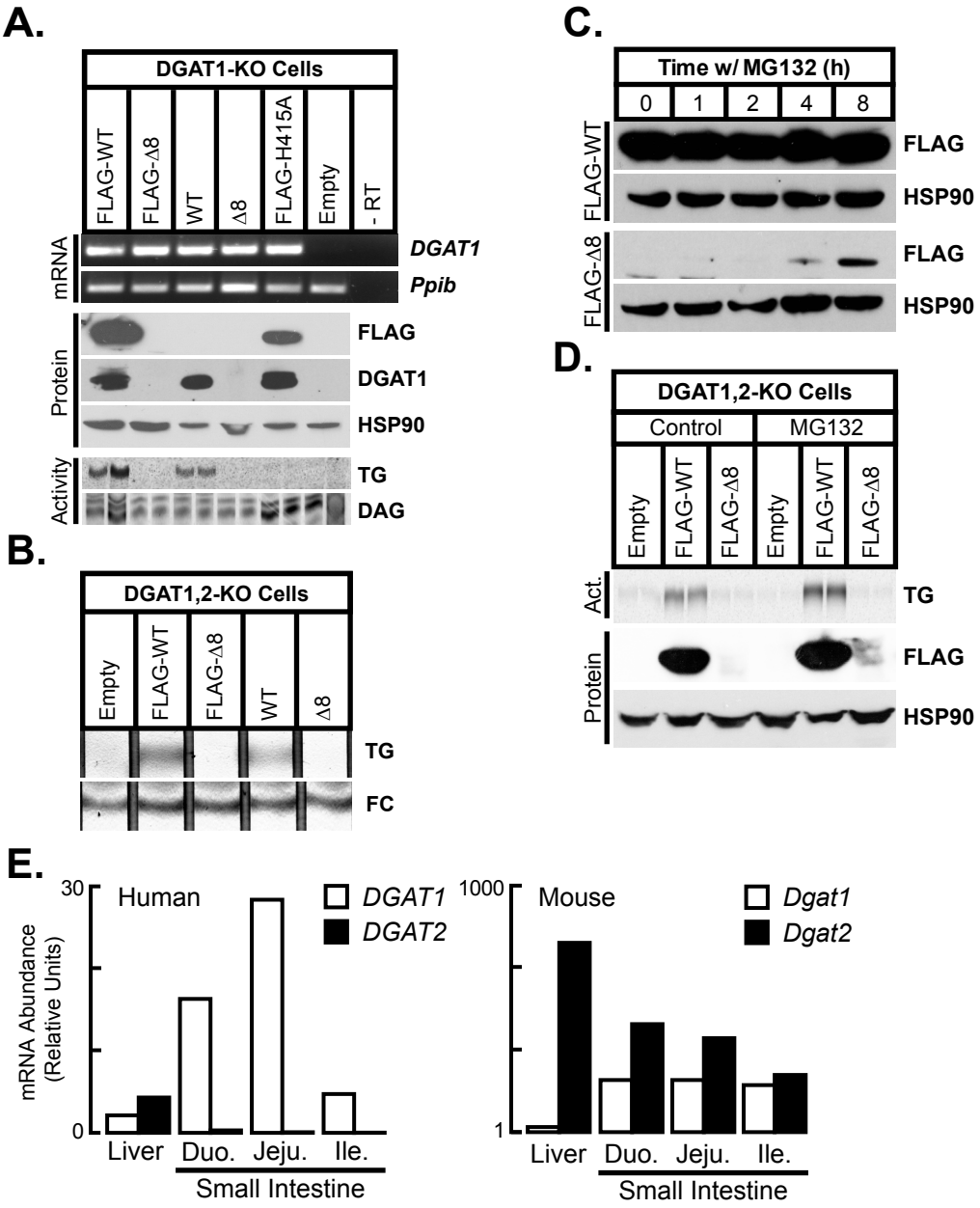

Figure 2. DGAT1-KO or DGAT1,2-KO MEFs expressing DGAT1 cDNAs reveal that Δ8 mRNA yields an unstable protein, resulting in loss of DGAT1 activity. **A.** DGAT1 activity, indicated by accumulation of [^{14}C]-TAG, was absent in lysates from Δ8-expressing cells despite the presence of mRNA. All lysates synthesized [^{14}C]-DAG (internal control). **B.** Intact Δ8-expressing cells do not accumulate TG, as measured by TLC in DGAT1,2-KO cell lines after incubation with 200 mM oleic acid:BSA complex. Free cholesterol (FC) provides a loading control. **C.** Immunoblotting shows proteasome inhibition rescues Δ8 protein expression in MG132-treated DGAT1,2-KO MEFs. **D.** MG132-treated DGAT1,2-KO MEFs expressing Δ8 do not accumulate [^{14}C]-TG after a 2-hour treatment with 200 mM [^{14}C]-oleic acid. **E.** Quantitative RT-PCR showing that humans lack DGAT2 expression in the small intestine.

CDD can be caused by mutations in *APOB*, *MTP*, and *SAR1B* (Zamel et al., 2008), which function in chylomicron assembly and export. These mutations yield defective intestinal fat absorption and consequent steatorrhea. These defects differ from the current report in that they occur distal to TG synthesis whereas, with DGAT1 deficiency, the defect is in TG synthesis itself.

The phenotype of DGAT1 deficiency in humans differs from that of DGAT1-KO mice, which exhibit reduced body fat, increased energy expenditure, improved glucose tolerance, resistance to diet-induced obesity, and extended longevity (Smith et al., 2000; Streeper et al., 2012). The mice also have delayed fat absorption and decreased post-prandial excursions of plasma TG, but not excess fecal fat or diarrhea (Buhman et al., 2002). These findings suggest species-specific differences for DGAT1 deficiency. In mammals, DGAT1 and DGAT2 account for nearly all TG synthesis (Harris et al., 2011). Using quantitative PCR, we found that both *Dgat1* and *Dgat2* are expressed in murine intestine, but only *DGAT1* is expressed highly in human intestine (**Figure 3.2E**), as we reported (Cases et al., 2001; Smith et al., 2000). Thus, human intestine may be more sensitive to DGAT1 inhibition, owing to lack of *DGAT2* expression.

How human DGAT1 deficiency causes diarrhea is unclear, but build-up of DGAT1 lipid substrates in the intestinal mucosa or lumen likely contributes. Excess diacylglycerols or fatty acids could become toxic, by acting as bioactive signalling lipids or by detergent-like behaviour of fatty acid moieties. Toxicity to enterocytes could result in protein-losing enteropathy. Alternatively, bile acid malabsorption can cause diarrhea, and DGAT1 deficiency could affect bile acid metabolism. Unfortunately, no information on fecal bile acid levels in the affected individuals was available.

The different clinical outcome of the affected children remains unclear. Case 2 suggests there may be aging-associated increases in intestinal DGAT2 expression or other adaptation to DGAT1 deficiency. Without complications from sepsis, the Case 1 individual might also have improved. The two children were different sexes, but relative levels of *DGAT2* expression in male and female children are unknown. Treatment with a bile acid–binding resin might have helped in Case 2. However, timing of this treatment did not correspond with clinical improvement.

Moderate hyperlipidemia, including hypertriglyceridemia, occurred in the affected children and parents. Whether this is causally linked to the *DGAT1* mutation or an independent trait is unclear. Mice lacking DGAT1 have normal fasting levels of serum TGs (Smith et al., 2000) and reduced TGs after fat intake (Buhman et al., 2002), thus hypertriglyceridemia linked to DGAT1 deficiency would be specific to humans. If hypertriglyceridemia is associated, overcompensation from hepatic DGAT2 may contribute via lipoprotein-mediated secretion of TGs. Alternatively, interruption of bile acid absorption in the distal small intestine is associated with very low-density lipoprotein overproduction and hypertriglyceridemia (Beil et al., 1982). The identification of more individuals with homozygous DGAT1 deficiency could shed light on this issue.

Notably, recent studies of DGAT1 inhibitors in humans reported dose-related adverse effects of mild-to-moderate diarrhea in some patients (Novartis, 2011). Our findings suggest this effect results from DGAT1 inhibition, rather than being off-target. A better understanding of DGAT1's role in the intestine and how DGAT1 deficiency causes diarrhea will be useful for developing or improving therapies with DGAT1 inhibitors.

Table 3.I. Blood lipid levels for Case 1 and Case 2 (mg/dl).

Age (months)	Triglycerides	Total Cholesterol	LDL-C	HDL-C	VLDL-C
Case 1					
1	325	105	15	25	65
3	284	88	17	14	57
6	260	90	10	28	52
9	252	148	65	34	50
12	291	106	19	29	58
14	256	99	12	36	51
16	188	97	25	34	38
Case 2					
6	204	120	67	29	41
8	172	112	62	28	34
12	193	116	60	33	39
14	359	152	74	26	72
16	288	150	80	28	58
27*	300	188	117	32	60
28	275	149	86	33	55
30	120	108	58	29	24

*Questran started.

References

(ESP), N.E.S.P. Exome Variant Server. (Seattle, WA).

Adzhubei, I.A., Schmidt, S., Peshkin, L., Ramensky, V.E., Gerasimova, A., Bork, P., Kondrashov, A.S., and Sunyaev, S.R. (2010). A method and server for predicting damaging missense mutations. Nat Methods 7, 248-249.

Beil, U., Crouse, J.R., Einarsson, K., and Grundy, S.M. (1982). Effects of interruption of the enterohepatic circulation of bile acids on the transport of very low density-lipoprotein triglycerides. Metabolism 31, 438-444.

Berni Canani, R., Terrin, G., Cardillo, G., Tomaiuolo, R., and Castaldo, G. (2010). Congenital diarrheal disorders: improved understanding of gene defects is leading to advances in intestinal physiology and clinical management. J Pediatr Gastroenterol Nutr 50, 360-366.

Birch, A.M., Buckett, L.K., and Turnbull, A.V. (2010). DGAT1 inhibitors as anti-obesity and anti-diabetic agents. Curr Opin Drug Discov Devel 13, 489-496.

Buhman, K.K., Smith, S.J., Stone, S.J., Repa, J.J., Wong, J.S., Knapp, F.F., Jr., Burri, B.J., Hamilton, R.L., Abumrad, N.A., and Farese, R.V., Jr. (2002). DGAT1 is not essential for intestinal triacylglycerol absorption or chylomicron synthesis. J Biol Chem 277, 25474-25479.

Cao, G., Konrad, R.J., Li, S.D., and Hammond, C. (2012). Glycerolipid acyltransferases in triglyceride metabolism and energy homeostasis-potential as drug targets. Endocr Metab Immune Disord Drug Targets 12, 197-206.

Cao, J., Zhou, Y., Peng, H., Huang, X., Stahler, S., Suri, V., Qadri, A., Gareski, T., Jones, J., Hahm, S., Perreault, M., McKew, J., Shi, M., Xu, X., Tobin, J.F., and Gimeno, R.E. (2011). Targeting Acyl-CoA:diacylglycerol acyltransferase 1 (DGAT1) with small molecule inhibitors for the treatment of metabolic diseases. J Biol Chem 286, 41838-41851.

Cases, S., Smith, S.J., Zheng, Y.W., Myers, H.M., Lear, S.R., Sande, E., Novak, S., Collins, C., Welch, C.B., Lusis, A.J., Erickson, S.K., and Farese, R.V., Jr. (1998). Identification of a gene encoding an acyl CoA:diacylglycerol acyltransferase, a key enzyme in triacylglycerol synthesis. Proc Natl Acad Sci U S A 95, 13018-13023.

Cases, S., Stone, S.J., Zhou, P., Yen, E., Tow, B., Lardizabal, K.D., Voelker, T., and Farese, R.V., Jr. (2001). Cloning of DGAT2, a second mammalian diacylglycerol acyltransferase, and related family members. J Biol Chem 276, 38870-38876.

Harris, C.A., Haas, J.T., Streeper, R.S., Stone, S.J., Kumari, M., Yang, K., Han, X., Brownell, N., Gross, R.W., Zechner, R., and Farese, R.V., Jr. (2011). DGAT enzymes are required for triacylglycerol synthesis and lipid droplets in adipocytes. J Lipid Res 52, 657-667.

Hofmann, K. (2000). A superfamily of membrane-bound O-acyltransferases with implications for wnt signaling. Trends Biochem Sci 25, 111-112.

Krawczak, M., Thomas, N.S., Hundrieser, B., Mort, M., Wittig, M., Hampe, J., and Cooper, D.N. (2007). Single base-pair substitutions in exon-intron junctions of human genes: nature, distribution, and consequences for mRNA splicing. Hum Mutat 28, 150-158.

McLaren, D.G., He, T., Wang, S.P., Mendoza, V., Rosa, R., Gagen, K., Bhat, G., Herath, K., Miller, P.L., Stribling, S., Taggart, A., Imbriglio, J., Liu, J., Chen, D., Pinto, S., Balkovec, J.M., Devita, R.J., Marsh, D.J., Castro-Perez, J.M., Strack, A., Johns, D.G., Previs, S.F., Hubbard, B.K., and Roddy, T.P. (2011). The use of stable-isotopically labeled oleic acid to interrogate lipid assembly in vivo: assessing pharmacological effects in preclinical species. J Lipid Res 52, 1150-1161.

Nakada, Y., Aicher, T.D., Le Huerou, Y., Turner, T., Pratt, S.A., Gonzales, S.S., Boyd, S.A., Miki, H., Yamamoto, T., Yamaguchi, H., Kato, K., and Kitamura, S. (2010). Novel acyl coenzyme A (CoA): diacylglycerol acyltransferase-1 inhibitors: synthesis and biological activities of diacylethylenediamine derivatives. Bioorg Med Chem 18, 2785-2795.

Novartis (2011). DGAT1 Inhibitor Clinical Trial Results.

Project, G. (2010). A map of human genome variation from population-scale sequencing. Nature 467, 1061-1073.

Slatkin, M. (2004). A population-genetic test of founder effects and implications for Ashkenazi Jewish diseases. Am J Hum Genet 75, 282-293.

Smith, S.J., Cases, S., Jensen, D.R., Chen, H.C., Sande, E., Tow, B., Sanan, D.A., Raber, J., Eckel, R.H., and Farese, R.V., Jr. (2000). Obesity resistance and multiple mechanisms of triglyceride synthesis in mice lacking Dgat. Nat Genet 25, 87-90.

Streeper, R.S., Grueter, C.A., Salomonis, N., Cases, S., Levin, M.C., Koliwad, S.K., Zhou, P., Hirschey, M.D., Verdin, E., and Farese, R.V., Jr. (2012). Deficiency of the lipid synthesis enzyme, DGAT1, extends longevity in mice. Aging (Albany NY) 4, 13-27.

Terrin, G., Tomaiuolo, R., Passariello, A., Elce, A., Amato, F., Di Costanzo, M., Castaldo, G., and Canani, R.B. (2012). Congenital diarrheal disorders: an updated diagnostic approach. Int J Mol Sci 13, 4168-4185.

Willnow, T.E., and Herz, J. (1994). Genetic deficiency in low density lipoprotein receptor-related protein confers cellular resistance to Pseudomonas exotoxin A. Evidence that this protein is required for uptake and degradation of multiple ligands. J Cell Sci 107 (Pt 3), 719-726.

Yen, C.L., Stone, S.J., Koliwad, S., Harris, C., and Farese, R.V., Jr. (2008). Thematic review series: glycerolipids. DGAT enzymes and triacylglycerol biosynthesis. J Lipid Res 49, 2283-2301.

Yin, W., Carballo-Jane, E., McLaren, D.G., Mendoza, V.H., Gagen, K., Geoghagen, N.S., McNamara, L.A., Gorski, J.N., Eiermann, G.J., Petrov, A., Wolff, M., Tong, X., Wilsie, L.C., Akiyama, T.E., Chen, J., Thankappan, A., Xue, J., Ping, X., Andrews, G., Wickham, L.A., Gai, C.L., Trinh, T., Kulick, A.A., Donnelly, M.J., Voronin, G.O., Rosa, R., Cumiskey, A.M., Bekkari, K., Mitnaul, L.J., Puig, O., Chen, F., Raubertas, R., Wong, P.H., Hansen, B.C., Koblan, K.S., Roddy, T.P., Hubbard, B.K., and Strack, A.M. (2012). Plasma lipid profiling across species for the identification of optimal animal models of human dyslipidemia. J Lipid Res 53, 51-65.

Zamel, R., Khan, R., Pollex, R.L., and Hegele, R.A. (2008). Abetalipoproteinemia: two case reports and literature review. Orphanet J Rare Dis 3, 19.

Zhao, G., Souers, A.J., Voorbach, M., Falls, H.D., Droz, B., Brodjian, S., Lau, Y.Y., Iyengar, R.R., Gao, J., Judd, A.S., Wagaw, S.H., Ravn, M.M., Engstrom, K.M., Lynch, J.K., Mulhern, M.M., Freeman, J., Dayton, B.D., Wang, X., Grihalde, N., Fry, D., Beno, D.W., Marsh, K.C., Su, Z., Diaz, G.J., Collins, C.A., Sham, H., Reilly, R.M., Brune, M.E., and Kym, P.R. (2008). Validation of diacyl glycerolacyltransferase I as a novel target for the treatment of obesity and dyslipidemia using a potent and selective small molecule inhibitor. J Med Chem 51, 380-383.

Lipid Droplet Formation in Mammalian Cells Requires TG Synthesis

Abstract

The lipid droplet (LD) is a dynamic, ubiquitous organelle that is central to cellular energy homeostasis. There is wide belief that LDs form from the endoplasmic reticulum (ER) membrane, however experimental data supporting this is lacking. To fill this void, we established several cell systems by which lipid droplets could be induced from a null background. In each case, our systems were based on the ability to modulate triglyceride (TG) synthesis as blocking neutral lipid synthesis is the only currently available way to ablate LD formation completely. Using DGAT2-KO adipocytes differentiated in the presence of a DGAT1 inhibitor, we found that LD formation was perfectly correlated with the cell's ability to synthesize TG. Immediately upon formation, we observed perilipin-1 present on the lipid droplets' surface. In a permeabilzed cell model, we found that the cell's ability to form LDs was, again, perfectly correlated with TG synthesis. We also found that providing di-C8:0 diacylglycerols for the DGAT substrate induced much larger LDs than providing di-C18:1. Finally, we used a BODIPY-C12 (B12), a fluorescent fatty acid analog, to visualize LD formation in living cells. Consistent with the other cell models, we found B12 spots closely associated with the ER within minutes after addition to the cells. However, we did not see perilipin-2 or perilipin-3 staining these nascent spots. Moreover, we also observed B12-induced spots in mouse embryonic fibroblasts lacking both DGAT1 and DGAT2. We were ultimately unable to determine the identity of the lipid species in the B12 spots and cannot be sure they reflect the behavior of endogenous lipid droplets.

Introduction

The lipid droplet (LD) is a unique dynamic organelle whose importance to cellular lipid metabolism is just beginning to be appreciated. As the major storage depot for TG, it plays a key role in regulating cellular energy balance. We are just beginning to fully appreciate this role and the various pathways that affect LDs.

Recent studies have uncovered important biological processes that can affect LD size and number. Two independent genome wide screens performed in Drosophila cells found that knockdown of the COPI complex affects the ability of cells to access their LD TG stores (Beller et al., 2008; Guo et al., 2008). Similar screens in yeast identified the ortholog for Seipin (BSCL2) as a key mediator of LD number and size (Fei et al., 2008; Szymanski et al., 2007). Finally, fat storage inducing transmembrane protein 2 (FIT2M) was identified and characterized as a modulator of TG partitioning between the ER and LDs. Despite this recent progress, the question of how exactly LDs form remains unanswered.

There are several specific question related to LD formation which are active areas of research. Firstly, what defines an LD formation site? There is general agreement that LDs form from the ER, though this has never been experimentally confirmed (Murphy and Vance, 1999; Wolins et al., 2005). Diacyglycerol acyltransferase (DGAT)-1, one of two TG synthesis enzymes, localizes to the ER, while DGAT2 has some ER and mitochondria-associated membrane localization. Additionally, TG below a concentration of 2-3 % (w/w) is soluble in the membrane bilayer (Hamilton and Small, 1981) and predicted to be highly mobile therein (Khandelia et al., 2010). These data present a second problem of how TG becomes locally concentrated into the nascent droplet.

In the ER, Seipin (BSCL2)(Szymanski et al., 2007), Lipin (Pah1p) (Adeyo et al., 2011) and Fat-storage inducing transmembrane protein (FITM)-2 (Gross et al., 2011) have alternatively been proposed to help confine TG molecules into the nascent LD core. Similarly, PLIN2 (Robenek et al., 2006), PLIN3 (Skinner et al., 2009) and PLIN4 (Wolins et al., 2003) have been proposed to perform a similar function by trafficking to the ER from the cytoplasm through largely unknown mechanisms. For Seipin, Lipin and FITM2, most studies have focused on their effects on LDs at steady state, rather than during *de novo* LD formation per se. This discounts the contributions of LD catabolism that would affect the presence or absence of LDs at later timepoints. In the case of the PLIN proteins, there are no known functional homologs in yeast, yet they retain the ability to store neutral lipid in LDs. Additionally, more precise studies of LD formation have been hampered by the availability of model systems.

Here we present three new models to study LD formation directly. In each case, we focus on the ability to control cells' ability to synthesize TG as a means to control subsequent LD formation; this is the only proven way to block LD formation completely (Harris et al., 2011; Sandager et al., 2002). With these three systems, we find that whenever TG synthesis is active, LDs are formed and were unable to separate these processes. Using DGAT2-KO adipocytes treated with a chemical inhibitor of DGAT1, we found that nascent LDs were coated by PLIN1 almost immediately after formation. These nascent droplets were always visible close to ER markers and were not sensitive to inhibitors of de novo lipogenesis, protein trafficking, cytoskeletal transport or protein synthesis.

Using digitonin permeabilized cells, we found that cells did not require cytosol or energy to synthesize TG and form LDs as assessed by BODIPY staining. Moreover, treating

cells with N-ethylmaleimide, a cysteine-modifying reagent, had no effect on their ability to form LDs. Interestingly, using short chain diacylglycerols, we found that the nascent LD size was strongly affected. We believe this may be linked to the fact that shorter chain fatty acids modulate the physical properties of the membrane bilayer and may stabilize the bud neck of a nascent LD.

Finally, we wanted to investigate the relationship of nascent lipid droplets to other organelles and used COS7 cells as a well-established model in the field of ER membrane morphology and dynamics (Klemm et al., 2013; Niu et al., 2005; Shibata et al., 2010; Voeltz et al., 2006). We also employed a fluorescent fatty acid analog, BODIPY-C12 (B12), to maximize our ability to visualize newly synthesized TG molecules. We found that nascent spots induced from B12 were always close to fluorescently marked ER membranes. Interestingly, we found that nascent B12 spots were not coated by PLIN proteins, but were coated by these proteins after overnight treatment. Puzzlingly, B12 spots still formed in cells lacking DGAT1 and DGAT2 or cells treated with inhibitors of DGAT1 and DGAT2, suggesting the spots may not be made of TGs. Ultimately, we were unable to definitively determine the identity of the lipids generated by B12 treatment and are unsure of whether the behavior of the spots accurately reflects nascent LD behavior.

Methods

Chemicals and Reagents

All chemicals were purchased from Sigma-Aldrich (St. Louis, MO) unless otherwise noted. BODIPY-C12 was purchased from Invitrogen (Carlsbad, CA).

Cell Culture

All cell lines were grown in DMEM with 25 mM glucose (Invitrogen, Carlsbad, CA) with 10% fetal bovine serum (FBS, Thermo Scientific, Waltham, MA). For transfection studies, we used Lipofectamine 2000 (Invitrogen) according to manufacturer's instructions. Digitonin permeabilization was carried out as described previously (Urano et al., 2008). Mouse embryonic fibroblasts (MEFs) were isolated as described previously (Harris et al., 2011) and immortalized by serial passaging. For differentiation of MEFs, immortalized MEFs were transduced with a murine stem cell virus (MSCV) retrovirus expressing PPARγ2 under control of the CMV promoter. Cells were selected to produce a polyclonal line expressing PPARγ2.

DGAT2-KO Adipocyte Differentiation

Differentiation of DGAT2-KO MEFs was carried out as described previously (Harris et al., 2011). To block LD formation, differentiation media was supplemented with 75 μM A-922500 (Cayman Chemicals, Ann Arbor, MI), a potent, selective DGAT1 inhibitor.

Microscopy

The day before imaging, cells were split onto glass-bottomed culture plates (Matrical

Bioscience, Spokane, WA) and allowed to adhere. Cells were imaged using a Nikon 60X ApoTIRF objective 1.49NA or Nikon 100X ApoTIRF objective 1.49NA on a Nikon ECLIPSE Ti 2000 inverted microscope fitted with a Yokogawa CSU-X1 spinning disk and Hamamatsu ImagEM EM CCD camera. In some experiments, imaging was performed in wide field mode with a Photometrics Cool Snap HQ2 CCD camera.

Immunofluorescence

For immunofluorescence studies, cells were fixed with 4% paraformaldehyde (Sigma Aldrich, St. Louis, MO) and permeabilized as described previously (DiDonato and Brasaemle, 2003). Antiserum raised against Perilipin-1 was a gift from Dr. Dawn Brasaemle (Rutgers University). For mitochondria staining an antibody raised against Complex I was used (Invitrogen).

In Situ DGAT Assay

Cells were grown in 24 well dishes and permeabilized as described above. To measure DGAT activity, 0.625 mg/mL fatty acid free bovine serum albumin (BSA), 5 mM $MgCl_2$, 200 μM 1,2-dioleoylglycerol and 25 μM either ^{14}C-oleoyl-CoA or cold oleoyl-CoA were added to the permeabilization buffer (10 mM HEPES-KOH pH 7.4, 125 mM potassium acetate). The radioactive assay was carried out for 5 minutes after which lipids were extracted by the Bligh-Dyer method (Bligh and Dyer, 1959) and resolved by TLC as described previously (Cases et al., 1998).

Real Time Quantitative PCR

Total RNA was isolated using Trizol and converted to cDNA using a mixture of random hexamer and oligo dT primers with the iScript reverse transcriptase kit (Biorad,

Hercules, CA). cDNA was diluted 10 fold and used for subsequent quantitative PCR reaction using a 2X SYBR Green qPCR reagent (Applied Biosystems, Foster City, CA). Primers were verified for efficiency and linearity prior to use.

Thin Layer Chromatography

For analysis of neutral lipids, a solvent system composed of hexanes:diethyl ether:glacial acetic acid (80:20:1) was used. For analysis of polar lipids, the solvent system contained methy acetate:isopropanol:chloroform:methanol:0.25% KCl (25:25:25:10:9).

Results

Inducible formation of lipid droplets in adipocytes using a chemical inhibitor

To begin to understand the process of lipid droplet formation, we first sought to build a model system in which formation could be rapidly induced from a null background. We have previously reported that murine adipocytes that lack DGAT1 and DGAT2 are totally devoid of lipid droplets, yet retain characteristics of adipocytes including adipose-specific gene expression and stimulated lipolysis (Harris et al., 2011). With the commercial availability of DGAT1 inhibitors, we established conditions for differentiating DGAT2-KO adipocytes in the presence of a DGAT1 inhibitor such that no LDs were formed during the differentiation protocol (**Figure 4.1A**). We loaded DGAT2-KO fibroblasts with 500 μM oleic acid and co-treated with increasing amounts of DGAT1 inhibitor. We found that it was possible to completely ablate TG formation in this system at 25 μM inhibitor (**Figure 4.1B**). To maintain an LD-null background throughout the adipocyte differentiation protocol, we determined that 75 μM inhibitor was required (data not shown). This concentration of inhibitor was used for all subsequent studies in the adipocytes.

To establish the timeframe for recovery of TG synthesis, and thus LD formation, we differentiated DGAT2-KO adipocytes in the presence of the DGAT1 inhibitor and measured the accumulation of TG upon release of the inhibitor by TLC (**Figure 4.1C**). Within 2 hours we saw an increase in TG synthesis that continued through 24 hours post release. As another, more sensitive assay of TG synthesis, we measured the incorporation of ^{14}C-oleate into TG (**Figure 4.1D**). In the presence of the inhibitor, TG synthesis is reduced more than 95%. After release, ^{14}C-oleate incorporation increased roughly two-fold within the first 30 mins

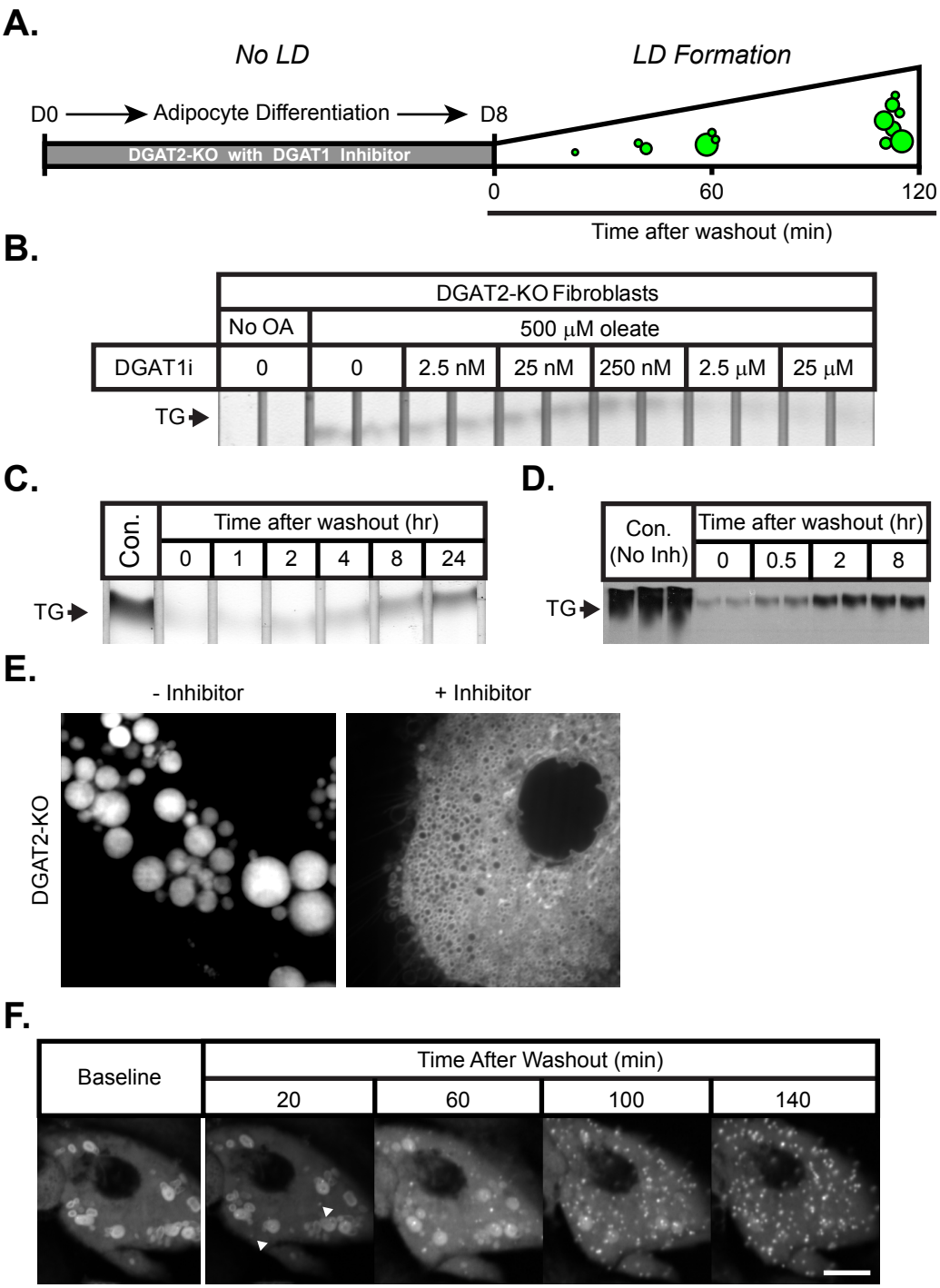

Figure 4.1: Lipid droplet formation correlates with TG synthesis in DGAT2-KO adipocytes. A. A schematic of the LD formation system. **B.** Titration of DGAT1 inhibitor to suppress TG synthesis in DGAT2-KO fibroblasts. **C.** Total TG mass accumulation after release of DGAT1 inhibitor in DGAT2-KO adipocytes. **D.** ^{14}C-oleate incorporation into TG after release of DGAT1 inhibitor in DGAT2-KO adipocytes. **E.** BODIPY staining of LDs in DGAT2-KO adipocytes with or without DGAT1 inhibitor. **F.** Timecourse of LD spot formation in DGAT2-KO adipocytes after release of DGAT1 inhibitor.

and up to 5.5-fold by 8 hours. These two results indicate that recovery of TG synthesis after inhibitor treatment is rapid and we should expect to see initial LD formation within 30 to 60 minutes after removing the inhibitor.

To visualize nascent LDs, we incubated DGAT2-KO adipocytes with BODIPY 493/503 (BODIPY), a vital dye that is well established for staining neutral lipids (Gocze and Freeman, 1994). To verify that LD formation was indeed inhibited in our working conditions, we stained DGAT2-KO adipocytes differentiated in the presence or absence of inhibitor (**Figure 4.1E**). As reported (Harris et al., 2011), DGAT2-KO adipocytes differentiated without inhibitor have abundant cytosolic LDs and are indistinguishable from WT adipocytes in this respect (**Figure 4.1E,** left, data not shown). Those that had been treated with inhibitor have no apparent LDs. Only background staining of the hydrophobic membranes is visible. (**Figure 4.1E**, right).

To determine the earliest time point at which LDs are visible, we performed live-cell imaging with BODIPY-stained adipocytes (**Figure 4.1F**). Prior to release of the inhibitor, only background staining of BODIPY is visible in cells. Within 20 minutes of the release, most cells show small punctae that continue to grow and accumulate for as long as we were able to follow the cells, more than 14 hours. These results demonstrate that TG synthesis and LD formation in DGAT2-KO adipocytes can be completely ablated by treatment with a reversible, competitive DGAT1 inhibitor. Further, recovery of TG synthesis and LD formation occurs within minutes after inhibitor release.

Nascent LDs form close to the ER and acquire PAT proteins almost immediately after formation

The findings of several groups has suggested that upon formation, LDs are constitutively coated by PAT proteins (Brasaemle et al., 1997; Dalen et al., 2007; Greenberg et al., 1991; Wolins et al., 2003). To test whether the BODIPY-stained spots act like LDs in that respect, we performed immunostaining for Perilipin 1 (PLIN1), the major adipocyte PAT protein. We found that PLIN1 was always coating the BODIPY-positive spots after inhibitor release (**Figure 4.2A**). Due to the dramatic change of fluorescence after inhibitor release, we suspected PLIN1 protein levels might be changing as it relocalizes on to the LD surface. To this end, we measured PLIN1 protein levels immediately after DGAT1 inhibitor release (**Figure 4.2B**). By Western blot, PLIN1 protein levels were stable over 8 hours. We were also interested in the localization of PLIN2 after LD formation (**Figure 4.2C**, top) and found it coated nascent LDs within 30 minutes of formation.

Because the enzymes that synthesize neutral lipids localize to the ER, there is general consensus that LDs form from ER membranes (Murphy and Vance, 1999). However, there is no direct experimental evidence supporting this idea. To investigate where the nascent LDs formed in this system, we performed live-cell fluorescence microscopy or immunofluorescence against markers for the ER and mitochondria. As expected, nascent LDs were first visible close to the ER markers KDEL and Sec61β **(Figure 4.2C**, middle). By contrast, mitochondria were more often separated from the LD markers (**Figure 4.2C**, lower). Altogether, these results confirm that the BODIPY-positive spots are nascent LDs and that they likely come from the ER or some very closely associated membranes.

Inhibitors of triglyceride synthesis block lipid droplet formation

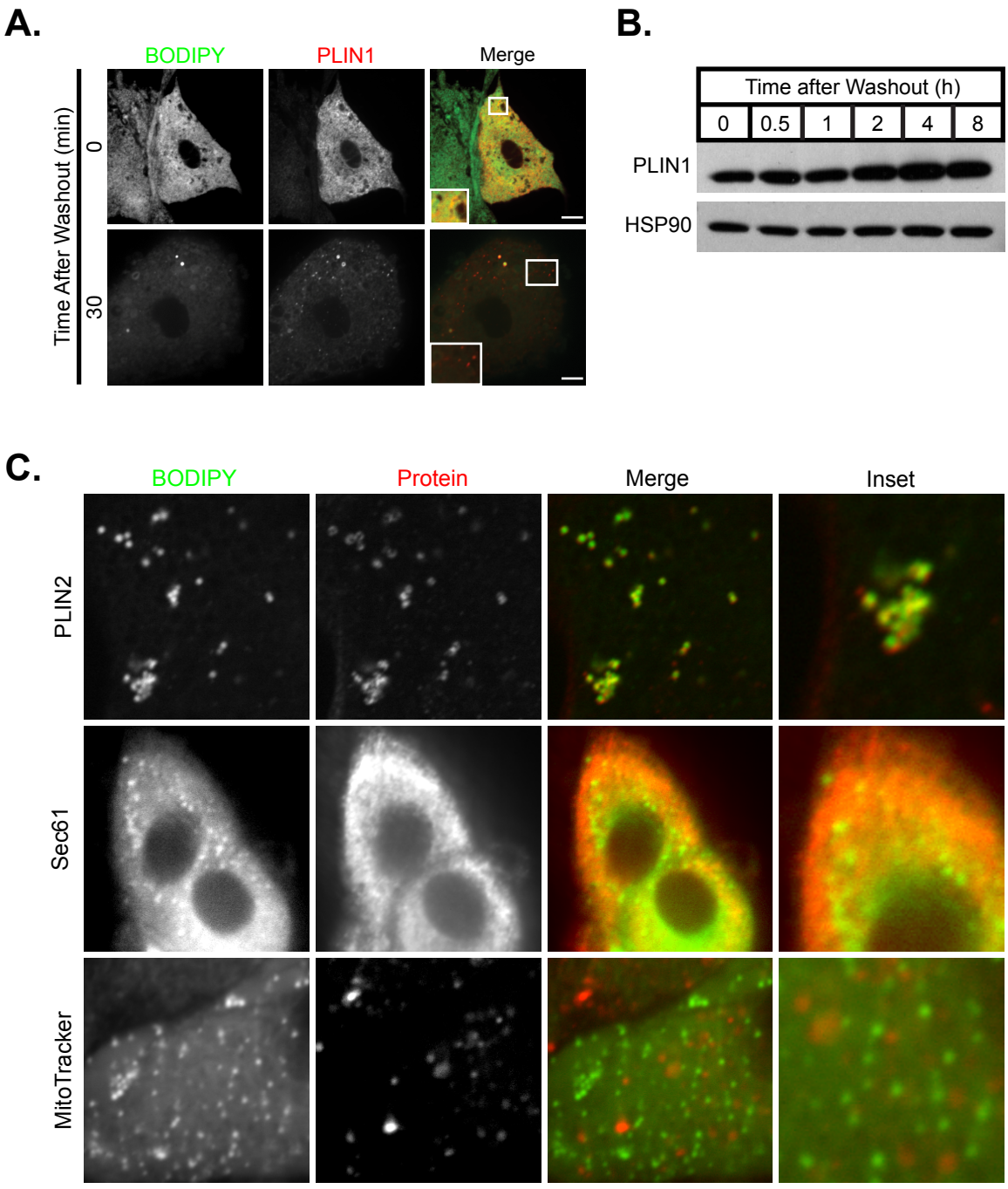

Figure 4.2. Nascent LDs are marked by PLIN Proteins and close to the ER. DGAT2 KO adipocytes were differentiated and treated with a DGAT1 inhibitor. Cells were fixed and stained at various timepoints after release of inhibitor. **A.** PLIN1 immunostaining at 0 and 30 minutes after inhibitor release. **B.** A Western blot of PLIN1 protein levels at various times after inhibitor release. **C.** Organelle markers of LDs (PLIN2), ER (Sec61) and mitochondria (Mitotracker Red) were visualized with nascent LDs 30 mins after inhibitor release.

We next wanted to determine what cellular processes might affect lipid droplet formation. We treated cells with the inhibitors nocodazole, brefeldinA, cycloheximide and latrunculinA. In each case, the cells were still able to make LDs that appeared qualitatively normal (**Figure 4.3A**). Without a strong phenotype, we decided to focus on inhibitors of de novo lipogenesis and the Kennedy pathway. Here we found that only inhibitors that also disrupted TG synthesis were capable of blocking LD formation (**Figure 4.3B-C**). Taken together, these results indicate LD formation explicitly requires TG synthesis and may not require the cytoskeleton, protein trafficking or new protein synthesis.

Increased triglyceride synthesis leads to increased lipid droplets

To determine whether we could separate TG synthesis from LD formation, we developed a digitonin permeabilized cell system to more easily manipulate DGAT substrates (oleoyl-CoA and 1,2-diacylglycerol) and cytosolic protein composition. We first measured DGAT activity in permeabilized cells in the presence or absence of a DGAT1 inhibitor (D1i), a DGAT2 inhibitor (D2i) or both inhibitors (**Figure 4.4A**). We confirmed that in vitro activity is dominated by DGAT1 (Cases et al., 2001), and that the dual inhibition completely ablates TG formation (Harris et al., 2011). We next wanted to determine whether TG synthesis in this system was affected by the addition of cytoplasm and/or an energy regeneration system (**Figure 4.4B**). To be sure that the newly formed TG was being packaged into LDs, we imaged permeabilized cells before and 100 minutes after addition of the DGAT substrates (**Figure 4.4C**). Again, we observed numerous new BODIPY-positive

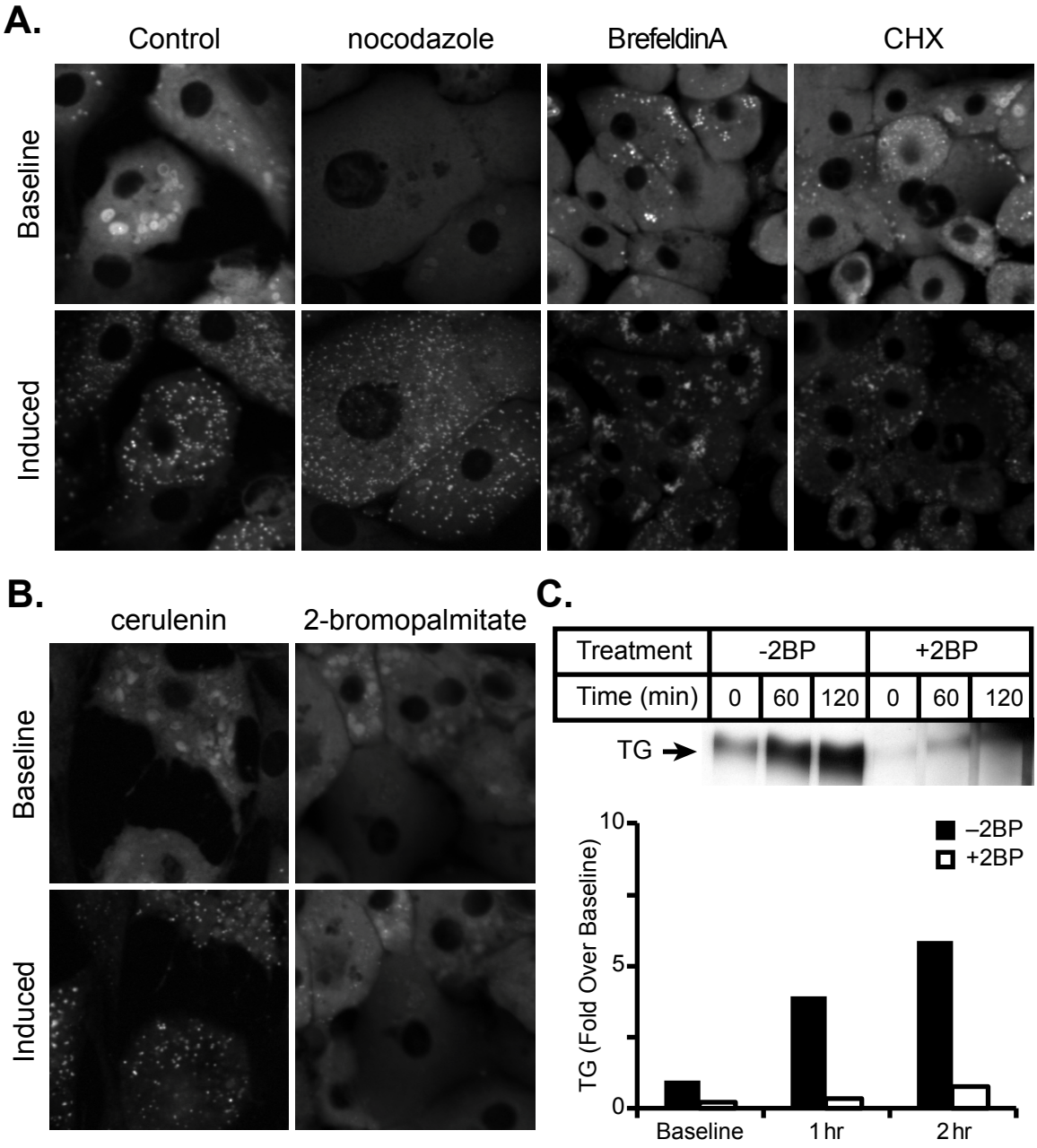

Figure 4.3: Only inhibitors which block TG synthesis also block LD Formation. A. Treatment of DGAT2-KO adipocytes with nocodazole, brefeldinA or cycloheximide does not affect their ability to form LDs. **B.** While the fatty acid synthase inhibitor cerulenin does not block LD formation, treatment with 2-bromopalmitate does. This is due to a strong decrease in TG synthesis. **C.** Using a 14C tracer, we measured TG synthesis in control and 2-bromopalmitate treated cells.

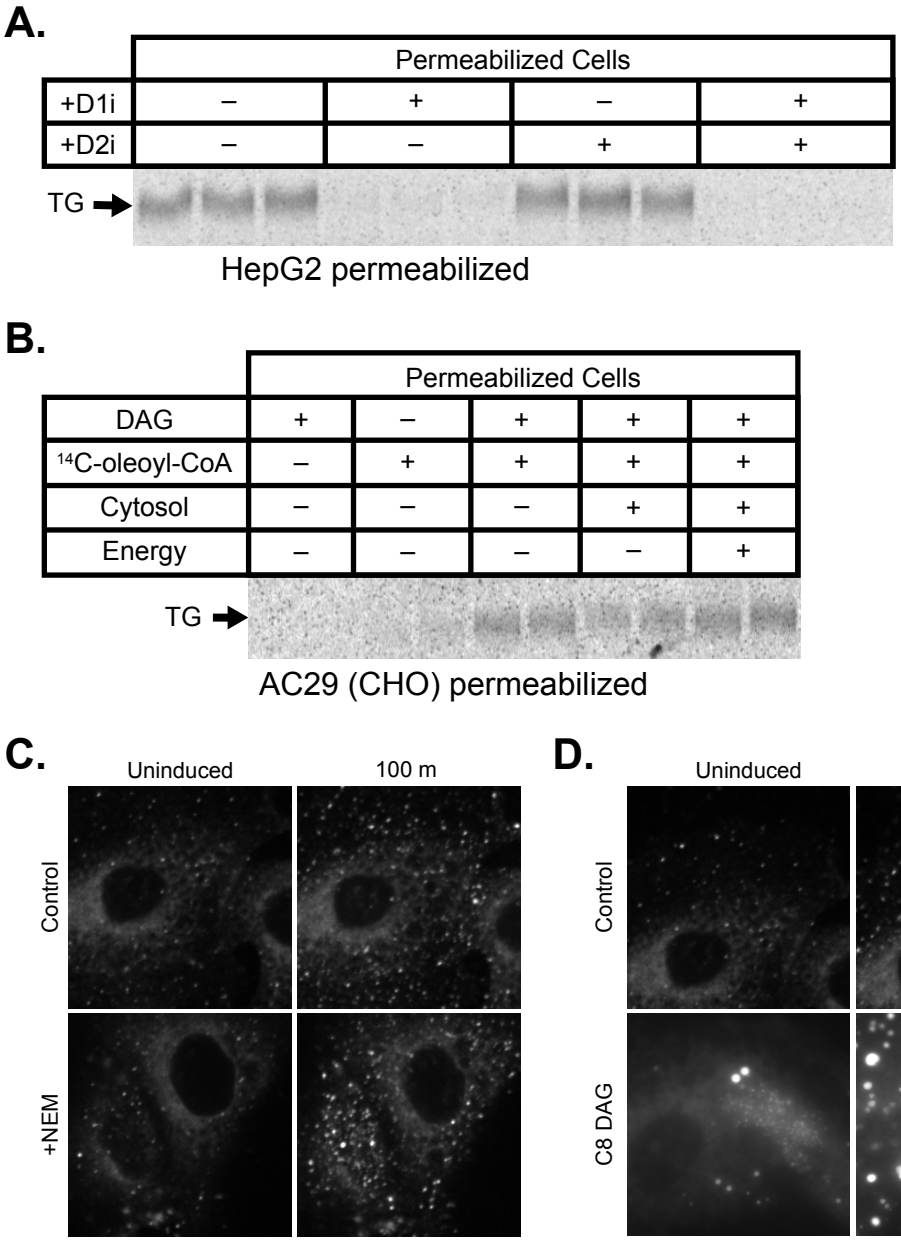

Figure 4.4: Triglyceride synthesis and LD formation remains intact in permeabilized cells. A. DGAT activity in permeabilized cells measured in situ as described in methods. **B.** The effect of cytosol and energy on DGAT activity in permeabilized cells. **C.** LD Formation in permeabilized cells as assessed by BODIPY 493/503 staining. Cells were treated or not with N-ethylmaleimide. **D.** Permeabilized cells were treated with either di-C18:1 (control) or di-C8:0 diacylglycerols.Di-C8:0 treated cells make dramatically larger lipid droplets.

spots 100 minutes after substrate suggesting that LD formation and TG synthesis are inextricably connected.

Due to these findings, we suspected the physical properties of TG accumulation may dominate the process of LD formation, rather than protein influence. Thus, we substituted dioctanoylglycerol (diC8:0) for dioleoylglycerol (diC18:1) in the DGAT substrate mixture provided to the permeabilized cells (**Figure 4.4D**). As shown previously, cells provided the usual di-C18:1 substrate developed many small lipid droplets that were visible within 100 minutes of addition. Cells provided the di-C8:0 substrate initially formed small droplets and these rapidly grew to an apparent size much larger than those with di-C18:1. These findings suggest that forming LD size can be modulated through alterations in substrate chain length or other potential modulators of surface and line tension.

Treatment with fluorescent fatty acids induces formation of lipid droplet-like spots

Finally, we sought to develop a model system in which we could visualize LD formation in the context of organelle structure. COS7 cells are a well established model that has been used for years to investigate the structure of the ER and its connections to other organelles (Klemm et al., 2013; Niu et al., 2005; Shibata et al., 2010; Voeltz et al., 2006). Growing cells in normal media, we observed many cytosolic LDs that averaged 410 nm in size (**Figure 4.5A**). Because we wanted to focus on de novo LD formation, we treated cells overnight with 2 μM TriacsinC in normal media. Upon staining these cells with BODIPY, we observed a complete loss of cytosolic LDs and only the background membrane staining was visible (**Figure 4.5B**). Interestingly, the LD size distribution in these cells suggested they might lack the LD-localized TG synthesis enzymes (DGAT2, AGPAT3 and GPAT4) that are

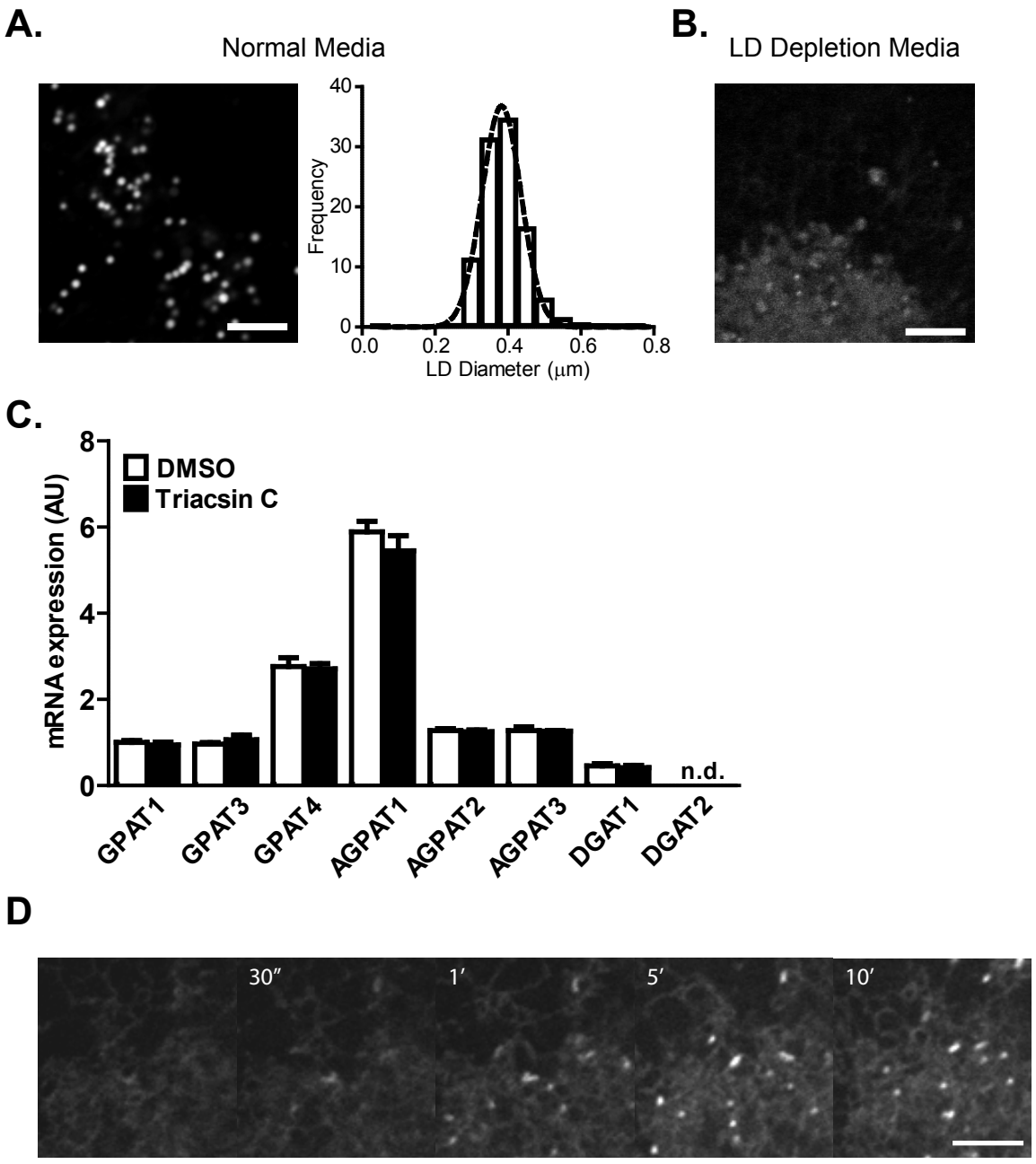

Figure 4.5: A COS7 cell model for induced LD formation using fluorescent fatty acid BODIPY-C12. A. COS7 cells make LDs when cultured in normal media. The lipid droplet size forms a normal distribution with mean 410 nm. **B.** Culturing cells in triacsinC depletes existing LDs. **C.** mRNA expression measurements indicate COS7 cells do not express DGAT2. **D.** Spots form within minutes after treatment with Bodipy-C12.

important for droplet growth (Wilfling et al., 2013). We measured gene expression of the TG synthesis enzymes and confirmed that mRNA for *DGAT2* was undetectable using two sets of primers, while the entire pathway of ER-localized enzymes was detected (**Figure 4.5C**). To determine whether we could observe nascent LD formation using B12, we performed live-cell imaging of LD-depleted cells immediately upon addition of B12 to the culture media. Within minutes, BODIPY-positive foci were visible at multiple spots throughout the cell (**Figure 4.5D**). These results suggest COS7 cells treated with B12 could be used to visually interrogate LD formation in living cells.

BODIPY-C12 induced spots initially appear close to endoplasmic reticulum

Though it is widely believed that LDs form from the ER, direct experimental evidence of this has never been observed. We sought to address this question in our COS7 cell model by expressing fluorescent markers of various cellular organelles and imaging them concomitantly with B12 treatment. We observed B12-induced spots close to ER within minutes after addition to cell culture media (**Figure 4.6A**). To quantify this behavior, we manually selected spots in the first image they were visible (usually 1-2 mins after addition) and measured the smallest radius from each spot that would encompass a red organelle marker. We found that spots localized close to the ER signal ~98% of the time, while mitochondria, golgi, and ERGIC had less than 40% overlap (**Figure 4.6B**). Because of the high density of ER, we wanted to be sure that the high degree of overlap was statistically different from a random result. We simulated random LD sites on the observed ER networks and plotted the distance from the ER as before. We found that simulated LDs overlapped with ER signal only 85% of the time, and that the distribution of distances measured in the

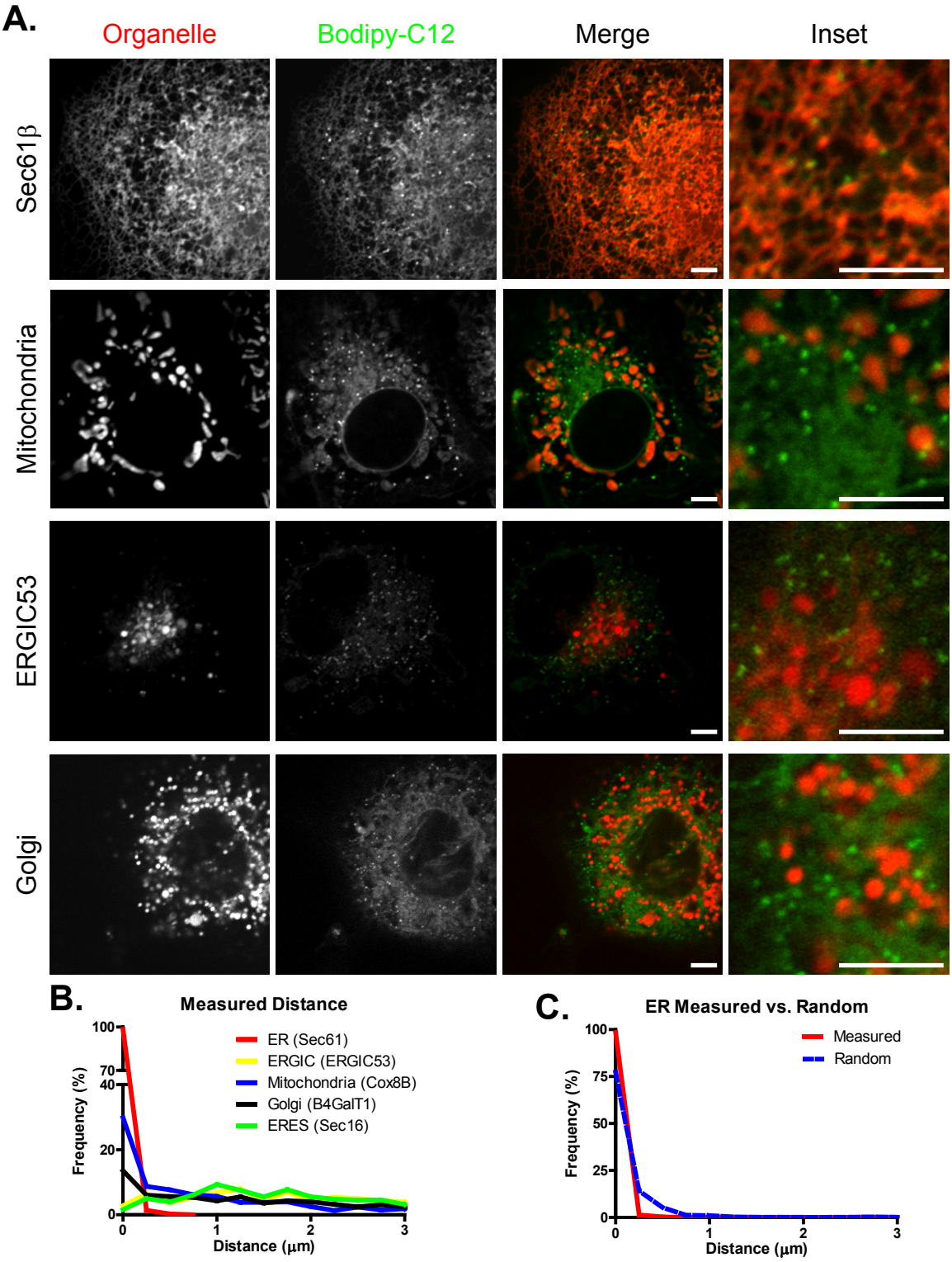

Figure 4.6: BODIPY-C12 spots initially appear close to the ER. A. Expression of organelle markers comparing localization B12 (green) and the organelle marker (red). **B.** Quantification of the distance between each B12 spot and the closest organelle marker. **C.** Comparison between experimentally measured and randomly simulated LD localization for overlap with ER markers.

experimental and simulated conditions was statistically different (**Figure 4.6C**). These data strongly support the idea the ER membrane is the donor membrane that gives rise to LDs.

BODIPY-C12 is incorporated into unidentifiable glycerolipids

We have previously been unable to visualize nascent LDs using oleate (data not shown). We suspected that the signal of BODIPY may be too low to visualize nascent LDs as compared to the much larger mature lipid droplets. To overcome this limitation, we decided to use BODIPY-conjugated fatty acids to give a ratio of 1:1 up to 3:1 of fluorophores to TG molecules. However, previous reports suggested BODIPY-C12 (B12) may not behave like an endogenous fatty acid (Huang et al., 2002; Kuerschner et al., 2008). We compared B12 and oleate treatment of COS7 cells that had been depleted of LDs. At 2 hours and 16 hours after treatment, B12-treated cells and oleate were indistinguishable with respect to LD size and morphology (**Figure 4.7A**).

We next wanted to investigate whether the biochemical species of lipids produced by B12 and oleate were similar at early time points. We treated cells with 50 μM B12 or 0.5 μCi/mL ^{14}C oleate, and separated neutral lipid species by TLC. Within 5 minutes, ^{14}C oleate is incorporated into triglyceride, consistent with the timing of the appearance of B12 spots (**Figure 4.7B**). Similarly, B12 is incorporated into many glycerolipid species (**Figure 4.7C**), but they run significantly slower than the endogenous oleate lipids (**Figure 4.7D**). To verify that the prominent band is a DGAT product, we treated cells with DGAT1 and DGAT2 inhibitors together (**Figure 4.8A**). In this case, band 1 is uniquely sensitive to DGAT inhibition and strongly suggests it is a TG species. Band 2 is also somewhat sensitive and may also be a TG. Finally, we labeled cells with ^{3}H-glycerol simultaneously with B12 and

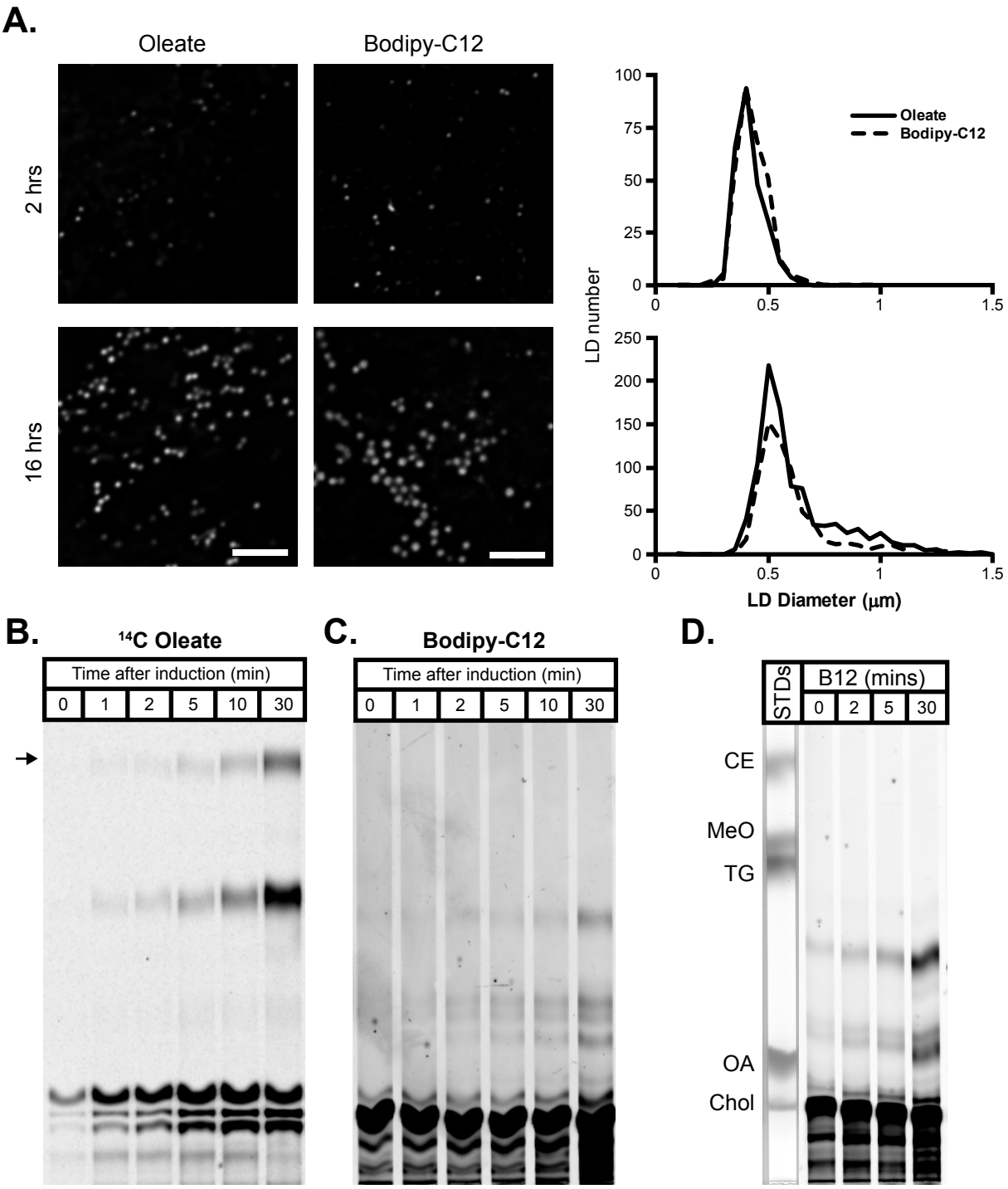

Figure 4.7: Bodipy-C12 and Oleate are incorporated into glycerolipids at similar timepoints. A. Oleate and B12 treatment at 2 hours and 16 hours gives similar morphology and size of LDs. **B.** 14C oleate incorporation into neutral lipids over a timecourse. TG (arrow) accumulates within minutes after addition **C.** B12 incorporation into neutral lipids occurs within minutes, though the lipids do not comigrate with their endogenous lipid counterparts. **D.** Direct comparison of B12 neutral lipids and normal lipid standards (STDs)

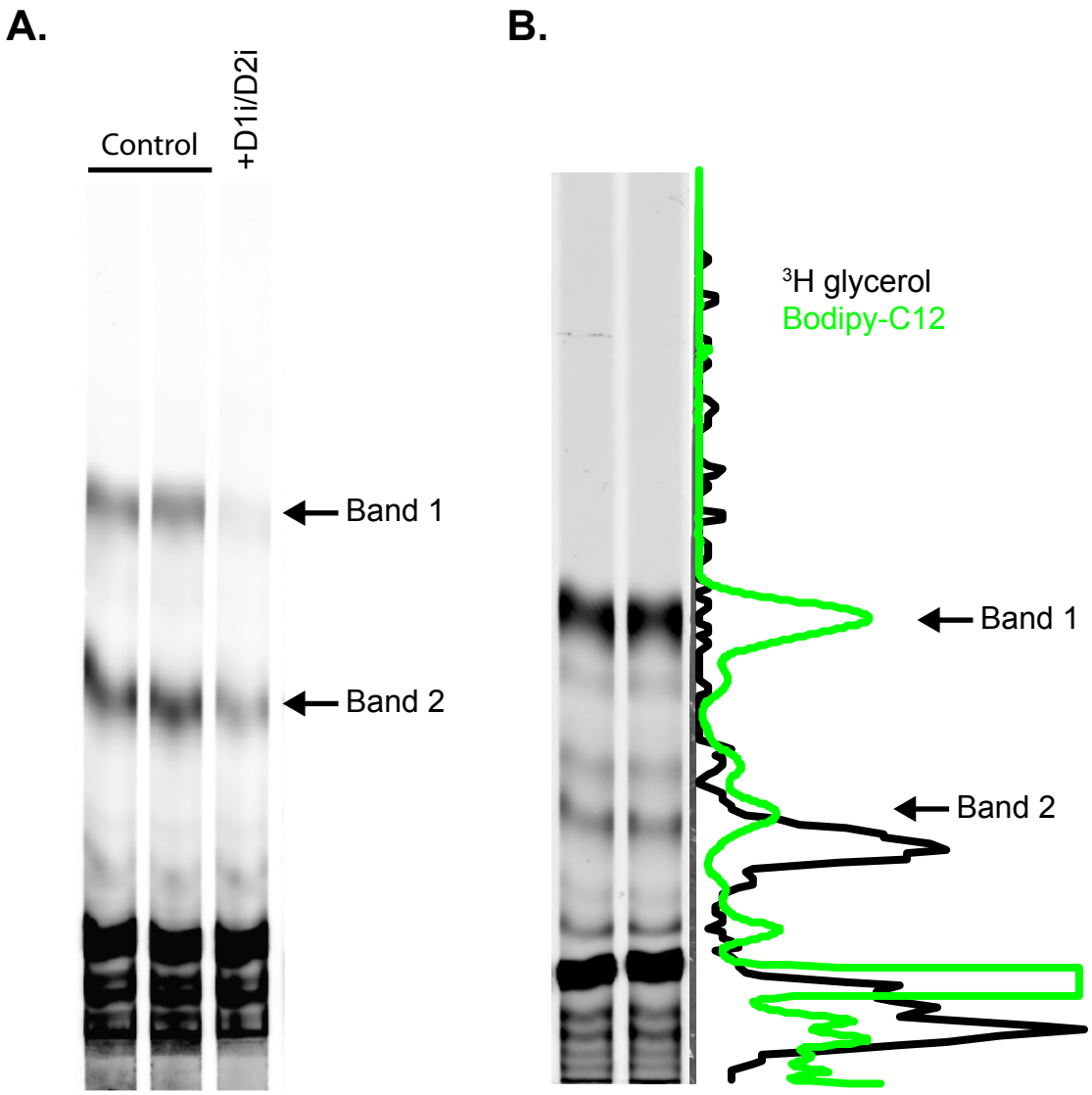

Figure 4.8 Bodipy-C12 lipid species are sensitive to DGAT inhibitors and do include a glycerol backbone. A. B12 incorporation for 1 hour in COS7 cells treated or untreated with DGAT1 and DGAT2 inhibitors (+D1i/D2i). **B.** B12 and ^{3}H glycerol were given to COS7 cells for 1 hour and lipids were resolved by TLC. The corresponding traces are included at the right. The image is the B12 fluorescence image.

resolved lipids by TLC (**Figure 4.8B**). We found that band 1, which has the same R_f as the band sensitive to the DGAT inhibitors, does not have an associated peak in the glycerol spectrum. However, band 2 and band 3 do have accompanying glycerol peaks, indicating they are glycerolipids.

Spots resulting from BODIPY-C12 may not be LDs

We next wanted to determine whether PAT proteins coat these BODIPY-C12 spots at early time points. This behavior of the PAT proteins has been widely described and would be strong evidence that the B12 spots are, in fact, nascent LDs. We expressed PLIN2 in COS7 cells and imaged them immediately after adding B12 to the culture media (**Figure 4.9A**). As seen in previous experiments, B12 induces formation of spots within minutes of addition. However, PLIN2 could not be seen coating these nascent spots. Interestingly, after overnight treatment with B12, PLIN2 forms clear rings around the B12 spots. PLIN3 was also investigated in this way and exhibited the same behavior (data not shown). These results suggest that B12-induced spots may not be LDs at the nascent stage, but do become LDs.

We also hypothesized that including DGAT inihibitors or other inhibitors of lipid metabolism should also inhibit B12 spot formation. We first treated cells with 2-bromopalmitate (2BP), which was sufficient to block LD formation in the DGAT2-KO adipocyte model. Indeed, 2BP was sufficient to block B12 spot formation (**Figure 4.9B**). Conversely, treatment with the DGAT inhibitors was not sufficient to block B12 spots. Inspection of the lipid species by TLC showed that several bands were ablated by 2BP treatment (**Figure 4.9C**). We concluded that nascent B12 spots may not be composed solely of TG species, but may also include other fatty acid metabolites.

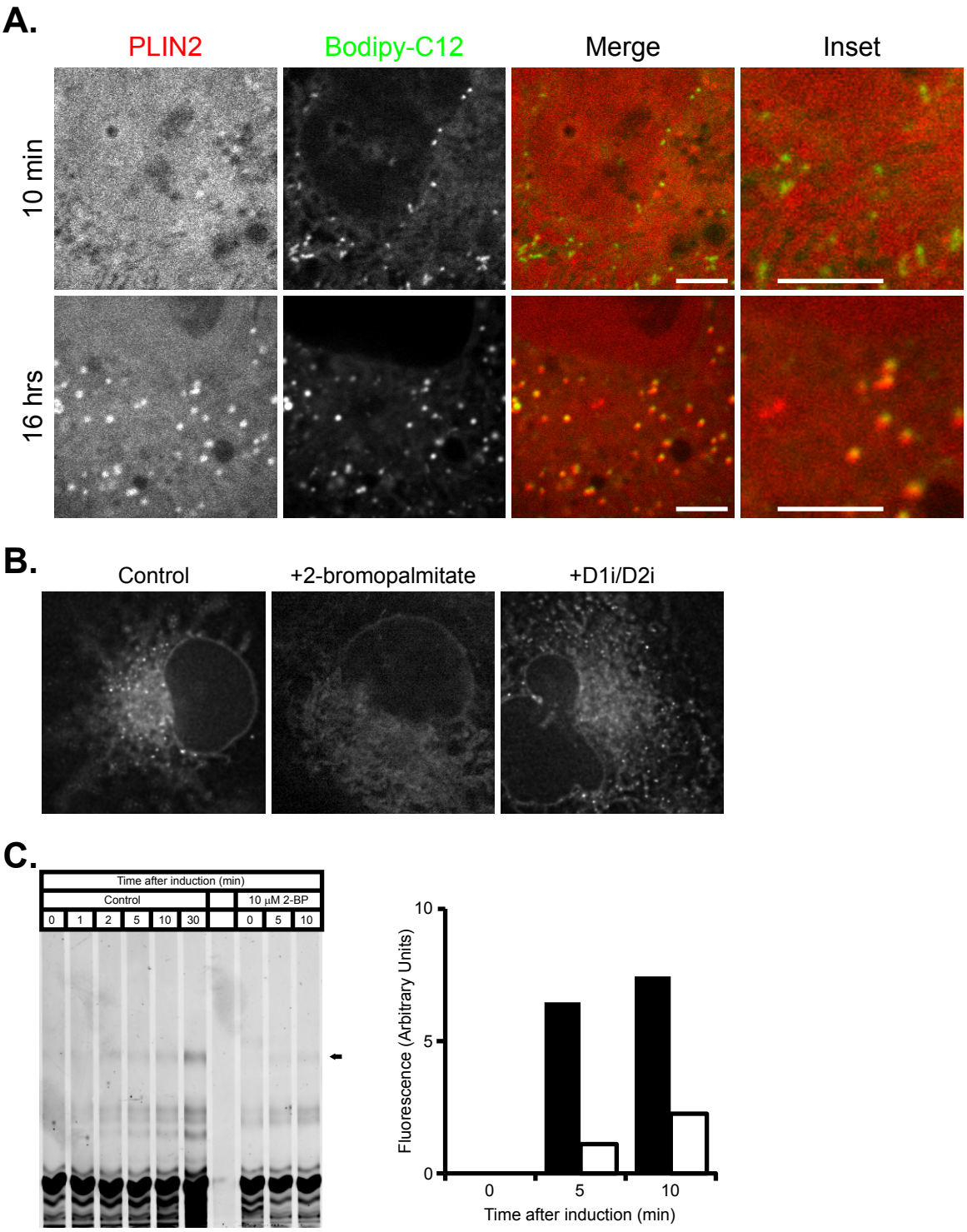

Figure 4.9: BODIPY-C12 spots are not only TGs. A. Expressing PLIN2 in COS7 cells did not mark B12 spots after 10 min of treatment, but did mark spots after overnight treatment. **B.** Cotreatment with 2-BP was sufficient to block B12 spot formation, but treatment with DGAT inhibitors was not. **C.** 2-BP treatment severely reduces B12 incorporation by TLC.

BODIPY-C12 spots are not affected by genetic loss of DGATs

In the DGAT2-KO adipocyte model, spot formation was explicitly correlated with DGAT activity (**Figure 4.1F**). To this end, we treated MEFs that lacked both DGATs with B12 and imaged them to observe spot formation. As expected, WT MEFs formed many spots in a pattern reminiscent of that seen in COS7 cells (**Figure 4.10A**). Surprisingly, DGAT1,2-KO MEFs also produced spots in response to B12 treatment. As previous results highlighted, it is possible that the early time points of B12 treatment may not accurately reflect nascent LDs, while later time points (hours) may more faithfully reproduce native LD behavior (**Figure 4.8B**). Thus, we treated WT and DGAT1,2-KO cells for 4 hours with B12 and costained cells with LipidTOX Red, another neutral lipid stain (**Figure 4.10B**). At this timepoint, B12 spots in the WT colicalized with LipidTOX Red, while those spots in the DGAT1,2-KO MEFs did not colocalize with the B12 spots. These results again suggest B12 spots may be derived from other fatty acid metabolites and not purely TG. While this may still reflect nascent LD behavior, we are unable to conclude with any certainty at this time.

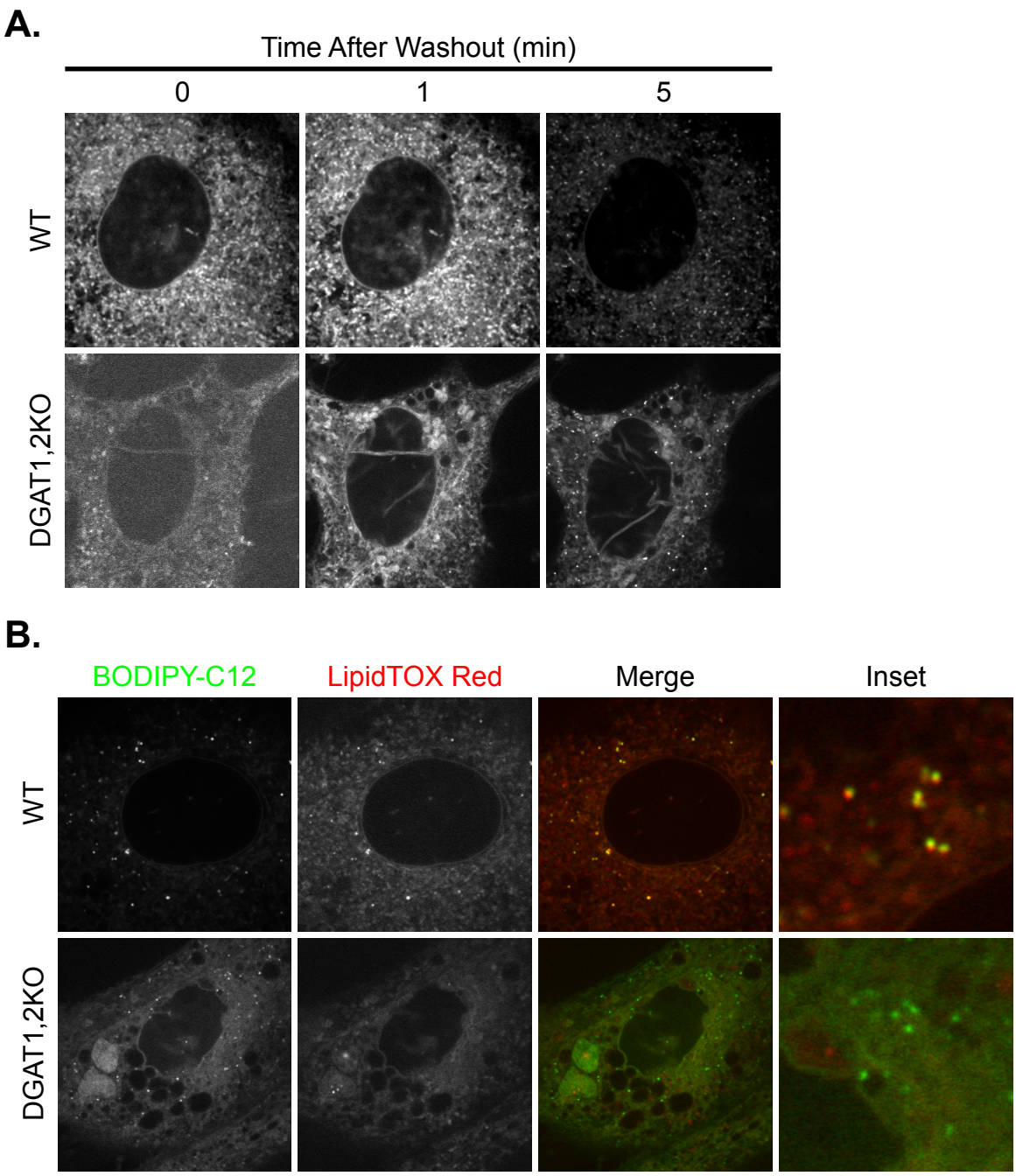

Figure 4.10: BODIPY-C12 spots may not reflect nascent LD behavior but do at later timepoints. A. B12 treatment of WT and DGAT1,2KO MEFs shows both cell types are capable of forming spots within minutes. **B.** After 2 hours of treatment, only B12 positive spots in WT MEFs also stain with LipidTOX Red, while the spots present in DGAT1,2-KO do not.

Discussion

Here we present three models that are capable of controlled, inducible formation of TG LDs from a null background. Using adipocytes lacking DGAT2, we established conditions for chemical inhibition of DGAT1 to completely block LD formation through the process of adipocyte differentiation. With this model, we found that LD formation was insensitive to inhibitors of protein synthesis, the secretory pathway and the cytoskeleton. Nascent LDs were always coated by PAT proteins, and stained specifically with BODIPY, a vital dye for visualizing neutral lipids. Indeed, treatments that altered the cells' ability to synthesize TG were effective in blocking LD formation.

We next developed a system of digitonin permeabilized cells to attempt to determine whether TG synthesis could be dissociated from LD formation. We found that permeabilized cells were capable of synthesizing TG and this was not influenced by the presence of cytosol, nor did it require an energy regeneration system. As seen previously, the majority of TG synthesis activity was derived from DGAT1 and it could be completely ablated by addition of DGAT1 and DGAT2 inhibitors together. As long as cells were able to synthesize TG, they were also able to form LDs as assessed by BODIPY staining.

Finally, we used a fluorescent fatty acid analog (B12) to attempt to interrogate the very early stages of LD formation. Nascent spots induced by B12 treatment in cells were seen always close to the ER, and were similar in size and morphology to oleate-induced LDs after hours of treatment. However, the nascent B12 spots were not coated by PLIN2 or PLIN3 and were not sensitive to inhibition or genetic ablation of the DGAT enzymes. Ultimately, we were unable to definitively determine whether the spots induced by B12

treatment were, in fact, TGs and cannot rule out that their presence is in some way artifactual.

References

Adeyo, O., Horn, P.J., Lee, S., Binns, D.D., Chandrahas, A., Chapman, K.D., and Goodman, J.M. (2011). The yeast lipin orthologue Pah1p is important for biogenesis of lipid droplets. J Cell Biol 192, 1043-1055.

Beller, M., Sztalryd, C., Southall, N., Bell, M., Jackle, H., Auld, D.S., and Oliver, B. (2008). COPI complex is a regulator of lipid homeostasis. PLoS Biol 6, e292.

Bligh, E.G., and Dyer, W.J. (1959). A rapid method of total lipid extraction and purification. Can J Biochem Physiol 37, 911-917.

Brasaemle, D.L., Barber, T., Wolins, N.E., Serrero, G., Blanchette-Mackie, E.J., and Londos, C. (1997). Adipose differentiation-related protein is an ubiquitously expressed lipid storage droplet-associated protein. J Lipid Res 38, 2249-2263.

Cases, S., Smith, S.J., Zheng, Y.W., Myers, H.M., Lear, S.R., Sande, E., Novak, S., Collins, C., Welch, C.B., Lusis, A.J., Erickson, S.K., and Farese, R.V., Jr. (1998). Identification of a gene encoding an acyl CoA:diacylglycerol acyltransferase, a key enzyme in triacylglycerol synthesis. Proc Natl Acad Sci U S A 95, 13018-13023.

Cases, S., Stone, S.J., Zhou, P., Yen, E., Tow, B., Lardizabal, K.D., Voelker, T., and Farese, R.V., Jr. (2001). Cloning of DGAT2, a second mammalian diacylglycerol acyltransferase, and related family members. J Biol Chem 276, 38870-38876.

Dalen, K.T., Dahl, T., Holter, E., Arntsen, B., Londos, C., Sztalryd, C., and Nebb, H.I. (2007). LSDP5 is a PAT protein specifically expressed in fatty acid oxidizing tissues. Biochim Biophys Acta 1771, 210-227.

DiDonato, D., and Brasaemle, D.L. (2003). Fixation methods for the study of lipid droplets by immunofluorescence microscopy. J Histochem Cytochem 51, 773-780.

Fei, W., Shui, G., Gaeta, B., Du, X., Kuerschner, L., Li, P., Brown, A.J., Wenk, M.R., Parton, R.G., and Yang, H. (2008). Fld1p, a functional homologue of human seipin, regulates the size of lipid droplets in yeast. J Cell Biol 180, 473-482.

Gocze, P.M., and Freeman, D.A. (1994). Factors underlying the variability of lipid droplet fluorescence in MA-10 Leydig tumor cells. Cytometry 17, 151-158.

Greenberg, A.S., Egan, J.J., Wek, S.A., Garty, N.B., Blanchette-Mackie, E.J., and Londos, C. (1991). Perilipin, a major hormonally regulated adipocyte-specific phosphoprotein associated with the periphery of lipid storage droplets. J Biol Chem 266, 11341-11346.

Gross, D.A., Zhan, C., and Silver, D.L. (2011). Direct binding of triglyceride to fat storage-inducing transmembrane proteins 1 and 2 is important for lipid droplet formation. Proc Natl Acad Sci U S A 108, 19581-19586.

Guo, Y., Walther, T.C., Rao, M., Stuurman, N., Goshima, G., Terayama, K., Wong, J.S., Vale, R.D., Walter, P., and Farese, R.V. (2008). Functional genomic screen reveals genes involved in lipid-droplet formation and utilization. Nature 453, 657-661.

Hamilton, J.A., and Small, D.M. (1981). Solubilization and localization of triolein in phosphatidylcholine bilayers: a 13C NMR study. Proc Natl Acad Sci U S A 78, 6878-6882.

Harris, C.A., Haas, J.T., Streeper, R.S., Stone, S.J., Kumari, M., Yang, K., Han, X., Brownell, N., Gross, R.W., Zechner, R., and Farese, R.V., Jr. (2011). DGAT enzymes are required for triacylglycerol synthesis and lipid droplets in adipocytes. J Lipid Res 52, 657-667.

Huang, H., Starodub, O., McIntosh, A., Kier, A.B., and Schroeder, F. (2002). Liver fatty acid-binding protein targets fatty acids to the nucleus. Real time confocal and multiphoton fluorescence imaging in living cells. J Biol Chem 277, 29139-29151.

Khandelia, H., Duelund, L., Pakkanen, K.I., and Ipsen, J.H. (2010). Triglyceride blisters in lipid bilayers: implications for lipid droplet biogenesis and the mobile lipid signal in cancer cell membranes. PLoS One 5, e12811.

Klemm, R.W., Norton, J.P., Cole, R.A., Li, C.S., Park, S.H., Crane, M.M., Li, L., Jin, D., Boye-Doe, A., Liu, T.Y., Shibata, Y., Lu, H., Rapoport, T.A., Farese, R.V., Jr., Blackstone, C., Guo, Y., and Mak, H.Y. (2013). A conserved role for atlastin GTPases in regulating lipid droplet size. Cell Rep 3, 1465-1475.

Kuerschner, L., Moessinger, C., and Thiele, C. (2008). Imaging of lipid biosynthesis: how a neutral lipid enters lipid droplets. Traffic 9, 338-352.

Murphy, D.J., and Vance, J. (1999). Mechanisms of lipid-body formation. Trends Biochem Sci 24, 109-115.

Niu, T.K., Pfeifer, A.C., Lippincott-Schwartz, J., and Jackson, C.L. (2005). Dynamics of GBF1, a Brefeldin A-sensitive Arf1 exchange factor at the Golgi. Mol Biol Cell 16, 1213-1222.

Robenek, H., Hofnagel, O., Buers, I., Robenek, M.J., Troyer, D., and Severs, N.J. (2006). Adipophilin-enriched domains in the ER membrane are sites of lipid droplet biogenesis. J Cell Sci 119, 4215-4224.

Sandager, L., Gustavsson, M.H., Stahl, U., Dahlqvist, A., Wiberg, E., Banas, A., Lenman, M., Ronne, H., and Stymne, S. (2002). Storage lipid synthesis is non-essential in yeast. J Biol Chem 277, 6478-6482.

Shibata, Y., Shemesh, T., Prinz, W.A., Palazzo, A.F., Kozlov, M.M., and Rapoport, T.A. (2010). Mechanisms determining the morphology of the peripheral ER. Cell 143, 774-788.

Skinner, J.R., Shew, T.M., Schwartz, D.M., Tzekov, A., Lepus, C.M., Abumrad, N.A., and Wolins, N.E. (2009). Diacylglycerol enrichment of endoplasmic reticulum or lipid droplets recruits perilipin 3/TIP47 during lipid storage and mobilization. J Biol Chem 284, 30941-30948.

Szymanski, K.M., Binns, D., Bartz, R., Grishin, N.V., Li, W.P., Agarwal, A.K., Garg, A., Anderson, R.G., and Goodman, J.M. (2007). The lipodystrophy protein seipin is found at endoplasmic reticulum lipid droplet junctions and is important for droplet morphology. Proc Natl Acad Sci U S A 104, 20890-20895.

Urano, Y., Watanabe, H., Murphy, S.R., Shibuya, Y., Geng, Y., Peden, A.A., Chang, C.C., and Chang, T.Y. (2008). Transport of LDL-derived cholesterol from the NPC1 compartment to the ER involves the trans-Golgi network and the SNARE protein complex. Proc Natl Acad Sci U S A 105, 16513-16518.

Voeltz, G.K., Prinz, W.A., Shibata, Y., Rist, J.M., and Rapoport, T.A. (2006). A class of membrane proteins shaping the tubular endoplasmic reticulum. Cell 124, 573-586.

Wilfling, F., Wang, H., Haas, J.T., Krahmer, N., Gould, T.J., Uchida, A., Cheng, J.X., Graham, M., Christiano, R., Frohlich, F., Liu, X., Buhman, K.K., Coleman, R.A., Bewersdorf, J., Farese, R.V., Jr., and Walther, T.C. (2013). Triacylglycerol synthesis enzymes mediate lipid droplet growth by relocalizing from the ER to lipid droplets. Dev Cell 24, 384-399.

Wolins, N.E., Quaynor, B.K., Skinner, J.R., Schoenfish, M.J., Tzekov, A., and Bickel, P.E. (2005). S3-12, Adipophilin, and TIP47 package lipid in adipocytes. J Biol Chem 280, 19146-19155.

Wolins, N.E., Skinner, J.R., Schoenfish, M.J., Tzekov, A., Bensch, K.G., and Bickel, P.E. (2003). Adipocyte protein S3-12 coats nascent lipid droplets. J Biol Chem 278, 37713-37721.

Perspectives and Future Directions

In this work, we have undertaken several lines of experimentation to uncover elucidate the mechanisms that activate triglyceride (TG) synthesis, the physiological contexts under which it is relevant, and the processes that facilitate LD formation.

Post translational regulation of DGAT1 activity

Studies in chapter 2 set the frame for the complex picture surrounding the regulation of DGAT1. We know from previously published studies that DGAT1 protein has a long half-life, there is some evidence of transcriptional and post-transcriptional regulation (Yu et al., 2002). We observed a clear change in DGAT1 activity with change in nutritional status in white adipose tissue, while brown adipose tissue did not show similar changes (**Figure 2.1A**). Interestingly, DGAT2 also showed meaningful regulation with respect to nutritional status and it was measured in both white and brown adipose tissues. Considering the character of white and brown adipose, it seems highly plausible that this discrepancy could arise from a signaling event.

However, our approach had a few limitations. The lack of a reliable antibody against DGAT1 is a significant impediment to a targeted approach for subsequent mass spectrometry. We also did not explore the effects of various hormone (insulin or glucagon) or nutrient (glucose, fructose or fatty acid) treatments on DGAT1 phosphorylation status. Using ^{32}P labeling and mass spectrometry we confirmed that DGAT1 is basally phosphorylated, but were unable to recreate the effect of nutritional status through phosphosite mutations. It is possible that such regulation does not exist, however, viewing our results in the context of others' work (Haagsman et al., 1981; Lau and Rodriguez, 1996) and P. Zhou and S Stone, unpublished observations), it is difficult to rationalize this outcome. Fortunately, there are

several new technologies that could facilitate future studies and help answer the question of whether and how DGAT1 is regulated through phosphorylation.

With the advent of more sensitive mass spectrometers and better enrichment methods for phosphopeptides, recent high throughput phosphoproteomics studies (Beltrao et al., 2012; Humphrey et al., 2013) have identified nearly as many sites in murine DGAT1 as our targeted approach. These high throughput approaches combined with SILAC or other quantitative comparison methods will be critical to determine the relative phosphorylation status of various residues. Indeed, searching the supplemental data for Humphrey, et al. yields a trove of data, including that phosphorylation status of murine DGAT1 at T15 changes with insulin treatment (from -0.43 at 15 sec to +2.26 after 1 minute, treated/untreated) (Humphrey et al., 2013). There are other changes observed, but the phosphorylation status was never tied to changes in DGAT1 activity as it was not the focus of the study.

In terms of relevance, there is currently a very active field of research into developing more active DGAT1 protein in plants to maximize food oil production (Siloto et al., 2009) and in oleaginous fungus for biofuel development (Pan and Hua, 2012). While it is possible to use directed evolution to accomplish the same goal, it seems plausible that a first step would be to access any existing biological regulation that might already increase activity. These methods may also converge on the same result.

Still, the main interest in our group remains the role of DGAT1 in normal mammalian energy homeostasis. Three major kinase cascades that are central to metabolic regulation, AKT, PKA, and AMPK, all have predicted phosphorylation sites on DGAT1 (**Table 2.I**).

Using a targeted approach including treatments affecting these pathways combined with direct measures of DGAT1 activity along with functional consequences for the cells (reduced or increased TG storage), are likely to be successful in answering the question of whether DGAT1 activity is regulated by phosphorylation.

DGAT1 and Intestinal Triglyceride Uptake

A prime example of our lack of understanding of DGAT1 in humans is evident in Chapter 3. Due to the phenotype of the DGAT1-KO mouse, obesity resistance (Smith et al., 2000), improved glucose tolerance (Chen et al., 2003), increased life span (Streeper et al., 2012), among others, there was wide agreement that DGAT1 inhibitors should be an effective therapy against obesity and obesity-related disorders (Chen and Farese, 2000). However, as numerous DGAT1 inhibitors have been developed, many have struggled through clinical trials due to gastrointestinal adverse effects including nausea and diarrhea (Devita and Pinto, 2013). Our findings in Chapter 3 strongly suggest this may be a direct effect of DGAT1 inhibition in the intestine, rather than another off target effect. However, the question of what exactly triggers the diarrhea remains open.

Recent work has identified that DGAT1 inhibition or knockout has a dramatic effect on the secretion of gut endocrine peptides, primarily GLP-1 and PYY (Ables et al., 2012; Lin et al., 2013). GLP-1 acts by sensitizing many different cell types to insulin action, thereby improving glucose uptake and reducing glycemia (Drucker and Nauck, 2006). PYY is also relevant to obesity as it is a known appetite suppressant (Murphy et al., 2006). The balance of gut secreted peptides is carefully balanced, and altering that balance (e.g. VIP secreting tumors) has been shown to cause diarrhea (Fabian et al., 2012). It is possible that diarrhea associated with DGAT1 inactivation could be related to changes in these or other gut peptides. However, downstream treatments affecting GLP-1 (Morales, 2011) directly do not induce diarrhea, while one of the major effects of PYY is slowing the intestinal tract (Moriya et al., 2010). Thus it seems unlikely that these two peptides are involved in the cause of the diarrhea.

Loss of DGAT1 in the intestine is known to cause delayed fat absorption in mice. Normally, more than 95% of dietary fat is absorbed in the duodenum, but in DGAT1-KO mice tracer studies indicate dietary fat reaches the proximal small intestine, including the jejunum and ileum (Buhman et al., 2002). As we noted (Haas et al., 2012), mice express both DGAT1 and DGAT2 in the small intestine, whereas humans only express DGAT1. Changing the mixture of nutrients in the small intestine can induce diarrhea (e.g. bile acid sequestrants have this effect).

The added element complicating DGAT1 inhibition as therapy for obesity and related disorders is the pleiotropic nature of the DGAT1-KO phenotype. For example, loss of DGAT1 in the liver is protective against steatosis (Villanueva et al., 2009), but DGAT1-KO in the macrophage compartment seems to sensitize the immune compartment to inflammatory stimulus (Koliwad et al., 2010). Similarly, feeding should induce DGAT1 activity in the small intestine, while DGAT1 activity is suppressed in the adipose during feeding (**Figure 2.1A**). The tissue-specific necessities for DGAT1 action require a refined view of DGAT1 inhibition rather than a blanket inactivation therapy.

Equally as interesting as the cause of the diarrhea, may be its resolution. Indeed, both reports of humans with homozygous loss of function mutations of DGAT1 reported severe congenital diarrhea that resolved early in the second year of life (Haas et al., 2012) (H. Winter, personal communication). Mostly, this offers hope that if DGAT1 inhibitors are to come to market, it may be possible for humans to adapt to DGAT1-loss. Unfortunately, a complete understanding of this phenomenon is unlikely to come soon as it will require more human studies or could perhaps be modeled in an intestine-specific DGAT2-KO mouse.

Lipid Droplet Formation in Mammalian Cells

Finally, our studies in Chapter 4 have attempted to address two key challenges of studies of LD formation; how to mark what is a nascent LD from a pre-existing LD, and how to increase the frequency of formation events. Without being able to distinguish a nascent LD from a preexisting one, it is impossible to study their behavior. Likewise, the very short time scale (seconds or milliseconds) and very small distance scale (potentially smaller than 100 nm) present a significant challenge to available technology for visualization of LD formation. These technological barriers combined with a paucity of models led us to develop cell systems where we could interrogate LD formation and eventually delineate some factors affecting their nascent LD size and the localization of the formation site.

We focused on the fact that the only reported cell types that lack LDs are those that also lack the enzymes that synthesize neutral lipids (Harris et al., 2011; Sandager et al., 2002). Others, working in yeast, have built a galatose-inducible LD strain and found that LDs are functionally connected to the ER (Jacquier et al., 2011). We took a similar approach in mammalian cells and used DGAT inhibitors and other inhibitors of lipid metabolism to define conditions in which LDs could be completely ablated and subsequently reinduced. We also pursued a strategy employing fluorescent fatty acid analogs to distinguish newly synthesized TG from any preexisting pool. However, due to the nature of this molecule and findings summarized in chapter 4, we were unable to determine whether the fluorescent lipid was faithfully recapitulating endogenous lipid behavior.

While we were successful in constructing these model systems, we were unable to move beyond the correlation of TG synthesis and LD formation. In the interim, we also

participated in several studies related to LD size (Wilfling et al., 2013) and protein targeting (Thiam et al., 2013) that have changed the way we think about LD formation as a problem; namely, lipid droplets in cells are an emulsion. Focusing on the physical properties of TG in a PC bilayer, there are some clear predictions that we can make relevant to LD formation that should facilitate future studies.

At a basic level, the size of emulsion particles depends on the surface tension of the donor membrane and the stability of the budding intermediate. We touched on this idea using di-C8:0 diacylglycerol in the permeabilzed cells (**Figure 4.4D**). Short chain diacylglycerols are known to lower surface tension, thus lowering the barier to membrane deformation and favoring larger droplets. This is exactly what we observed after di-C8:0 addition, but at the time we did not understand this finding. Future studies will be required to test a variety of different surfactants to determine the defining factor of a nascent LD's size, either stability of the bud neck or the surface tension of the membrane.

Unsurprisingly, these two parameters are often connected. However, there are lipids for which the effect of either surface tension or bud neck stability dominates. For example, recent work by our collaborators (Wilfling F and Thiam AR, et al. submitted) revealed that cholesterol addition was sufficient to raise surface tension of the LD surface and support fusion to ER tubules. This facilitated LD targeting of the TG synthesis enzyme complex when it was otherwise blocked by excess surfactant. Others have proposed a similar mechanism supporting LD fusion or fission through addition of synthetic surface-active molecules (Murphy et al., 2010). Similarly, biophysical studies have identified stearylamine as a synthetic lipid whose action primarily stabilizes a budding intermediate (Teixeira et al.,

2000). Thus, we feel that addition of synthetic lipids offers an appealing line of experimentation for understanding the determination of nascent LD size.

It is important to note that proteins can also lower surface tension or stabilize a budding intermediate. Indeed, even positive results showing a clear effect of synthetic lipid additions cannot rule out that proteins may facilitate LD formation in cells. However, if modulating the surface properties of the membranes does significantly affect nascent LD size, we could conclude that biophysical properties have a dominating effect over some secondary protein action.

Lastly, the technological barriers discussed above are largely still present. Electron microscopy (EM) is still the gold standard in terms of spatial resolution. However, there are significant a significant trade-offs; EM is static and does not offer the same ability to mark structures as with fluorescent light microscopy. Similarly, it is debatable as to whether common fixation methods, e.g. glutaraldehyde with osmium post-fixation, are sufficient to preserve a nascent lipid droplet structure. Careful optimization needs to be performed to ensure such a case. Fluorescence light microscopy is also limited by spatial and temporal resolution. Increased temporal resolution is often associated with increased light toxicity to living cells. New methods for enhancing spatial resolution including 3D STORM, STED and SIM currently rely on very high light intensity, though technological development in this area is very active (Chmyrov et al., 2013; Zhu et al., 2012). A combination of increased light sensitivity with better fluorophores and image processing techniques could very well prove essential to further study of LD formation.

Our work summarized here offers an important view into the complex connections of triglyceride synthesis, physiology and lipid droplets. Through our work in chapter 2, we confirmed for the first time that DGAT1 is multiply phosphorylated, and its activity is regulated in a nutrient-state and tissue specific manner. In chapter 3, we characterized the first case of a human with DGAT1 deficiency which offers a view of the potential pitfalls of DGAT1 inhibition as a therapy for obesity and associated disorders. Finally, we present several cell systems for interrogating the process of LD formation in chapter 4 and a potential framework for continued experimentation. These advances are an important stepping stone toward an integrated view of molecular energy homeostasis at the cellular and physiological level.

References

Ables, G.P., Yang, K.J., Vogel, S., Hernandez-Ono, A., Yu, S., Yuen, J.J., Birtles, S., Buckett, L.K., Turnbull, A.V., Goldberg, I.J., et al. (2012). Intestinal DGAT1 deficiency reduces postprandial triglyceride and retinyl ester excursions by inhibiting chylomicron secretion and delaying gastric emptying. J Lipid Res *53*, 2364-2379.

Beltrao, P., Albanese, V., Kenner, L.R., Swaney, D.L., Burlingame, A., Villen, J., Lim, W.A., Fraser, J.S., Frydman, J., and Krogan, N.J. (2012). Systematic functional prioritization of protein posttranslational modifications. Cell *150*, 413-425.

Buhman, K.K., Smith, S.J., Stone, S.J., Repa, J.J., Wong, J.S., Knapp, F.F., Jr., Burri, B.J., Hamilton, R.L., Abumrad, N.A., and Farese, R.V., Jr. (2002). DGAT1 is not essential for intestinal triacylglycerol absorption or chylomicron synthesis. J Biol Chem *277*, 25474-25479.

Chen, H.C., and Farese, R.V., Jr. (2000). DGAT and triglyceride synthesis: a new target for obesity treatment? Trends Cardiovasc Med *10*, 188-192.

Chen, H.C., Jensen, D.R., Myers, H.M., Eckel, R.H., and Farese, R.V., Jr. (2003). Obesity resistance and enhanced glucose metabolism in mice transplanted with white adipose tissue lacking acyl CoA:diacylglycerol acyltransferase 1. J Clin Invest *111*, 1715-1722.

Chmyrov, A., Keller, J., Grotjohann, T., Ratz, M., d'Este, E., Jakobs, S., Eggeling, C., and Hell, S.W. (2013). Nanoscopy with more than 100,000 'doughnuts'. Nat Methods *10*, 737-740.

Devita, R.J., and Pinto, S. (2013). Current Status of the Research and Development of Diacylglycerol O-acyltransferase 1 (DGAT1) Inhibitors. J Med Chem.

Drucker, D.J., and Nauck, M.A. (2006). The incretin system: glucagon-like peptide-1 receptor agonists and dipeptidyl peptidase-4 inhibitors in type 2 diabetes. Lancet *368*, 1696-1705.

Fabian, E., Kump, P., and Krejs, G.J. (2012). Diarrhea caused by circulating agents. Gastroenterol Clin North Am *41*, 603-610.

Haagsman, H.P., de Haas, C.G., Geelen, M.J., and van Golde, L.M. (1981). Regulation of triacylglycerol synthesis in the liver: a decrease in diacylglycerol acyltransferase activity after treatment of isolated rat hepatocytes with glucagon. Biochim Biophys Acta *664*, 74-81.

Haas, J.T., Winter, H.S., Lim, E., Kirby, A., Blumenstiel, B., DeFelice, M., Gabriel, S., Jalas, C., Branski, D., Grueter, C.A., et al. (2012). DGAT1 mutation is linked to a congenital diarrheal disorder. J Clin Invest *122*, 4680-4684.

Harris, C.A., Haas, J.T., Streeper, R.S., Stone, S.J., Kumari, M., Yang, K., Han, X., Brownell, N., Gross, R.W., Zechner, R., et al. (2011). DGAT enzymes are required for triacylglycerol synthesis and lipid droplets in adipocytes. J Lipid Res *52*, 657-667.

Humphrey, S.J., Yang, G., Yang, P., Fazakerley, D.J., Stockli, J., Yang, J.Y., and James, D.E. (2013). Dynamic adipocyte phosphoproteome reveals that Akt directly regulates mTORC2. Cell Metab *17*, 1009-1020.

Jacquier, N., Choudhary, V., Mari, M., Toulmay, A., Reggiori, F., and Schneiter, R. (2011). Lipid droplets are functionally connected to the endoplasmic reticulum in Saccharomyces cerevisiae. J Cell Sci *124*, 2424-2437.

Koliwad, S.K., Streeper, R.S., Monetti, M., Cornelissen, I., Chan, L., Terayama, K., Naylor, S., Rao, M., Hubbard, B., and Farese, R.V., Jr. (2010). DGAT1-dependent triacylglycerol storage by macrophages protects mice from diet-induced insulin resistance and inflammation. J Clin Invest *120*, 756-767.

Lau, T.E., and Rodriguez, M.A. (1996). A protein tyrosine kinase associated with the ATP-dependent inactivation of adipose diacylglycerol acyltransferase. Lipids *31*, 277-283.

Lin, H.V., Chen, D., Shen, Z., Zhu, L., Ouyang, X., Vongs, A., Kan, Y., Levorse, J.M., Kowalik, E.J., Jr., Szeto, D.M., et al. (2013). Diacylglycerol acyltransferase-1 (DGAT1) inhibition perturbs postprandial gut hormone release. PLoS One *8*, e54480.

Morales, J. (2011). The pharmacologic basis for clinical differences among GLP-1 receptor agonists and DPP-4 inhibitors. Postgrad Med *123*, 189-201.

Moriya, R., Shirakura, T., Hirose, H., Kanno, T., Suzuki, J., and Kanatani, A. (2010). NPY Y2 receptor agonist PYY(3-36) inhibits diarrhea by reducing intestinal fluid secretion and slowing colonic transit in mice. Peptides *31*, 671-675.

Murphy, K.G., Dhillo, W.S., and Bloom, S.R. (2006). Gut peptides in the regulation of food intake and energy homeostasis. Endocr Rev *27*, 719-727.

Murphy, S., Martin, S., and Parton, R.G. (2010). Quantitative analysis of lipid droplet fusion: inefficient steady state fusion but rapid stimulation by chemical fusogens. PLoS One *5*, e15030.

Pan, P., and Hua, Q. (2012). Reconstruction and in silico analysis of metabolic network for an oleaginous yeast, Yarrowia lipolytica. PLoS One *7*, e51535.

Sandager, L., Gustavsson, M.H., Stahl, U., Dahlqvist, A., Wiberg, E., Banas, A., Lenman, M., Ronne, H., and Stymne, S. (2002). Storage lipid synthesis is non-essential in yeast. J Biol Chem *277*, 6478-6482.

Siloto, R.M., Truksa, M., Brownfield, D., Good, A.G., and Weselake, R.J. (2009). Directed evolution of acyl-CoA:diacylglycerol acyltransferase: development and characterization of Brassica napus DGAT1 mutagenized libraries. Plant Physiol Biochem *47*, 456-461.

Smith, S.J., Cases, S., Jensen, D.R., Chen, H.C., Sande, E., Tow, B., Sanan, D.A., Raber, J., Eckel, R.H., and Farese, R.V., Jr. (2000). Obesity resistance and multiple mechanisms of triglyceride synthesis in mice lacking Dgat. Nat Genet *25*, 87-90.

Streeper, R.S., Grueter, C.A., Salomonis, N., Cases, S., Levin, M.C., Koliwad, S.K., Zhou, P., Hirschey, M.D., Verdin, E., and Farese, R.V., Jr. (2012). Deficiency of the lipid synthesis enzyme, DGAT1, extends longevity in mice. Aging (Albany NY) *4*, 13-27.

Teixeira, H., Dubernet, C., Rosilio, V., Benita, S., Lepault, J., Erk, I., and Couvreur, P. (2000). New bicompartmental structures are observed when stearylamine is mixed with triglyceride emulsions. Pharm Res *17*, 1329-1332.

Thiam, A.R., Antonny, B., Wang, J., Delacotte, J., Wilfling, F., Walther, T.C., Beck, R., Rothman, J.E., and Pincet, F. (2013). COPI buds 60-nm lipid droplets from reconstituted water-phospholipid-triacylglyceride interfaces, suggesting a tension clamp function. Proc Natl Acad Sci U S A *110*, 13244-13249.

Villanueva, C.J., Monetti, M., Shih, M., Zhou, P., Watkins, S.M., Bhanot, S., and Farese, R.V., Jr. (2009). Specific role for acyl CoA:Diacylglycerol acyltransferase 1 (Dgat1) in hepatic steatosis due to exogenous fatty acids. Hepatology *50*, 434-442.

Wilfling, F., Wang, H., Haas, J.T., Krahmer, N., Gould, T.J., Uchida, A., Cheng, J.X., Graham, M., Christiano, R., Frohlich, F., et al. (2013). Triacylglycerol synthesis enzymes mediate lipid droplet growth by relocalizing from the ER to lipid droplets. Dev Cell *24*, 384-399.

Yu, Y.H., Zhang, Y., Oelkers, P., Sturley, S.L., Rader, D.J., and Ginsberg, H.N. (2002). Posttranscriptional control of the expression and function of diacylglycerol acyltransferase-1 in mouse adipocytes. J Biol Chem *277*, 50876-50884.

Zhu, L., Zhang, W., Elnatan, D., and Huang, B. (2012). Faster STORM using compressed sensing. Nat Methods *9*, 721-723.

Appendices

Appendix 1: Supplemental Material for Chapter 3

Exome Capture and Sequencing

Exome capture was performed on genomic DNA with Agilent Whole Exome SureSelect v2 kit according to manufacturer's instructions. Captured exome DNA was then subjected to Illumina sequencing. Reads were processed by Picard and aligned to the human reference genome hg19 (Wheeler et al., 2008) with Burrows-Wheeler Aligner (Li and Durbin, 2009), and then single nucleotide variant (SNV) calling on the exomes was performed by using the GATK toolkit (McKenna et al., 2010). Search parameters were set for identification of rare (frequency < 1% in available exome pool) alleles with predicted nonsense, splice or frameshift, or non-synonymous and predicted deleterious (Adzhubei et al., 2010). Criteria were further constrained by searching for mutations with expected Mendelian ratio in parents and affected child.

Restriction Fragment Length Polymorphism Assay

A restriction fragment length polymorphism assay was designed with the following primers: F-*TGAGCTCGTAGCACAAGGTG,* R-*TAGCCTCTGCAGGGAAGAAG*. PCR on genomic DNA was performed with subsequent digestion by the restriction enzyme *Fnu*4-HI. The digested products were separated by agarose gel electrophoresis. The wildtype allele yields bands sized 165, 32 and 3 bp (latter not resolved); the mutant allele yields bands sized 122, 43, 32 and 3 bp.

cDNAs and Plasmids

Wildtype *DGAT1* cDNA was isolated from HeLa cDNA by PCR and subcloned, with or without FLAG-tag sequences, into a modified pMSCV-puro vector containing a CMV promoter (Clontech). The PGK:puromycin cassette was replaced with a PGK:mRuby-T2A-Zeocin cassette encoding the red fluorescent protein mRuby (Kredel et al., 2009), the T2A self cleaving peptide,

and a Zeocin resistance gene. Δ8 *DGAT1* cDNA was generated as described (Gibson et al., 2009). FLAG-H415A *DGAT1* was generated with Site-Directed Mutagenesis kit (Stratagene).

Cell Lines

Mouse embryonic fibroblasts (MEFs) were isolated from E14.5 embryos and immortalized by serial passaging (Willnow and Herz, 1994). Immortalized cells were transduced with retrovirus encoding *DGAT1* cDNAs. Cells were cultured in DMEM-High Glucose medium (Invitrogen) with 10% FBS (Thermo Fisher). Stable cell lines were selected in 300 μg/mL Zeocin (Invitrogen).

DGAT1 Activity

DGAT activity was measured as described (Cases et al., 2001) with conditions specific for DGAT1. Briefly, 7.5 μg of microsomal proteins were added to a reaction mix of 100 mM Tris-HCl pH 7.5, 50 mM $MgCl_2$, 0.625 mg/mL BSA, 25 μM [^{14}C]-oleoyl-CoA, and 200 μM 1,2-dioleoyl-glycerol (DAG) in a final volume of 200 μL. The assay was carried out at 37 °C for 5 min and quenched with 2:1 chloroform:methanol. Lipids were separated by TLC and visualized and quantified with a phosphorimage screen.

RT-PCR

For cells, total RNA was isolated with Trizol (Invitrogen). For patient samples, total RNA was isolated from whole blood collected in Paxgene (Qiagen) tubes. White cells were isolated by centrifugation and washed twice with PBS. RNA was isolated from white cells using RNEasy spin columns (Qiagen) according to manufacturer's instructions. RNA samples were reverse-

transcribed (RT) using the iScript cDNA Synthesis kit (BioRad). RT reaction products were diluted 10-fold for PCR reactions.

Immunoblotting

Anti-FLAG monoclonal antibody M2 (Sigma Aldrich) was used to detect the FLAG epitope (1:2000). Other antibodies were anti-DGAT1 polyclonal antibody NB110-41487 (1:1000, Novus Biologicals) and anti-HSP90 (1:2000, BD Biosciences). Secondary antibodies conjugated to HRP (1:5000, Amersham) were used for detection with ECL reagents (Pierce).

Statistics

The probability of the Δ8 mutation causing the CDD phenotype was calculated empirically from the frequency of any homozygous or compound heterozygous and deleterious mutations (9).

Study Approval

Eight members of one family with two affected individuals were studied. Written informed consents for all adult participants and the parents of the children were obtained to permit genetic studies of their samples which are included in a biorepsitory (HSW) that was approved by the Partners Institutional Review Board.

References

Adzhubei, I.A., Schmidt, S., Peshkin, L., Ramensky, V.E., Gerasimova, A., Bork, P., Kondrashov, A.S., and Sunyaev, S.R. (2010). A method and server for predicting damaging missense mutations. Nat Methods 7, 248-249.

Cases, S., Stone, S.J., Zhou, P., Yen, E., Tow, B., Lardizabal, K.D., Voelker, T., and Farese, R.V., Jr. (2001). Cloning of DGAT2, a second mammalian diacylglycerol acyltransferase, and related family members. J Biol Chem 276, 38870-38876.

Gibson, D.G., Young, L., Chuang, R.Y., Venter, J.C., Hutchison, C.A., 3rd, and Smith, H.O. (2009). Enzymatic assembly of DNA molecules up to several hundred kilobases. Nat Methods 6, 343-345.

Kredel, S., Oswald, F., Nienhaus, K., Deuschle, K., Rocker, C., Wolff, M., Heilker, R., Nienhaus, G.U., and Wiedenmann, J. (2009). mRuby, a bright monomeric red fluorescent protein for labeling of subcellular structures. PLoS One 4, e4391.

Li, H., and Durbin, R. (2009). Fast and accurate short read alignment with Burrows-Wheeler transform. Bioinformatics 25, 1754-1760.

McKenna, A., Hanna, M., Banks, E., Sivachenko, A., Cibulskis, K., Kernytsky, A., Garimella, K., Altshuler, D., Gabriel, S., Daly, M., and DePristo, M.A. (2010). The Genome Analysis Toolkit: a MapReduce framework for analyzing next-generation DNA sequencing data. Genome Res 20, 1297-1303.

Wheeler, D.A., Srinivasan, M., Egholm, M., Shen, Y., Chen, L., McGuire, A., He, W., Chen, Y.J., Makhijani, V., Roth, G.T., Gomes, X., Tartaro, K., Niazi, F., Turcotte, C.L., Irzyk, G.P., Lupski, J.R., Chinault, C., Song, X.Z., Liu, Y., Yuan, Y., Nazareth, L., Qin, X., Muzny, D.M., Margulies, M., Weinstock, G.M., Gibbs, R.A., and Rothberg, J.M. (2008). The complete genome of an individual by massively parallel DNA sequencing. Nature 452, 872-876.

Willnow, T.E., and Herz, J. (1994). Genetic deficiency in low density lipoprotein receptor-related protein confers cellular resistance to Pseudomonas exotoxin A. Evidence that this protein is required for uptake and degradation of multiple ligands. J Cell Sci 107 (Pt 3), 719-726.

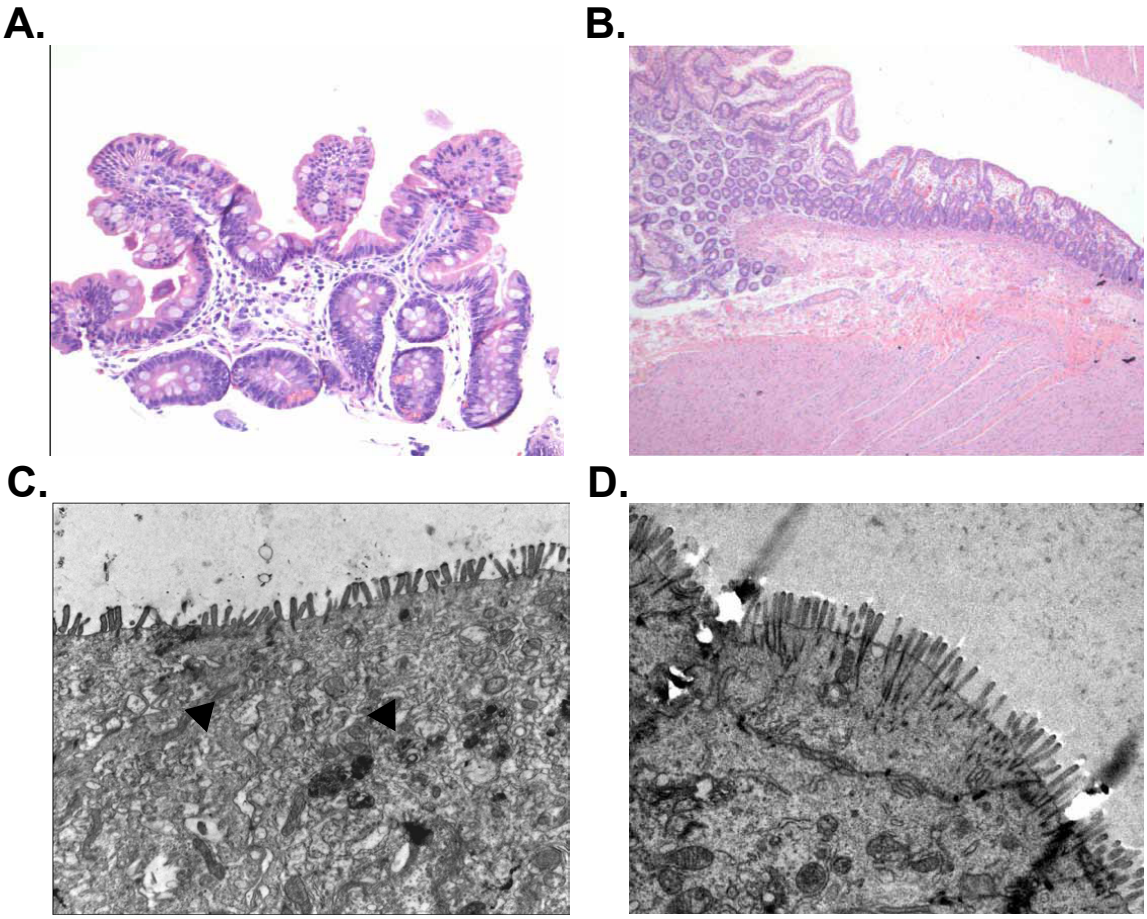

Figure A1.1 Histopathology of Case 1 shows areas of villous atrophy and microvillous dystrophy in proximity to areas of normal morphology.
A. Jejunal biopsy at 1 month of age shows preserved villi and normal crypts with Paneth cells. There was no evidence for increased intraepithelial lymphocytes. **B.** A duodenal biopsy shows an area of sever enteritis adjacent to an area with intact villi. There does not appear to be increased inflammation in the lamina propria. **C.** Distorted and separated microvillia are present in some areas of the biopsy. Enterocytes show well preserved cytoplasmic organelles, including mitochondria, endoplasmic reticulum and lysosomes. There is slight dilation of the ER and an increase in number of lysosomes, but intracellular junctions and basement membranes appear intact. **D.** A second biopsy taken 11 months later still shows some areas of poorly formed microvilli and overall cellular morphology appears unchanged from first biopsy.

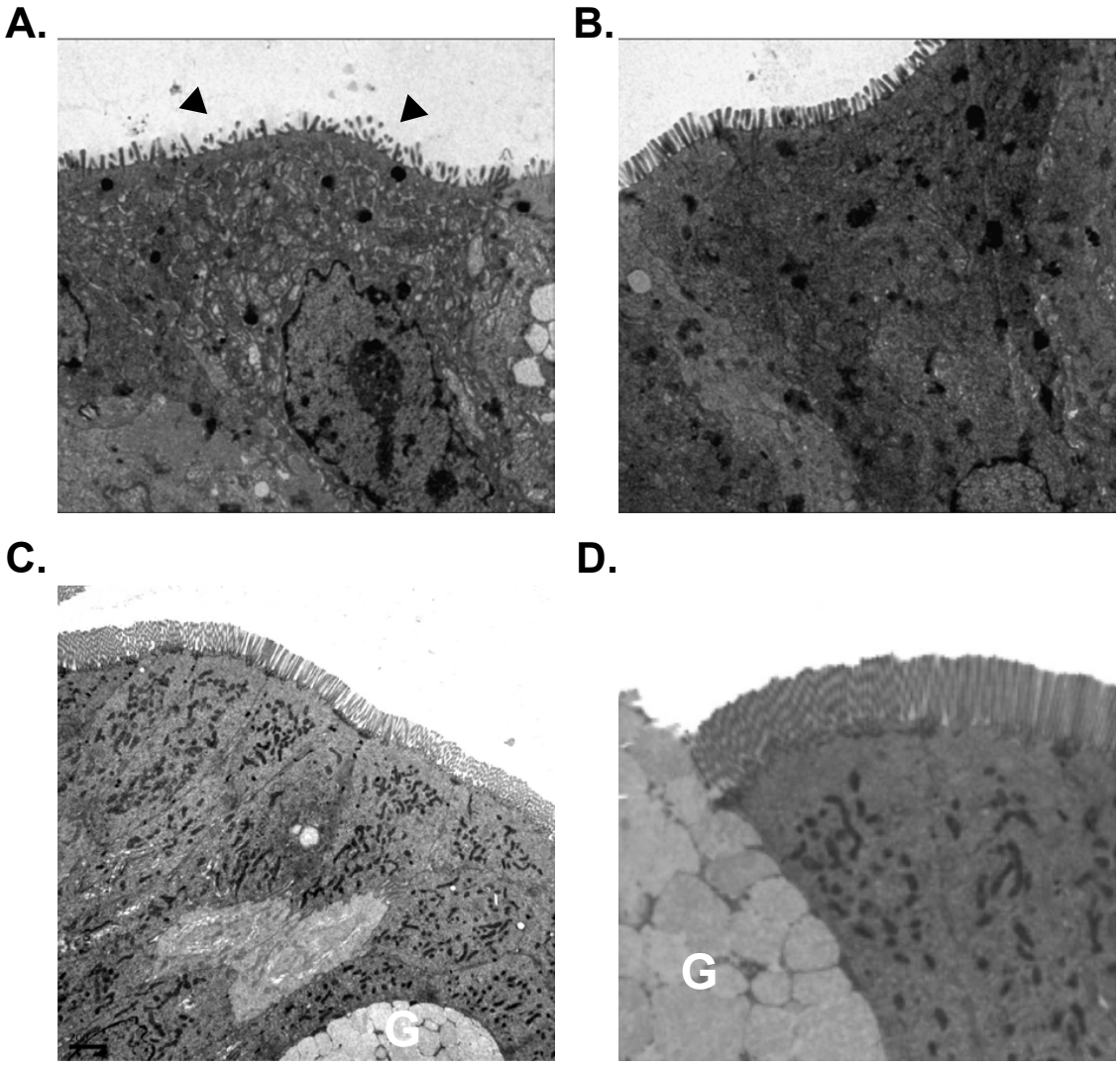

Figure A1.2 Electron micrographs of duodenal biopsies from Case 2 show areas of microvillous dystrophy with moderate improvement over time.
A. Microvillous malformations (arrows) present in duodenal biopsy taken from Case 2 at age two months. Similar characteristics as Case 1, including slight dilation of the ER and increased lysosome numbers, but otherwise good preservation of cytoplasmic organelles, intracellular junctions and basement membranes. **B.** Another field taken at age 2 months shows better preservation of microvilli **C.** and **D.** A second biopsy taken after impprovement of symptoms (age 13 months) shows improved morphology of microvilli. Goblet cells (G) can be seen, some with depleted mucin vacuoles.

Publishing Agreement

It is the policy of the University to encourage the distribution of all theses, dissertations, and manuscripts. Copies of all UCSF theses, dissertations, and manuscripts will be routed to the library via the Graduate Division. The library will make all theses, dissertations, and manuscripts accessible to the public and will preserve these to the best of their abilities, in perpetuity.

Please sign the following statement:

I hereby grant permission to the Graduate Division of the University of California, San Francisco to release copies of my thesis, dissertation, or manuscript to the Campus Library to provide access and preservation, in whole or in part, in perpetuity.

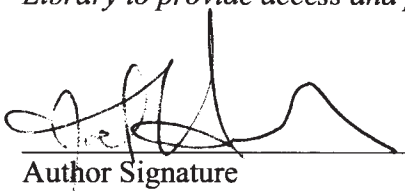

Author Signature

9/3/13

Date